THE HONG KONG
POLYTECHNIC UNIVERSITY

DEPARTMENT OF MECHANICAL ENGINEERING

Development of CNT-reinforced Polymer Composite

Wong Ka Keung

A thesis submitted in partial fulfilment of the requirements for the
Degree of Master of Philosophy

August 2007

Certificate of originality

I hereby declare that this thesis is my own work and that, to the best of my knowledge and belief, it reproduces no material previously published or written, nor material that has been accepted for the award of any other degree or diploma, except where due acknowledgement has been made in the text.

Wong Ka Keung

Abstract

Light and strong material will be essential in everyday life in the future. Research into this kind of material has never stopped. In 1991, NEC researcher, Iijima, discovered a tube-like structure of carbon: Carbon nanotubes (CNTs). Many reports showed that CNTs have novel mechanical, electrical, thermal and chemical properties. This tube-like structure was expected to improve human life.

Fillers such as glass fiber, Kevlar, graphite, ceramics, metal particles and clays are commonly used in polymer composites. However, these fillers offer only a limited contribution to the mechanical properties of the composites. With the advance of nano-technology, more researchers have focused on the application of nano-materials such as nano-clays and CNTs to reinforce polymer-based composites.

Although many studies have been conducted in the past few years on the possibility of using CNTs to improve the performance of polymer-based materials, some of the results have been contradictory and lacked coherence. Thus, an in-depth understanding of CNT-reinforced composites is required.

It is now known that the dispersion of CNTs and interfacial bonding between CNTs and polymer chains affect the performance of reinforcements. Thus, these two key issues need to be solved in order to make the best use of CNTs as reinforcement. The Van der Waals force between the nanotubes is rather strong, so nanotubes usually form bundles and are difficult to separate. The dispersion quality of CNTs directly affects the stress transfer efficiency from a polymer matrix to CNTs. In addition, the smooth tube body makes it difficult to bond with the host matrix, which results in a poor interfacial strength between CNTs and polymer.

This research project aims to solve the problems by functionalizing the CNTs (fCNTs) with carboxyl function group (COOH) to improve the stress transfer efficiency from polymer to CNTs body. These functional groups of CNTs provide sites for covalent integration of the CNTs into polymer structures to produce the reinforcement. Both thermosetting and thermoplastic polymers were used to fabricate CNTs polymer-based composites in this work. CNTs and fCNTs were blended with polypropylene (PP) and epoxy by different fabrication processes. The experimental results on both CNT/epoxy and CNT/PP composites were presented. fCNTs showed a positive effect on mechanical properties of the composites when comparing with non-functionalized ones. fCNTs formed cross-link with polymer chains. Thus, it can enhance the stress transfer efficiency between CNTs and polymer matrix.

On the other hand, UV degradation has been a critical problem for polymers. There is a need to study the UV effects on CNTs polymer composites when applying them in outdoor environments. fCNT/PP composites were fabricated for UV irradiation. Through mechanical and thermal properties analyses, it has been found that fCNTs can diminish the negative effects of UV irradiation on PP. fCNTs absorbs the UV energy to form bonds with polymer chains, while the layer that the polymer chains formed bonding with fCNTs would be stronger. This strengthened layer can protect the inner part of the composite.

From the experimental results, CNT-reinforced polymer composites showed its high potential for multi-purpose applications. If more effort is put into related research, it will become a useful material in the future.

Publications arising from the thesis

[1] K.K. Wong, S.Q. Shi and K.T. Lau, Mechanical and Thermal Behavior of a Polymer Composite Reinforced with Functionalized Carbon Nanotubes, Key Engineering Materials, Vol. 334-335, pp.705~708, 2007

[2] K.K. Wong, S.Q. Shi and K.T. Lau, Practical Issues on Carbon Nanotubes Reinforced Polymer Composites and its Mechanical Properties, The 11th Annual Conference of the Hong Kong Society of Theoretical and Applied Mechanics and the 3rd Jiangsu-Hong Kong Forum on Mechanics and Its Application, 10 March 2007, Hong Kong, China

[3] K.K. Wong, S.Q. Shi and K.T. Lau, Effects of UV Exposure on an Oxidized Carbon Nanotube Polymer Composite, The 16th International Conference on Composite Materials, 8-13 July 2007, Kyoto, Japan

Acknowledgments

I would like to express my great appreciation to my supervisors, Prof. San-qiang Shi and Dr. Alan, Kin-tak Lau for their valuable and constructive suggestions, and enthusiastic encouragement throughout my research study. Their willingness to give their time so generously has been very much appreciated.

I would thank the Hong Kong Polytechnic University (PolyU) providing an opportunity for me to gain more knowledge and experience in research activities. I would also thank the Institute of Textiles and Clothing, and Materials Research Centre of PolyU that allowing me to use their facilities to conduct my research work.

Finally, I wish to thank my parents and friends for their support and encouragement during my study.

List of abbreviations

ABS	Acrylonitrile-butadiene-styrene
AFM	Atomic force microscopy
Arc-	Arc discharge method
CNT	Carbon nanotube
COOH	Carboxyl function group
CVD	Chemical vapor deposition
DGEBA	Diglycidyl ether of bisphenol
DMF	N,N-dimethylformamide
DMSO	Dimethyl sulfoxide
DSC	Differential scanning calorimetry
DTG	Thermogravimetric
f CNT	Functionalized carbon nanotube
fMWNT	Functionalized multi-walled nanotube
fSWNT	Functionalized single-walled nanotube
GNP	Graphite nano platelet
MWNT	Multi-walled nanotube
NMP	1-methyl-2-pyrrolidinone
ODCB	1,2-dichlorobenzene
PHAE	Polyhydroxyaminoether
PMMA	Polymethlymethacrylate
PolyU	The Hong Kong Polytechnic University
PP	Polypropylene
PVA	Polyvinylalcohol
SDS	Sodium dodecyl sulfate
SEM	Scanning electron microscope
SWNT	Single-walled nanotube
TCE	1,1,2,2-tetrachloroethane
TG	Thermogravimetric
Tg	Glass transition temperature
TGA	Thermogravimetric analyzer
THF	Tetrahydrofuran
UV	Ultraviolet

Table of Contents

Chapter 1 Introduction

1.1 Background

With the recent advance of materials science, many synthetic materials with high performance in mechanical and chemical properties have been produced. The conventional fiber-reinforced composites, such as carbon fiber reinforced polymer, glass fiber reinforced polymer and Kevlar fibers, are largely employed in industry. Definitely, lighter and stronger materials would benefit the sports, automotive and aerospace industries to improve the energy efficiency and performance of their products. On the other hand, using recycled polymers to fabricate polymer composites, which incorporate strong reinforcement fillers, would create a new direction for future development. With the advance of nano-technology, more researchers focus on the application of nano-materials such as nano-clays and carbon nanotubes (CNTs) to reinforce polymer-based composites. It is believed that nano-scaled fillers can provide unique properties to polymer matrices [1]. The discovery of CNTs [2] in 1991 introduced the possibility of fabricating high performance materials. The elastic modulus of the CNTs was reported [3, 4] as high as 1TPa and the elastic strain as high as 5%. In addition, with the improved quality and quantity of CNTs by recent advance of the synthesis of CNTs [5], many research activities have been stimulated by the attractive mechanical and thermal properties of CNTs.

Carbon nanotubes were discovered by Iijima [2] in 1991. Because of their remarkable physical and chemical properties, many potential applications of CNTs are suggested. The Young’s modulus of CNTs was estimated to be the order of 1 TPa [4, 5] by atomic force microscopy (AFM), while the Young’s modulus of convention carbon fiber and glass fiber are 800 GPa and 70 GPa respectively [7]. CNTs have three classes of structure (Fig. 1), armchair, zigzag and chiral. The Carbon-Carbon (C-C) bonds of the armchair structure are perpendicular to the tube axis and the compound has metallic properties. The C-C bonds of the zigzag structure are parallel to the tube axis. The C-C bonds of the chiral structure make an angle to the tube axis. Carbon nanotubes exist in two forms: single-walled nanotubes (SWNTs) and multi-walled nanotubes (MWNTs). CNTs often twist together to form ropes consisting of dozens or hundreds of individual tubes. MWNTs can be either coaxial tubes stuck inside one another or a single long sheet rolled up like a scroll.

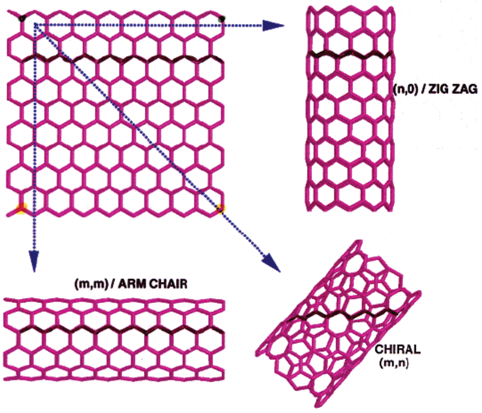

Fig. 1. 3 Classes of structure of carbon nanotubes (arrows: rolling direction)

Many studies about using SWNTs and MWNTs as nano-reinforcements for composite materials have been conducted in recent years [7 – 9]. Qian et al [10] found that the addition of only 1 wt% CNTs to polystyrene increases the polymer mechanical properties significantly, while about 10 wt% of carbon fiber was needed in order to get a similar tensile modulus. However, previous studies of the CNTs composite were mainly focused on randomly orientated CNTs. The performance of the composite is related to the orientation of the CNTs. If well-aligned CNTs composites were produced, the mechanical performance of the composites would be greatly improved. The degree of dispersion of CNTs and the strength of interfacial bonding between CNTs and polymer matrix are the keys to produce a high mechanical performance CNTs composite.

CNTs are easily to agglomerate and bundle together due to very high Van der Waals forces of individual nanotubes [10]. Sonication (physical blending) and chemical functionalization are the most common dispersion methods for CNTs [11]. The strength of interfacial bonding between CNTs and the polymer matrix is an important factor in controlling the mechanical properties of CNTs composites at different loading conditions. Good interfacial bonding ensures the stress transfer from the polymer matrix to the CNTs. However, the agglomeration of CNTs would also affect the stress transfer from the matrix to CNTs. Agglomeration of CNTs would incur slippage[12], which would affect the mechanical properties of the composite. Functionalization of CNTs is a method to solve the problem of CNTs agglomeration. The fabrication process of CNT-reinforced polymer composites can be categorized into three main methods: solvents-solution mixing [8, 10 & 16], melt-mixing [5] and in-situ polymerization [27]. The alignment methods of CNTs can be categorized into three main areas: Ex situ alignment of CNTs [13, 14], field-induced alignment of CNTs [15 – 21] and force-induced alignment of CNTs [5, 22 – 29].

UV degradation has been a critical problem for polymers. CNT-reinforced polymer composites also face the same problem when they are used in outdoor applications. However, there are only a very limited number of scientific studies focusing on this issue for CNT/polymer composites. Thus, this study will also study the UV effects on functionalized CNT/polymer composites.

1.2 Objectives

The objectives of this project are to study the effects of functionalized CNTs on the dispersion quality of CNTs and the load transfer properties between CNTs and a polymer matrix. The fabrication methods and the mechanical properties of CNT-reinforced polymer composites are also discussed. Epoxy and polypropylene (PP) were used for the fabrication of CNT-reinforced polymer composites. The main reason for using these two materials is that these materials are commonly available in the market. Epoxy is largely used in structural applications. PP is always used as a material for fabricating car components, plastic bags and soft drink bottles. The recycling of PP would be a worthwhile area for investigation. If the material properties of PP were improved, there would be more applications and opportunities for recycled PP. Here are the objectives of this research project:

1. Develop techniques for fabricating CNT-reinforced polymer composite;
2. Study the effects of functionalization on CNTs;
3. Study the mechanical and thermal performance of CNT-reinforced composite and functionalized CNT-reinforced polymer composite; and
4. Study the effects of UV on functionalized CNT-reinforced polymer composite.

1.3 Layout of the thesis

The present thesis is divided into seven chapters. Chapter 1 provides an overview for the background of the present work. Due to the needs of society, four objectives were developed to gain more knowledge in carbon nanotube reinforced polymer composites. The research of carbon nanotubes is a hot topic in the world. Chapter 2 summarizes related studies of carbon nanotubes and carbon nanotube-reinforced polymer composites. Both the work of functionalization of carbon nanotubes and the fabrication processes of carbon nanotube-reinforced polymer composites are reviewed in this chapter. Through out the reviewing process, the fundamental ideas of this research work are presented.

Chapter 3 introduces the experimental equipment required in this study. The procedures for conducting the experiments are mentioned. The critical functionalization process of carbon nanotubes will also be discussed in this chapter.

Chapter 4 and 5 present the experimental results of SWNT/epoxy and MWNT/PP composites respectively. The theoretical study incorporating comprehensive experimental findings concludes the role of functionalization of carbon nanotubes in these two chapters. In order to extend the usefulness for daily application of this research, Chapter 6 focuses on the effects of UV exposure on the carbon-nanotube-reinforced polymer composites. This chapter will also present the experimental findings and theoretical study.

The findings from this research study are concluded in Chapter 7. The possibility of transferring the experience and techniques used in the study to industry is discussed. Future work is also recommended and proposed.

Chapter 2 Literature Reviews

2.1 Carbon nanotube

Carbon nanotubes can have varies diameters ranging from 1 to 100 nm and lengths of up to millimeters [2]. Their densities can be as low as 1.3 g/cm^3 and Young's modulus values can be greater than 1 TPa [3, 4]. The tensile strength of CNTs can be a 100 times of steel but have less density than steel. Thus, CNTs would be an attractive material for engineering applications. There are three important synthesis produces for CNTs, electric arc-discharge, laser ablation and catalytic decomposition of gaseous hydrocarbons. The early method to fabricate CNTs was electric arc-discharge method, which was used for Fullerene fabrication [27, 28]. Electric arc-discharge and laser ablation requires very high operation temperature (> 3000^{o}C) and with many impurity inside the final product. On contrast, catalytic decomposition of gaseous hydrocarbons requires lower operation temperature (1000 -1100^{o}C) with better purity and higher production rate (50 kg/day) [30]. Chemical vapor deposition (CVD) (Fig. 2) is a common method of catalytic decomposition of gaseous hydrocarbons for mass product of CNTs with high quality and low cost.

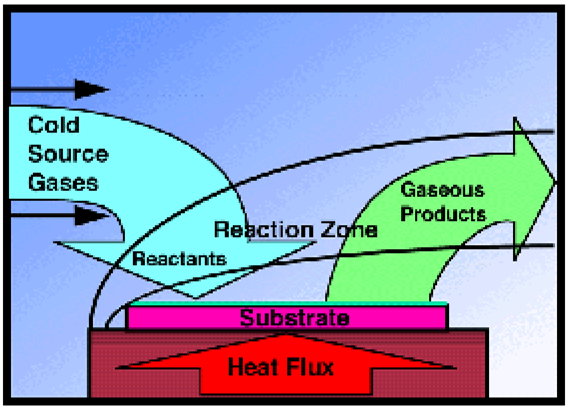

Fig. 2. Schematic diagram for chemical vapor deposition

2.1.1 Properties of carbon nanotubes

CNT is very conductive, they can carry up to 100MA/cm^2 of current density theoretically. The theoretical thermal conductivity of CNT is also as high as 6000W/mK [31 – 33]. However, these value were only in theoretic calculation, experiment is difficult to conduct due to they are easy to agglomerate together. The Young's modulus of in-plane graphite sheet is 1.06TPa [35], CNTs were expected in similar value. A number of computer simulations were carried out in the past decade to calculate the Young's modulus of CNTs. The calculation of Young's modulus of CNTs was 1.5 TPa by Overney et al [36] in 1993. Then a serial of papers predicted the modulus of CNTs with similar values [37]. The actual mechanical properties measurements (Fig. 3) of CNTs were carried until year 2000 by Yu et al. [31]. They have done the stress–strain measurements on individual arc discharge MWNTs between the tips of Atomic Force Microscope (AFM). They obtained the Young's modulus values of 0.27–0.95 TPa for a range of MWNTs. The fracture of MWNT at strains of was up to 12% and with strengths in the range 11–63 GPa. The first measurement of SWNT was carried out by Salvetat et al. using AFM [38]. They obtained a tensile modulus of 1 TPa for SWNT bundles by bending methods. The properties of larger diameter bundles were dominated by shear slippage of individual nanotubes within the bundle.

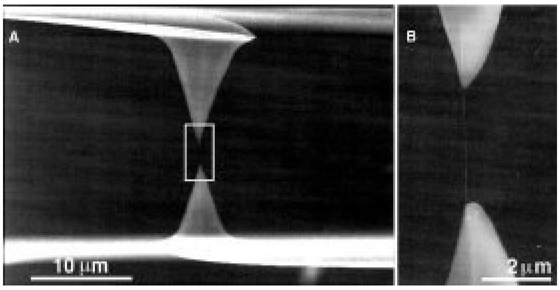

Fig. 3. An SEM image of two AFM tips holding a MWNT [31]

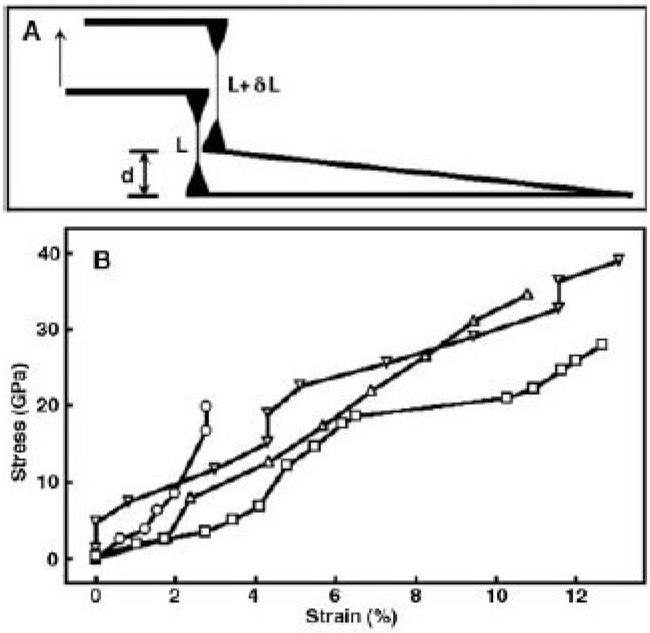

Fig. 4. Schematic showing the principle of the tensile-loading experiment. (B) Plot of stress versus strain curves for individual MWNTs [31]

With the outstanding mechanical properties of the CNTs, CNTs containing composite would be an interesting and fast growing subject [7]. Among of different types of matrix, polymer matrix could be a focus since our industry relies on polymer heavily. CNTs is small enough to inhibit the nano and micro cracks inside the polymer composite, the nanotube was found to bridge the microvoids (microcrack) in the matrix and presumably enhanced the strength of the composite [39]. However, there are some contradicting results for the performance of the CNTs composite [40]. Thus, more investigations about CNT-reinforced polymer composites are needed.

The stress transfer ability between the CNTs and polymer matrix at the interface is an important issue that governs the mechanical performance of the CNTs composite under different load condition. There are three main mechanisms of load transfer from a matrix to filler. The first is micromechanical interlocking; but it is not applicable for nanotube composites due to their atomically smooth surface. The second is chemical bonding between the nanotubes and the matrix. The third mechanism is a weak Van der Waals bonding between the fiber and the matrix. CNT-reinforced polymer composites would base on the third mechanisms to reinforce the composite. However, the second mechanism could be effective for chemical treated CNTs.

The dispersion issues of CNTs would affect the stress transfer efficient from CNTs to polymer matrix. As the Van der Waals force of the nanotube lead the nanotubes form agglomerates [10], the agglomeration of the CNTs will occur during CVD-growth nanotubes. It will also reduce the aspect ratio of the reinforcements. The CNTs will have slippage inside the bundles and it will affect stress transfer efficiency. Thus, CNTs need to be dispersed in the matrix so that the composite has uniform properties.

As pointed out by Harris et al. [7], there are two common methods to enhance the dispersion of the CNTs in the polymer. They are physical sonication/blending and chemical functionalization. High power dispersion methods (ultrasound / high-speed stirring) are the simplest dispersion methods. With the addition of surfactants, the dispersion would be enhanced. Many chemicals were used for the sonication of the CNTs while fabricating CNTs composites, such as, chloroform ($CHCl_3$) [39], ethanol [22], N,N-dimethylformamide (DMF) [5, 16], sodium dodecyl sulfate (SDS) [24] and quinoline [41]. Some studies about the dispersion issues of the CNTs were also conducted in the pervious years. Foster et al. [40] have studied four solvents: toluene, chloroform, tetrahydrofuran (THF), and 1-methyl-2-pyrrolidinone (NMP), he found that toluene and chloroform have the relative poor dispersion characteristics when compare with THF and NMP. The SWNT/polymer dispersions in NMP were stable for several months without any noticeable precipitation. However, the thermal and mechanical properties of CNTs composite would be affected by the use of the chemical solvents for sonication as pointed out by Lau et al. [43]. The higher boiling point of the solvent, the easier to have residue of solvent in CNTs composite. Although DMF have been used for sonication in many studies [5, 16], it have relatively high boiling point (130°C). Thus, it is quite inconvenience to evaporate out.

2.2 Functionalization of CNTs

Chemical functionalization of CNTs would be another approach to disperse the CNTs. By functionalizing the CNTs, both the dispersion quality of CNTs and interfacial bonding between CNTs and polymer will be enhanced. The end-caps of the SWNTs can be opened under oxidizing conditions and terminated with the oxygenated functionalities including carboxylic [44-45], carbonyl, and hydroxyl groups [30]. Oxidized nanotubes have better solubility and it can form well-dispersed electrostatically stabilized colloids in water and ethanol [46]. These functional groups are also necessary for providing sites for covalent integration of the SWNTs into organic/inorganic polymer structures to produce nanotube-reinforced composite materials (Fig. 5). Several chemical functionalization methods have been suggested for both SWNTs [44, 47-48] and MWNTs [45, 49-50].

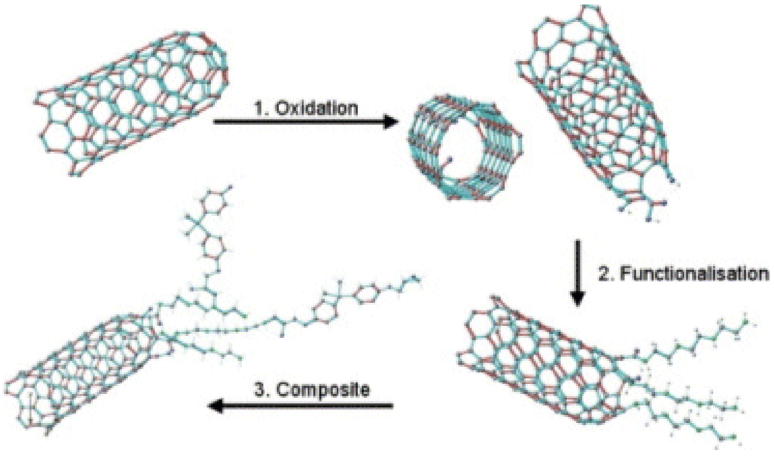

Fig. 5. The procedures for fabricating functionalized CNTs composite

The SWNTs was functionalized by refluxing the mixture of H_2SO_4 and HNO_3 (3:1 in ratio) and subsequent fluorination [46] (Fig. 6). It was found that the CNTs was highly dispersed and well integrated in the epoxy composites. The addition of (R-)oxycarbonyl nitrenes [47] to the sidewall of SWNTs allows for the covalent binding of a variety of different groups such as alkyl chains, aromatic groups, dendrimers, crown ethers, and oligoethylene glycol units. Such additions lead to a considerable increase in the solubility in organic solvents such as 1,1,2,2-tetrachloroethane (TCE), dimethyl sulfoxide (DMSO), and 1,2-dichlorobenzene (ODCB).

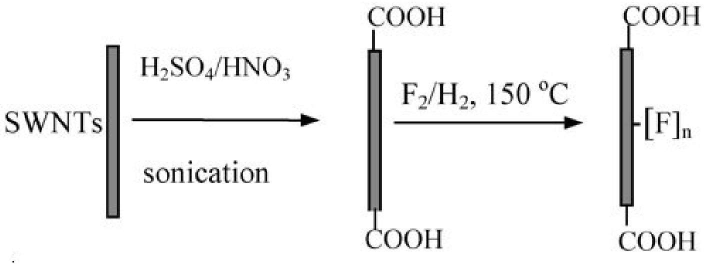

Fig. 6. End-functionalized SWNTs

Velasco Santos et al [49] functionalizated the MWNTs by an oxidation and silanization process in 2002. Different organo-functional groups were attached to the MWNTs, which improves the chemical compatibility of MWNTs with specific polymers for producing the nanotube-based composites.

Functionalization is able to let different functional groups attached to the surface of CNTs. Functionalization can improves the interfacial bonding between CNTs and different polymers for producing new CNTs-based composites. The smooth and non-reactive surface of nanotubes causes a poor load transfer from the polymers to nanotubes. Thus, CNTs are pulled out easily from the matrix and it cannot play the role of reinforcement. Tiano et al [48] studied use of functionalized nanotubes for epoxy composite fabrication. The sidewall surfaces of the nanotubes were functionalized via free-radical polymerization of polymethylmethacrylate (PMMA). The Young's modulus was increased 21% when comparing the unfilled epoxy with only 1 wt% of functionalized nanotubes epoxy. The result was different from the observed decrease of the mechanical properties when using the non-functionalized nanotubes. They showed the functionalization of CNTs able to improve the interfacial bonding between CNTs and the polymer.

2.3 CNTs composites fabrications

Haque et al. [40] noticed that there are large different in Poisson's ratio between the CNTs and polymer, and it generates a resistance from the CNTs to the polymer. They suggested that the Young's modulus of composite would be enhanced even without a very good bonding between CNTs and the matrix materials. Besides the strength of interfacial bonding between CNTs and polymer, the aspect ratio (surface force), CNTs volume fraction, matrix modulus and the orientation of the CNTs would affect the load transfer from CNTs to polymers. Some of the mathematical models [39, 49] about the interfacial bonding have been developed.

It can be classified into three main types of methods for preparing CNT-reinforced polymer composites. Solvents solution mixing [22-24, 65-67], melt mixing [68-70] and in situ polymerization [64-65, 74] are the commonly used methods.

2.3.1 Solvents solution mixing

Solvents solution mixing method is that the CNTs were dispersed with chemical solvent and mixed with the polymer solution. In general, high power agitation is applied into the CNTs/solvent mixture. These agitations are usually provided by magnetic stirring, shear mixing, reflux and ultrasonication [92]. After the dispersion of CNTs into the solvent, polymer will be added in to have further agitation. For the thermoset, resin will be added in before hardener is added. The mixture will then be placed in a mold at room temperature or a heated environment for the evaporation of the solvent. Finally, the CNTs composite is prepared. Very often, per-treatment such as functionalization of CNTs would be carried to enhance both the dispersion and the interfacial bonding between CNTs and polymer chains.

Jin et al [52] fabricated polyhyryoxyaminoether/MWNTs in chloroform with up to 50 wt%. Shaffer et al [53] dissolved polyvinylalcohol (PVA) in water with up to 60 wt% CNTs. This method relies on the dispersion quality of CNTs in the solvent. The choice of solvent would base on the solubility of the polymer [92]. However, CNTs cannot be dispersed effectively in many solvents. Thus, some people used surfactant to enhance the quality of CNTs dispersion. Sodium dodecylsulfate would be one of most common surfactant [52, 53]. The addition of surfactant resulted in very good dispersion with no derogatory effects on film properties [92]. Epoxy would be the most common thermoset for CNT-reinforced polymer composites. Many researchers would like using epoxy due to its easy available and widely used in our daily life.

The first paper studying about CNT/epoxy was done by Ajayan [22] in 1994. They also mentioned about the shear force induced by diamond knife's cutting could align the CNTs in epoxy matrix. The Young's modulus of 5 wt% MWNT/epoxy was improve from 3.1 GPa to 3.71 GPa by Schadler et al [79] in 1998. Most of the studies observed moderate improvement in Young's modulus but with little effect for strength and toughness [54, 55].

2.3.3 Melt mixing

Melt mixing is to use of the softening properties of the thermoplastic to disperse the CNTs in polymer matrix. The advantage of melting mixing would be its simplicity and speed. In addition, melting mixing can be done by common industrial equipments, such as extruder and injection molding machine [40, 56]. Extrusion will also induces high shear mixing force to align CNTs in polymer matrix [57, 58].

Andrew et al. [41] compounded MWNTs with the copolymer of polypropylene and acrylonitrile-butadiene-styrene (ABS) by high shear mixer. Gorga and Cohen [59] extrude polymethlymethacrylate (PMMA) with MWNTs at 130^{o}C by twin screws extruder. However, CNTs tends to stick together and the wall of the mixer for melting mixing. Tetrahydrofurane [60] or other solvents could help to reduce the problem, but it need to take care about the boiling point of the solvent during melting the polymer.

The improvement of Young’s modulus of CNT-reinforced polymer composites by melt mixing was wide in range. Jin et al. observed 130% improvement of Young’s modulus of 17 wt% MWNT/PMMA [61] in 2001, while Potschke et al. [62] observed only a 30% improvement of Young’s modulus with 15 wt% of MWNTs in polycarbonate matrix. However, the effectiveness of CNTs reinforcement was higher with the draw-out of composite fiber. 55% improvement of Young’s modulus was achieved for 1 wt% SWNT/PP which fabricated by Kearns and Shambaugh [63] in 2002.

2.3.3 In situ polymerization

In situ polymerization involves monomer instead of polymer to prepare CNTs composites. CNTs were sonicated in a chemical solution/solvent and process the polymerization reaction with the monomer. It is possible to prepare a composite with high CNTs loading (up to 50 wt %). In situ polymerization can be applied for the preparation for most of the polymer composites containing CNTs. There are two bonding mechanism with the polymer molecules, non-covalently or covalently [92]. Non-covalent is the binding between polymer and CNTs involves physical adsorption and wrapping of polymer molecules through Van der Waals force and π–π interactions. For covalently mechanism, it is mainly talking about the functionalized CNTs grafted with polymer. The grafted CNTs would then involve with the polymerization. This method has been intensively explored due to its effective reinforcement performance.

Velasco-Santos et al. [64] polymerized the PMMA with 1 wt% of MWNTs. The Young’s modulus of this composite was increased from 1.5 to 2.5 GPa. The strength was also increased from 30 MPa to 50 MPa. Putz et al. [65] also studied the SWNT/PMMA, but in extremely low volume fraction of 8×10^{-5}. The increase in Young’s modulus was from 0.3 GPa to 0.38 GPa as measured by DMA. This result was close to the rule of mixtures for long, well-aligned and little defect’s CNTs. However, some literatures pointed out that this study was carried out at 100 rad/s, which is a reasonably high frequency. Time temperature equivalence of mechanical properties for visco-elastic materials suggests that this may be an overestimate as compared to values obtained by pseudo-static measurements [72, 92].

2.4 Alignment methods

With the increased concern of alignment of CNTs, many CNTs alignment methods had been proposed. Generally, “Ex situ” and “In situ” alignment can be classified for CNTs composite. For the “Ex situ” one, the CNTs are aligned in advance, and then compounded with the polymer matrix by in situ polymerization of the monomers. “In situ”, on the other hand, the CNTs are aligned in the polymer.

Magnetic fields and electric fields were the most common methods for ex situ CNTs alignment. Smith et al [13] developed a "buckypaper" (thick film) by deposition from suspension on to a nylon filter membrane. The CNTs lie in the plane of the buckypaper in same alignment, with the addition of magnetic field during filter deposition. Beside magnetic field, electric fields can be used for aligning the CNTs. A low plasma intensity (15 mA/cm^2) [14] was applied when the growth of CNTs. The growth of perpendicular CNTs was carried out when the anode was installed directly above the substrate (electrical field E, normal to substrate, Fig. 7). The electron charged catalytic particles on the growth end of CNTs were forced to move along the E field. The electrical force imparted on the catalytic particle has been proposed as the reason for the aligned growth. This suggested that the existence of a directional electrical field and an abundance of electrons are the main reasons for the aligned growth.

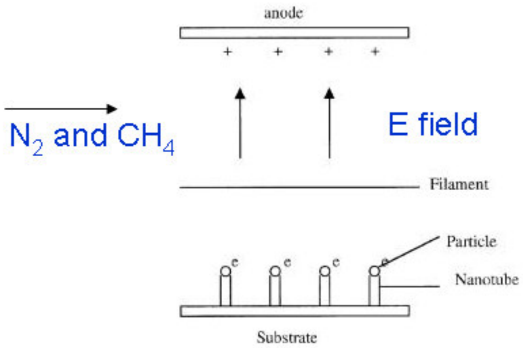

Fig. 7. The growth of aligned CNTs

The method of mechanical stretching can be also used for aligning the CNTs. MWNTs were ground and sonicated in chloroform for 1 hour at room temperature [39], and polyhydroxyaminoether (PHAE) was then dissolved into the nanotube/chloroform suspension. The solution was finally transferred into a Teflon mold and air-dried in a fume hood overnight. Pure PHAE and composite films with nanotube weight fraction up to 50% were made and cut into ~ 5 × 3 mm strips. The strips were mechanically stretched by applying a constant load at 95–100 °C. Under optimum conditions, most composites can be stretched up to 500% (final length L over initial length L_0) without fracture. After the desired stretching ratio was obtained, the sample was first cooled down to room temperature then the load released.

In the electrospinning technique [16] (Fig. 8) polymer nanofibers were produced from an electrostatically driven jet of polymer solution. The polymer solution was prepared similar to many studies before; sonicating CNTs into a solvent and then adding into polymer solution. The discharged polymer solution jet underwent a whipping process wherein the solvent evaporates and the highly stretched polymer fiber deposits on a grounded target. The nanofibers can be fabricated into a variety of forms such as membranes, coatings and films.

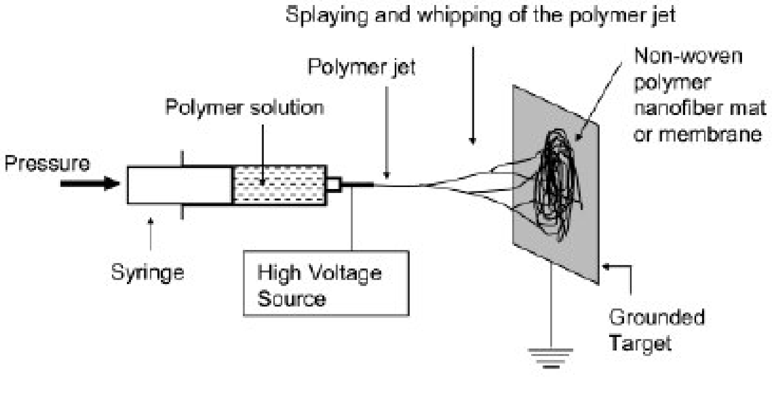

Fig. 8. Schematic representation of the electrospinning or electrospraying apparatus

Haggenmueller et al [5], studied two methods to prepare nanocomposite films. Method 1: 10 wt% of Poly(methyl methacrylate) (PMMA) was dissolved in DMF, and then dispersed SWNTs was added into this solution and sonicated for 3 hours. The mixtures were dried at 20°C in Teflon dishes. Method 2: The composite films from Method 1 were folded and broken into small pieces. The films then stacked between two metal plates. 3000lb load was applied on the stack at 180°C for 3 minutes. The 50–100 μm thick films were formed and then these films were broken again into small pieces, the stacking procedures repeated, and hot pressed again. This melt mixing procedure was repeated 25 times. The films were dried under vacuum at 180°C for 20 hour again. Finally, the films were mixed five more times at 180°C and 3000 lb for 3 minutes. The polymer fiber was then extruded by air-cooled melt spinning apparatus.

2.5 UV irradiation on CNTs composite

There are only a very limited number of scientific studies [17 - 19] focusing on UV effect for CNT/polymer composites. Najafi [17] found that the radiation of UVC (λ =254nm) on MWNTs would oxidize the surface of the nanotubes. It would be an indication that UVC may improve the interfacial interaction of CNTs and polymer matrix. He also observed that the addition of CNTs had a reinforcement effect against the degradation by UV irradiations [19]. Beside the studies of UV effect on CNTs composite showed positive results, UV/ozone treaded graphite nano-platelet (GNP)/epoxy also showed the improved interfacial interaction between GNP and epoxy [20].

For summary, the research of CNTs composite is just in beginning stage. There are many ways to produce CNT-reinforced polymer composites. Although many studies were conducted to show the possibility to improve the performance of the polymer, some of the results were contradictory [40] and lack of coherent. Thus, more understanding of CNTs composite is required. The main issues of the CNT-reinforced polymer composites would be focused on the dispersion problem and load transfer properties. The following study would focus on the functionalization of CNTs to improve the dispersion quality and the interfacial interaction between CNTs and polymer chains.

Chapter 3 Experimental Arrangement

3.1 Equipments

3.1.1 Chemical apparatus

In order to functionalize the CNTs, a series of chemical reaction were carried out. These chemical processes include acid and heat purification, reflux oxidation and filtration. The main purpose of these series processes is to purify the CNTs and to add the COOH functional group on the CNTs surface. Here are the required apparatus for the chemical reaction:

Reflux oxidation: electrical heater, metal stand, conical flask, tubing and condenser.

Filtration: filter flask, Buchner funnel, tubing and 0.2 μm millipore filter membrane.

Fig. 9. Reflux setup inside fume cupboard

3.1.2 Extrusion

Hakke MiniLab twin-screw micro extruder (Germany) (Fig. 10) was used to disperse the nanotubes into the PP pellets. The dry mixture of PP pellets and nanotubes were compounded inside the extrusion chamber for 15 minutes in co-rotating mode at 100 rpm and 177^{o}C. The blended materials were extrude and transferred into the barrel of Thermo Hakke small-scale injection molding machine (Germany) (Fig. 11). The temperature of barrel of injection molding machine was keep at 177^{o}C. The blended materials were injected into a dumbbell shaped mold (mold temperature: 50^{o}C)

Fig. 10. Hakke MiniLab twin-screw micro extruder

Fig. 11. Thermo Hakke small scale injection molding machine and mold

3.1.3 UV lamp chamber

In order to study the effect on the composite sample after UV exposure, UV irradiation was conducted under ambient condition in a UV lamp chamber (40 cm × 40 cm × 13.5 cm) which had a layer of reflective aluminum foil inside to ensure all the sample would have an even exposure to UV. The temperature during UV irradiation was maintained at around 25 °C. The neat PP and fMWNT/PP composite samples were irradiated under a 25 W ultraviolet lamp (Sylvania, Japan) for 72 hours. The primary wavelength of the lamp was 254 nm. Fig. 12 showed the spectral energy distribution of the lamp.

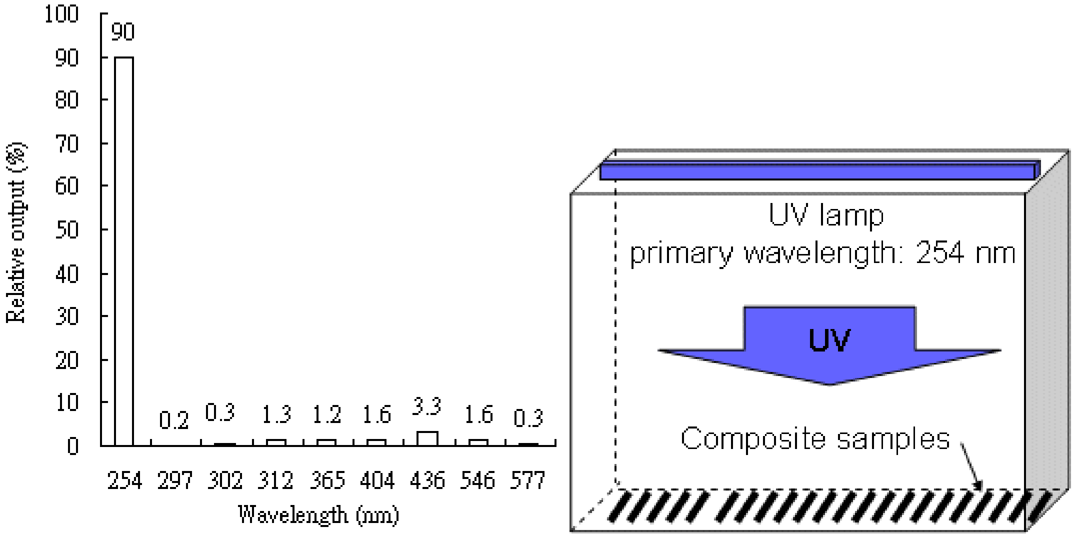

Fig. 12. The spectral energy distribution of the UV lamp and the set- up of the UV chamber.

3.1.4 Tensile tester

50kN MTS Alliance RT/50 tensile machine was used in the experiment. Young's modulus, tensile strength and the tensile strain was calculated after the tensile test. The tensile facture surface will be useful for the scanning electron microscope (SEM) observation. The loading speed of the cross head was 1 mm/minute. Moreover, the strain value was measured by an extensometer (MTS 632 24f-50) with 25mm gauge length.

Fig. 13. 50kN MTS Alliance RT/50 tensile machine and extensometer

3.1.5 Micro-hardness tester

The hardness of all nanotube composites was measured using Future-tech FM series micro-hardness tester. The unit and magnitude of the hardness are defined by Vickers hardness (Hv). The value was determined by measuring the average diagonal length, d (mm), of the indentation mark on the sample surface.

$$H_v = \frac{8F\sin(\theta/2)}{[(d_1+d_2)/2]^2} \tag{2}$$

where θ, d_1, d_2 and F are the face angle of a pyramidal diamond indenter (136°), two diagonal lengths and loading force (N), respectively. Fig. 14, showed the micro hardness tester and an indentation mark on a sample surface that observed by an optical microscope.

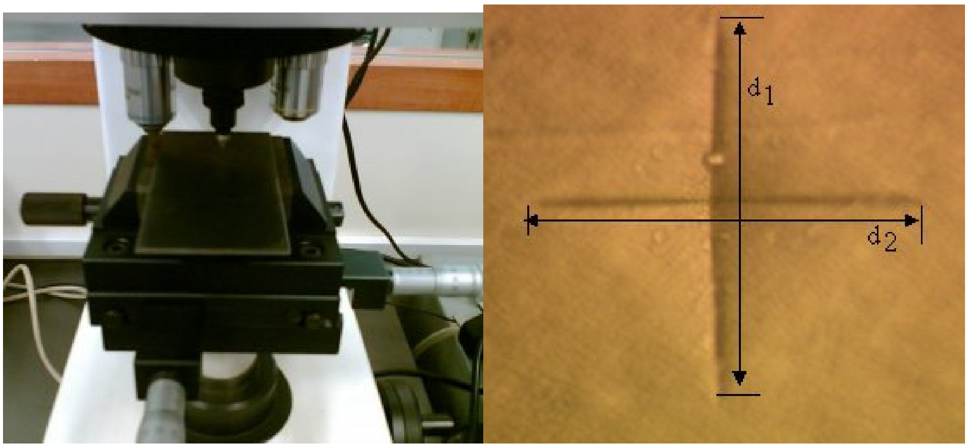

Fig. 14. Future-tech FM series micro-hardness testing machine and indention mark

3.1.6 Thermogravimetric analyzer (TGA)

The thermogravimetric (TG) curve and differential thermogravimetric (DTG) curve of the composites sample were determined by Setaram Labsys TG-DTA/DSC system. Thermogravimetric analysis is a type of testing that performed on samples to determine changes in weight in relation to change in temperature. It relies on a high degree of precision in three measurements: weight, temperature and temperature change. TGA is able to determine characteristics of materials such as polymers, to determine degradation temperatures, absorbed moisture content of materials.

Fig. 15. Setaram Labsys TG-DTA/DSC system and crucible

3.1.7 Differential Scanning Calorimetry (DSC)

The Differential Scanning Calorimeter (DSC) is a thermal analysis instrument that determines the temperature and heat flow associated with material transitions as a function of time and temperature. Power compensated calorimeter (Perkin-Elmer DSC7, Fig. 16) was used for the DSC test. In power compensated calorimeter, the sample and reference pan were in separate furnaces heated by separate heaters. Both the sample and reference were maintained at the same temperature and the difference in thermal power required to maintain them at the same temperature was measured and plotted as a function of temperature or time. Around 5 mg of composite samples were chopped into small pieces and placed into the heating pans. The pans were heated from 25°C to 200°C at a rate of 10°C/minute to evaluate the melting temperature of the composite samples.

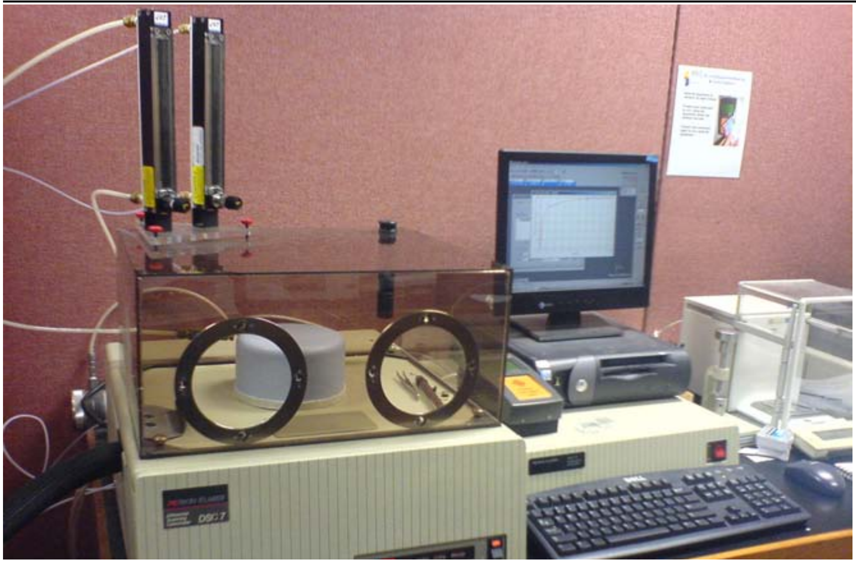

Fig. 16. Perkin-Elmer DSC7

3.1.8 Scanning Electron Microscope (SEM)

Scanning Electron Microscope (SEM) was used to investigate the failure mechanism of the composites after tensile test. SEM would also be used to observe whether the pull out of CNTs were happened or not. A beam of electrons is produced at the top of the SEM by heating of a tungsten filament. The electron beam follows a vertical path through the column of SEM. It makes its way through electromagnetic lenses which focus and direct the beam down towards the sample. Once it hits the sample, backscattered or secondary electrons are ejected from the sample. Detectors collected the ejected electrons, and converted them into a signal to form image. The SEM specimens are required to be conductive. The nonconductive specimen will build up negative charge on its surface and will deflect the incident electron beam and ruin the image. Thus, the nonconductive specimens should be coated with a conductive layer such as Au, Pt or carbon.

Fig. 17. Leica Stereoscan 440 scanning electron microscope and samples

3.2 Experimental works

3.2.1 Sources of CNTs

The sources of CNTs that used in the experiments:

1. SWNTs (arc-SWNTs) produced by hydrogen arc discharge method [75] from Institute of Metal Research, Chinese Academy of Sciences, Shenyang, China
2. SWNTs (CVD-SWNTs) produced by chemical vapor deposition method (CVD) from Shenzhen Nanotech Port Company Limited, Shenzhen, China
3. MWNTs (CVD-MWNTs) produced by chemical vapor deposition method (CVD) from Shenzhen Nanotech Port Company Limited, Shenzhen, China

	SWNTs labeled	MWNTs labeled
External Diameter	<2 nm	<10 nm
Contents of CNTs	SWNTs：50% MWNTs：40%	MWNTs≥95 %
Amorphous Carbon	＜5 %	＜2 %
Ash	≤2 wt%	≤0.2 wt%
Length	5～15μm	
Special Surface Area	450~600 m^2/g	40～300 m^2/g
Electric Conductivity		$10x10^{-4}$ s/cm
Thermal Conductivity		2800W/m•K
Ablating Temperature	520~610^{o}C（in air）	

Table 1. Specification of CVD-CNTs from Shenzhen Nanotech Port [88]

3.2.2 Sources of Polymer

In order to have a comprehensive study of CNT-reinforced polymer composites, both thermoset and thermoplastic were used for fabricating CNT-reinforced polymer composites. Epoxy was used to fabricate CNTs/thermoset composite in Chapter 4's study. Commercially available Araldite GY 251 epoxy resin DGEBA (diglycidyl ether of bisphenol A, Scheme 1) was used with Ciba HY 956 ethane-1,2-diamine hardener (Scheme 1). Polypropylene (PP, Scheme 2) was used to fabricate CNTs/thermoplastic composite in Chapter 5 & 6's studies.

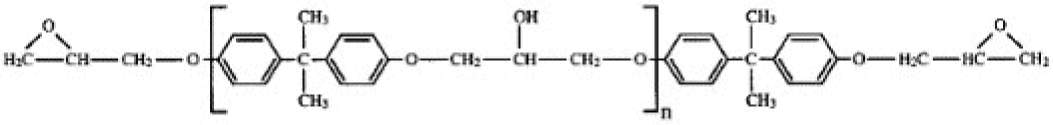

Chemical structure of epoxy resin

$H_2N\text{-}CH_2\text{-}CH_2\text{-}NH_2$

Chemical structure of hardener

Scheme 1. Chemical structure of epoxy resin and hardener

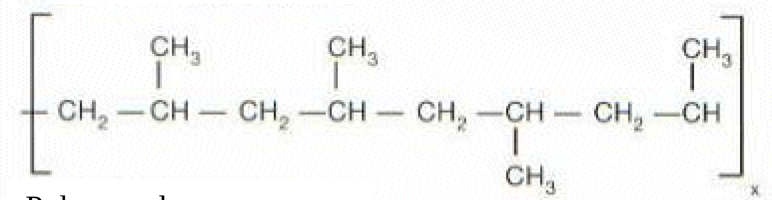

Polypropylene

Scheme 2. Chemical structure of polypropylene

3.2.3 Purification

3.2.3.1 arc-SWNTs

In order to minimize the effect of the impurity during the fabrication process of the composite material, purification of the raw material should be done. According to the specification of the arc-SWNTs from Institute of Metal Research, there were no any treatments after the production. Thus, it was needed to do the purification of the nanotubes. The purification procedure was followed as mentioned by Hou & Liu et al. [76, 77]. Thermogravimetric analysis (TGA) was performed to understand the composition of the raw nanotubes before and after the purification.

The as-prepared arc-SWNTs were first weighted, and acetone was then added into the SWNTs. The mixture was sonicated for 1 hour in room temperature. An electrical heater was used to evaporate the acetone at 55^{o}C. The SWNTs were then put into a ceramic crucible and oxidized in an electrical oven at 550^{o}C for 40 minutes. The SWNTs were cooled down at room temperature. 37wt% of HCl was added into the SWNTs and soaked for 12 hours. SWNTs were filtered and washed by de-ionized water. SWNTs were dried at 98^{o}C and the purified SWNTs were obtained.

Setaram Labsys TG-DTA/DSC system was used for TGA. The samples were heated from 25 ^{o}C to 1100 ^{o}C at a rate of 10^{o}C/minute in air. About 4mg of arc-SWNTs were tested. From the TGA result, there were some amorphous carbon and carbon nano-particles. The result can be reflected by the TGA graph between 300 ^{o}C to 600 ^{o}C. The circled area in Fig. 18 represents the oxidized amorphous carbon in the sample. There were about 56% of impurities left in the crucible after heating to 1100^{o}C. After the purification, only about 7% (Fig. 19) of impurities left. It was expected that, the purity could be increase by repeating the purification procedures that mentioned before.

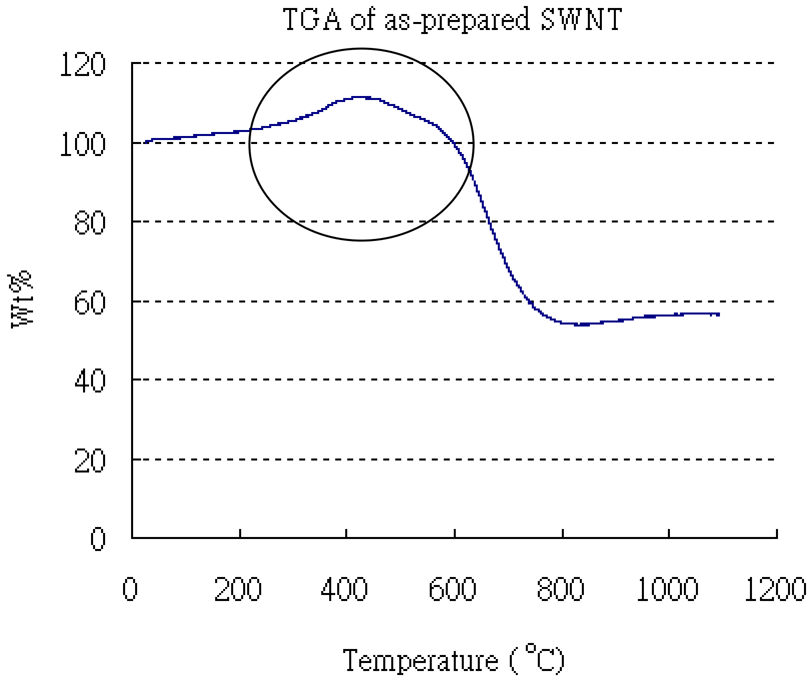

Fig. 18. TGA curve of arc-SWNTs

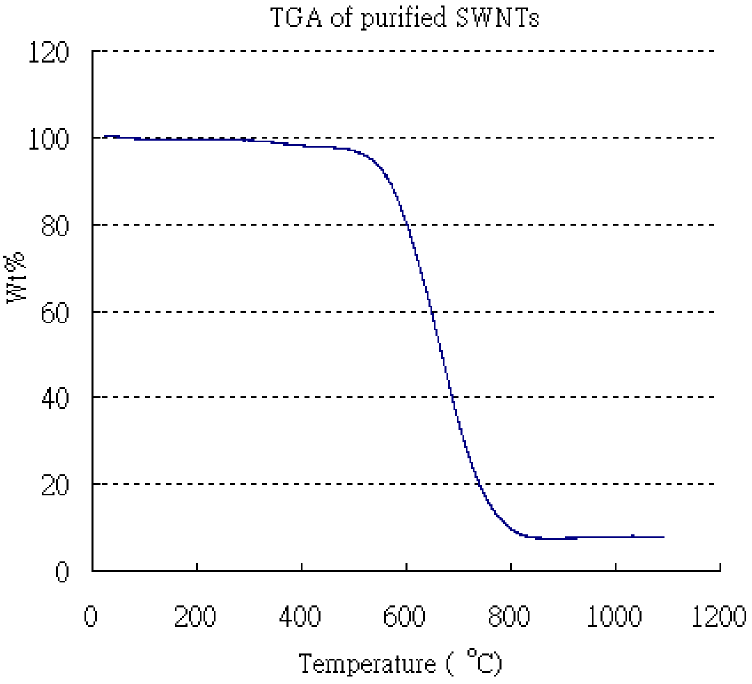

Fig. 19. TGA curve of purified arc-SWNTs

Result of purification

Impurities of SWNTs before purification: ~56%

Impurities of SWNTs after purification: ~7%

3.2.3.2 CVD-SWNTs

The specification of CVD-SWNTs from Shenzhen Nanotech Port was shown in Table 1. The SEM image of CVD-SWNTs was shown in Fig. 20. Form Fig 21, it could be seen that the purity of CVD SWNTs were much purer than the as-prepared arc-discharge SWNTs, which showed agreement with the literatures [27]. Thus, there was no need to conduct further complex purification since the acid treatments during fictionalization was proved effective to remove the metal catalyst.

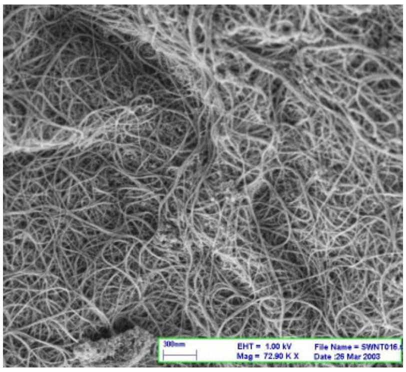

Fig. 20. SEM image of CVD-SWNTs

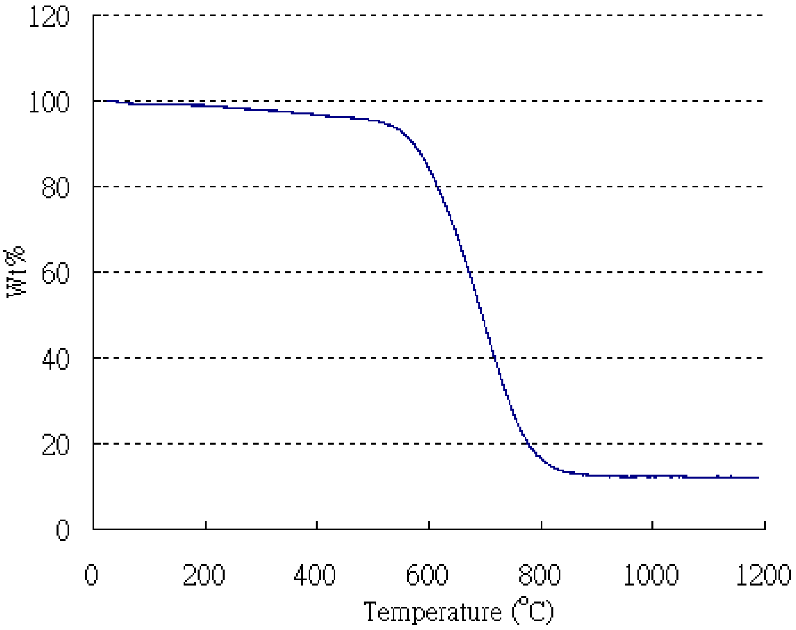

Fig. 21. TGA curve of as-received CVD-SWNTs

3.2.4 Functionalization of CNTs

Since the CNTs are insoluble in organic solvent, functionalization of CNTs would help solve the problem of dispersion. There are two reasons for functionalizing the CNTs. Firstly, it improves the dispersion / solubility of CNTs in chemical solvents: secondly it improves the interfacial bonding between the CNTs and polymer matrix. With the help of functionalization of CNTs, the time of sonication is reduced. Smalley reported that [78], the end caps of CNTs were opened and terminated with carboxylic acid groups, which allowed covalent linkages of polymers with the CNTs. Two methods (reflux and sonication) for functionalizing CNTs were carried out.

3.2.4.1 Reflux functionalization

Fig. 22 was shown the experimental set-up for the reflux finctionalization of CNTs. The purified CNTs were refluxed with a 3:1 mixture of concentrated H_2SO_4/HNO_3 (98%, and 70% respectively) for 3 hours at 120°C to add the COOH groups on the tube body. After the mixture was cooled down, the solution was washed with water and a NaOH solution [44] to get a neutral solution. The mixture was then diluted by large amount of de-ionized water (Fig. 23). The acid-treated nanotubes were collected by filtration by using double layer of 0.2 μm millipore membrane (Tianjin Tengda Filter Equipment Plant). It was noted that the reflux could not be conducted for too long time, otherwise; the nanotube would be cut into smaller pieces in scale, and it was difficult to collect after dilution by using millipore membrane.

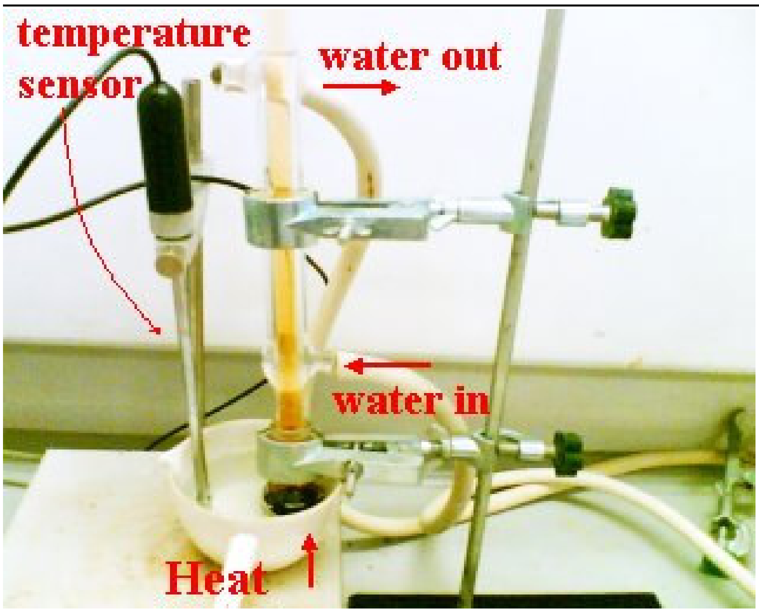

Fig. 22. The set-up of reflux system

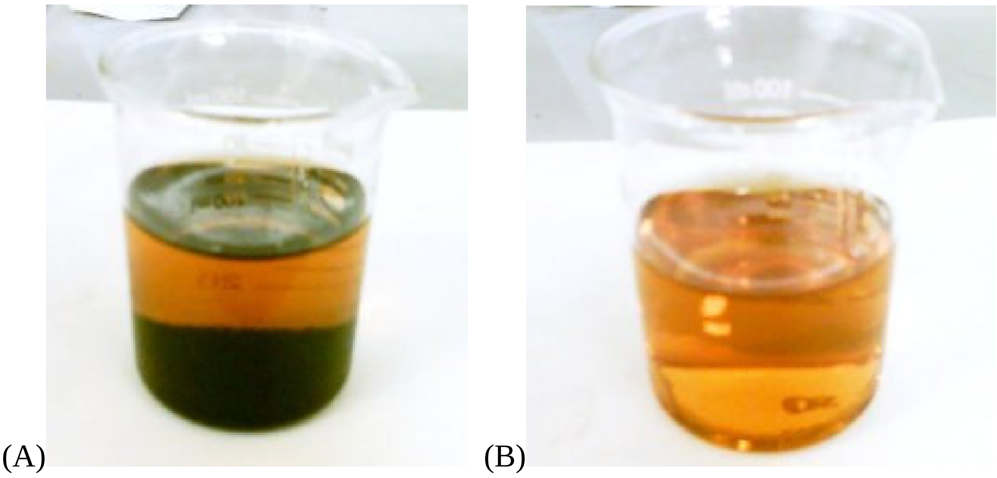
(A) (B)

Fig. 23. (A) SWNT mixture after dilution, (B) the filtered solution

During the process of reflux functionalization, an interesting phenomenon was observed. That was, the solution turned into dull black in color (Fig. 24) after several dilutions. After investigating and discussing with chemical professional, it was believed that a chemical equilibrium was happening inside the solution. Equation 3 helps explain this phenomenon as follows.

Fig. 24. Black solution of SWNT

$$\text{CNT-COOH}_{(s)} \leftrightarrow \text{CNT-COO}^{-}_{(aq)} + \text{H}^{+}_{(aq)} \quad (3)$$

The CNT-COO$^{-}_{(aq)}$ and H$^{+}_{(aq)}$ ions will keep in a constant molarity/concentration on the right hand side of the equation. If the acidity decreases, meaning that the molarity/concentration of H^{+} decreases, then more CNT-COOH$_{(s)}$ will change into the ionic form in order to attain equilibrium. As a result, the functionalized SWNTs are unable to be collected by filtration. Thus, this method is not preferred.

3.2.4.2 Sonication functionalization

According to the literature, sonication can also provide the functionalization effect of CNTs [78]. The purified CNTs were suspended into a 3:1 mixture of concentrated H_2SO_4/HNO_3 (98%, and 70% respectively) in a sonicated water bath for 3 hours to add the COOH groups on the tube body. HCl was added to ensure that the cut nanotube pieces were themselves molecularly perfect and chemically clean. Finally, the solution was washed with water and a NaOH solution [44] to get a neutral solution. The acid-treated nanotubes were collected by filtration by using double layer of 0.2 μm millipore membrane.

After several dilutions, it was found that using acetone to assist the washout of the acid would have better performance. In Fig. 25, the acetone assisted dilution got deep brown color when compared with the ethanol mixture. It suggested that acid mixture dissolved in acetone was easier.

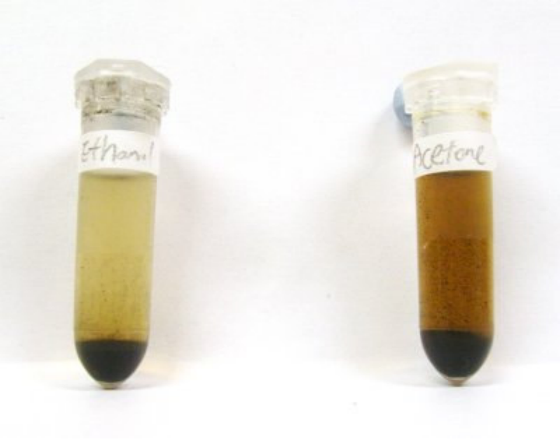

Fig. 25. Dilution of CNTs/acid mixture by ethanol (left), and acetone (right)

The method that Smalley mentioned was adopted to produce CNTs with COOH group (Fig. 26). The acid-treated nanotubes were then used for the fabrication of CNTs composite. Since the CNTs were tube-end modified, the load transfer property of CNTs composite was needed to go through a mechanical test to have a further in-depth study. As the novel mechanical property of CNTs is governed by tube body, removing the tube cap does not greatly affect the tube structure [30].

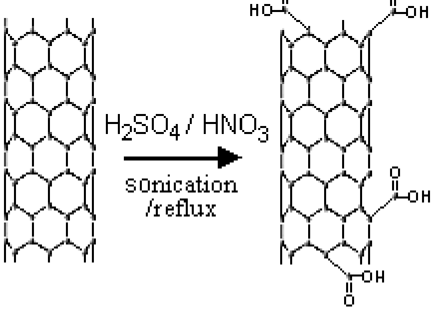

Fig. 26. Oxidized functionalization with COOH on SWNT

A further functionalization of CNTs could be conducted if the effect of adding COOH group was not satisfied. Besides functionalizing the end cap of the tube, it might be necessary to functionalize the sidewall of the tubes if needed.

3.2.5 Dispersion of CNTs

Sonication is a method of blending CNTs with chemical solvent and surfactant, followed by the addition of the well-dispersed CNTs solution to the polymer solution which undergo sonication aftwerwards. By combining high power dispersion methods, such as ultrasound and high speed shearing, with organic solvents, such as acetone, ethanol, toluene, chloroform, tetrahydrofuran, dimethylformamide (DMF) and sodium dodecyl sulfate (SDS), the performance of dispersion will be enhanced [80].

However, the use of the solvent directly affects the properties of polymer. Prudent decision on which solvents to be used was necessary. As mentioned by Lau et al [43], although the solvent effect of SWNTs were in the order of DMF>ethanol>acetone, the mechanical properties of the SWNT/epoxy composite were in the reverse order. Thus, acetone was used as the solvent during fabrication process of the composite to minimize the effect of residue solvent. Cole Parmer 8890 sonicator (42 kHz) was used to sonicate the SWNTs / fSWNTs with acetone for 1 hour. This sonication process was to disperse CNTs into the solvent so that it would be easier to disperse the CNTs into the polymer matrix during further mixing.

Chapter 4 CNT/Thermoset Composite

As mentioned before, due to the outstanding mechanical properties of the CNTs, CNTs related metallic and polymer-based composites has been becoming an interesting and fast growing research subject [7]. Principally, a CNT is small enough to inhibit nano and micro cracks inside composites. As mentioned in Chapter 2 Literature Reviews, the nanotube was found to be able to bridge up microvoids (microcrack) in the matrix and presumably enhance the strength of the composites [39]. In this chapter, the role of functionalization for CNTs was studied using mechanical and thermal analysis. The chemical processes for functionalizing the CNTs were kept as simple as possible in order to meet the requirement for future industry application. It is the first step of this project, the experiments of later chapter will base on the result of this chapter.

In general, there are three main mechanisms of load transfer from a matrix to filler, the first one is micromechanical interlocking between the fiber and matrix; but it is not applicable for nanotube composites due to the atomically smooth surface of the CNTs. The second mechanism is the chemical bonding between the nanotubes and the matrix. The third mechanism is a weak Van der Waals interaction between the fiber and the matrix. An improved matrix/nanotube interaction can be achieved via an equivalent bonding between the functional groups on the nanotube surfaces and the polymer.

In order to study the effect of the addition of CNTs into the polymer matrix, both the pure polymer and CNTs polymer composite were fabricated. This was the pilot experiment to study the effect of functionalization of CNTs. Thus, the research should start with the best condition. SWNTs and epoxy were the suitable candidates for fabricating the CNTs composite to investigate the effect of functionalization of CNTs, since SWNTs have better mechanical properties than MWNTs and epoxy is suitable for using solution mixing, which is the best method to fabricate CNTs composite that mentioned in Chapter 2.

After the fabrication of the composite samples, the global mechanical properties of the composite were characterized. Tensile test was conducted to obtain the global mechanical properties of the composite. The failure part was further studied by SEM image. Tensile property test and micro-hardness test were carried out to examine the mechanical properties of the composites. Thermogravimetry Analysis (TGA) and Differential Scanning Calorimetry (DSC) were used to evaluate the thermal properties of the composites. SEM was also used to investigate the failure mechanism of the composites after tensile test. SEM was used to observe whether or not the pulling-out effect of CNTs took place..

4.1 Fabrication of CNTs composite

Pure epoxy, SWNT/epoxy and functionalized SWNT/epoxy (fSWNT/epoxy) composites were fabricated separately. The SWNT and fSWNT were sonicated in acetone for 1 hour. The first sonication was attempted to disperse the CNTs into the solvent so that the dispersion of the CNTs into the polymer matrix would be more easily during mixing. Then, each mixture was added into epoxy resin (Araldite GY 251) for further sonication of 2 hours. During sonication, the resin mixture was heated to reduce the viscosity of the mixture to improve dispersion of nanotubes, and to allow the evaporation of the acetone. The heating procedure was important to the fabrication process of composite because heating would reduce the viscosity of the polymer matrix. Less viscous mixture allowed the CNTs to penetrate into the polymer matrix chain and allowed a better dispersion. The mixture was then placed into a vacuum chamber for 12 hours for degassing. The mixture was kept until a constant weight was attained to ensure all the solvent was evaporated. Hardener (HY 956) was added into the mixture at a resin-to-hardener weight ratio of 5:1. After a long steady state and stirring with hardener, the CNTs would agglomerate again. Thus further sonication was needed. Another 1 hour of sonication was undergone to allow the nanotubes to distribute in the epoxy matrix uniformly. All composites were cured in a silicon rubber mould at room temperature for 48 hours.

4.2 Tensile test

The dimensions of the samples were 85mm x 6.45mm x 2mm. The tensile properties of the composites were determined by a 50kN MTS Alliance RT/50 tensile machine. The loading speed of the cross head was 1 mm/minute. Fig. 27 was shown the composite specimens after tensile test. In Fig. 28 - Fig. 30, the stress-strain curves of the samples were plotted. The fabrication process of the samples was same as the procedure that mentioned in Section 4.1. Epoxy is a type of thermoset polymer, its highly cross-linked polymer chains form a 3D network structure, Owing to its 3D network structure, the chains cannot slide and rotate easily, which results in high strength, stiffness and hardness. It was expected that adding the CNTs could enhance the mechanical properties of the composites due to the interlocking between the CNTs and 3D networks. Neat epoxy, 1wt% of non-functionalized SWNT/epoxy (SWNT/epoxy) and 1wt% of COOH functionalized SWNT/epoxy (fSWNT/epoxy) composites were tested and plotted in the following curves.

Fig. 27. Composite specimens after tensile test

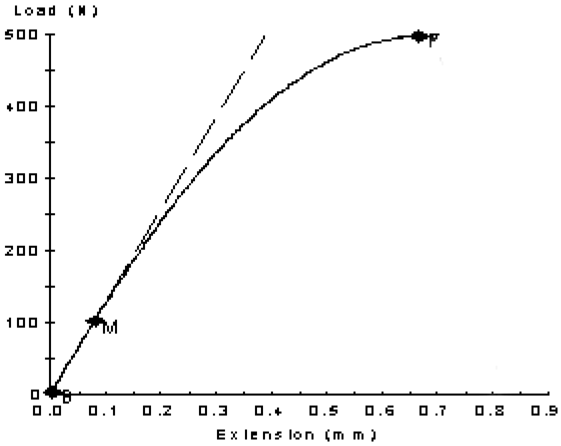

Fig. 28. Tensile curve of neat epoxy

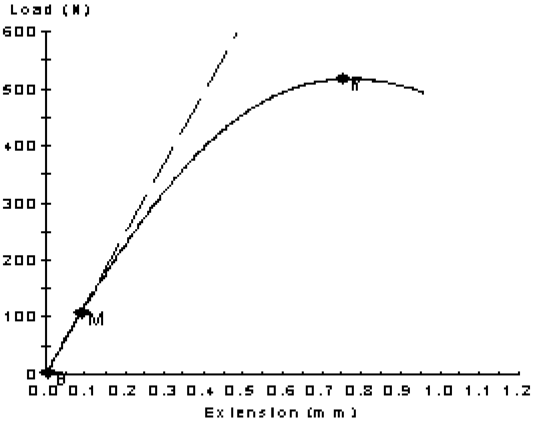

Fig. 29. Tensile curve of SWNT/epoxy

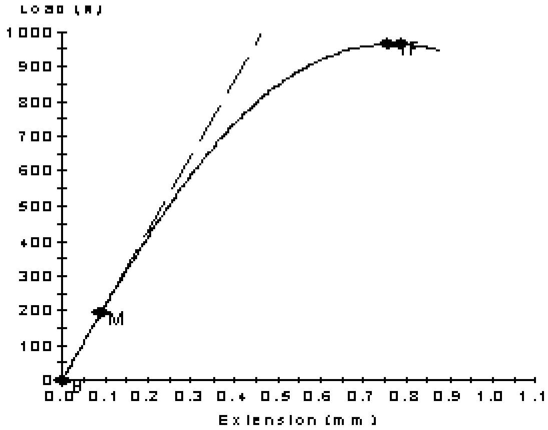

Fig. 30. Tensile curve of fSWNT/epoxy

The mechanical properties were summarized in Table 2. It was found that there was a reinforcement effect by using SWNTs. However, it was seen that the effect was very limited. On the other hand, there was an observable and significant improvement by using fSWNTs as the reinforcement filler to the polymer matrix. The direct comparison of the tensile performance of different samples was shown in Fig. 31.

	Epoxy	SWNT/ epoxy	fSWNT/epoxy
Peak Stress (MPa)	36.1±0.84	39.6±0.92	50.9±1.12
Improvement of Peak Stress	-	9.7%	41%
Modulus (GPa)	2.33±0.09	2.35±0.09	2.85±0.11
Improvement of Modulus	-	1.1%	21.3%

Table 2. Tensile test results of different specimens

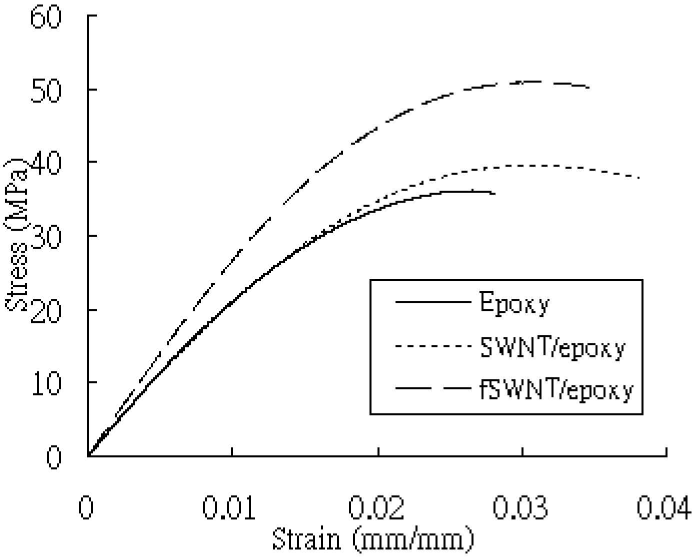

Fig. 31. Stress strain curves of epoxy and different nanotube composites

The Young's modulus of the epoxy, SWNT/epoxy and fSWNT/epoxy were 2.33 GPa, 2.35 GPa, 2.85 GPa respectively. The Young's moduli of both SWNT/epoxy composites were higher than that of neat epoxy. It showed that the reinforcement of the fSWNT was much better than the non-functionalized SWNT. The Young's modulus of fSWNT/epoxy was 21.3% higher than SWNT/epoxy. For the fSWNT/epoxy, about 41% improvement in tensile strength, from 36.1 MPa (pure epoxy) to 50.9 MPa, was achieved. On the contrary, the tensile strength of SWNT/epoxy was only improved by 9.7%.

The strength of the composites depends on the load transfer efficiency between the CNTs and the epoxy. The surface of the nanotube filler is the main factor that affects mechanical properties of the composite. The nature of the smooth tube body of CNTs makes it difficult to form bonding with epoxy. The non-functionalized SWNT has relatively smooth surface when compared with the fSWNTs, thus resulting in a poor interfacial strength between them. As a result, the SWNTs can only provide a limited interlocking with the 3D polymer chain networks. On the other hand, the fSWNTs provide sites to form chemical linkage with the polymer chains which play a vital role in the reinforcement.

A SEM observation was needed to examine the tensile fractured surface of the composite to explain the reinforcement mechanism of nanotubes. The details of the role of CNTs in the polymer matrix would be discussed in the Section of 4.5 Differential Scanning Calorimetry (DSC) and 4.7 Theoretical Study.

4.3 Microhardness test

The Vickers hardness (Hv) of the composites was measured by a microhardness testing machine (Future-tech FM series). The Microhardness test method according to ASTM E-384 specifies a range of loads using a diamond indenter to make an indentation that is measured and converted to a hardness value (equation 2 of Section 3.3). A square base pyramid was then used to shape diamond for testing in a Vickers tester subsequently.

Each specimen was measured five times at random locations respectively. The average value of tests was recorded as the hardness value. 100-gram force and 15 seconds of dwell time were used in indentation. All the specimens were polished before indentation. In Table 3, the hardness values of the different composites were shown. It showed that the result of the hardness test was consistent with the result of tensile test. The hardness of the composite was greatly improved for fSWNT/epoxy when compared with SWNT/epoxy. It was possible that the functionalized sites of fSWNTs were able to form cross-linkage with the thermoset matrix and therefore enhanced the hardness of the polymer. In addition, the standard deviation in the hardness values of all three samples were within 5%, it indicated that the dispersion of CNTs in the composites were uniform. The hardness of the polymer depends on the following factors: (i) the number of cross-linkage, (ii) the molecular weight of the polymer, and (iii) the degree of crystallinity. In the case of epoxy, factor (i) would be the dominant factor that affects the hardness value. From the hardness test result, fSWNTs performed a better reinforcement role. The functionalized sites of fSWNTs were possible to enhance cross-linkage, which also meant better interfacial bonding with the epoxy polymer chains, thereby enhancing the hardness of the polymer.

	Vicker hardness (Hv)	Improvement when comparing with epoxy
Epoxy	9.28±0.41	N/A
SWNT/epoxy	9.6±0.46	3.45%
fSWNT/epoxy	11.44±0.55	23.28%

Table 3. Hardness of epoxy, SWNT/epoxy and fSWNT/epoxy

4.4 Thermogravimetry Analysis (TGA)

TGA is a popular technique for the evaluation of the thermal decomposition kinetics of materials. The simultaneous TG/DTA system can be used for such applications as oxidation, heat resistance, amount of water, compositional analysis and the measurement of ash content in a sample. The thermal stability of the composites can be illustrated by thermogravimetric analysis (TGA). Setaram Labsys TG-DTA/DSC system was used for TGA. The samples were heated from 100 ^{o}C to 700 ^{o}C at a rate of 10 ^{o}C/minute with the flow of air (about 40cc/min).

Fig. 32 - Fig. 34 showed the TG-DTG curves of pure epoxy, SWNT/epoxy and fSWNT/epoxy respectively. Overall speaking, all three curves exhibited similar weight loss profile. It has been known that CNTs have extremely high thermal conductivity [71, 72]. The improvement of interfacial interaction between CNTs and the polymer matrix may raised the overall thermal conductivity of the composite, and thus enhanced its thermal stability. According to Chen et. al. [83], the more uniform the dispersion of CNTs, the higher thermal conductivity of the composite, and in turn the higher thermal stability.

For the pure epoxy (Fig. 32) (during 100 ^{o}C to 300 ^{o}C) in the TG-DTG curves, it could be seen that the curves are dropping. It was due to the volatiles of water and possibly residual solvents. In fact, all the three samples had similar behavior. There were two observable rapid dropping zones in 320 °C - 400 °C and 500 °C - 600 °C in TG curve. Its derivative curve (i.e. DTG curve), showed a sharper peak, which was due to the thermal decomposition of the epoxy.

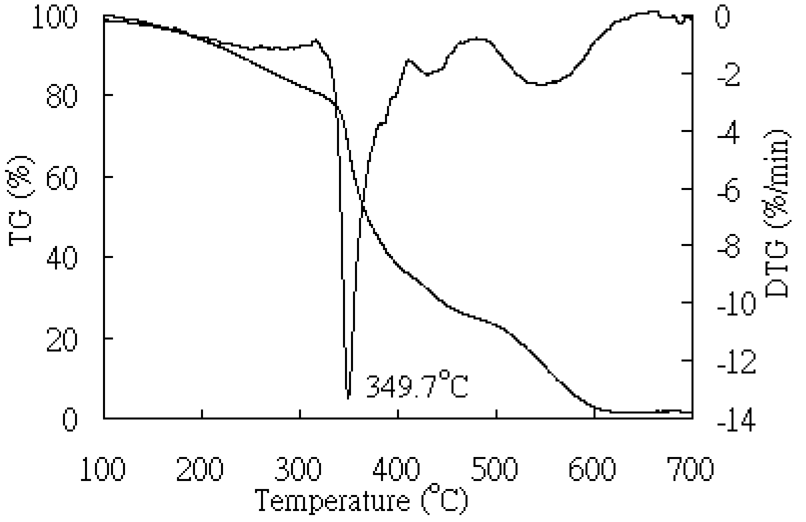

Fig. 32. TG-DTG curves of epoxy

During the first thermal decomposition, epoxy was oxidized into carbonaceous residue. Thus, the second thermal decomposition was described by an oxidative degradation mechanism of carbonaceous residue, which was more possible at slow heating scans [84].

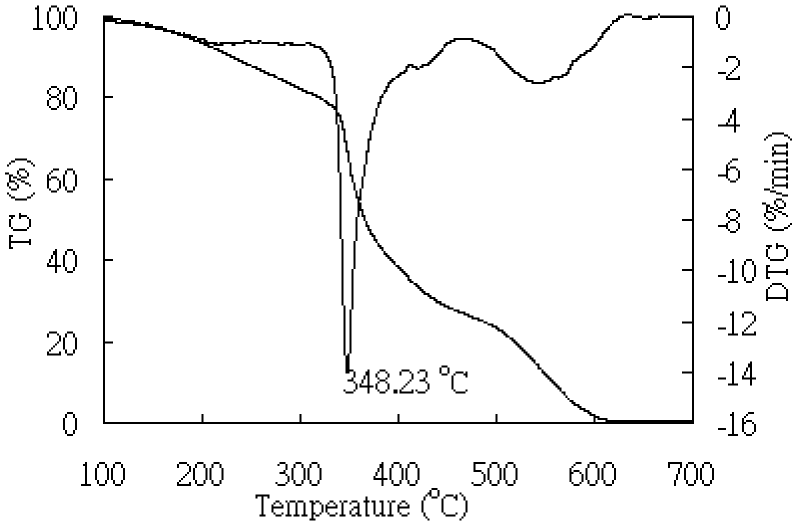

Fig. 33. TG-DTG curves of SWNT/epoxy

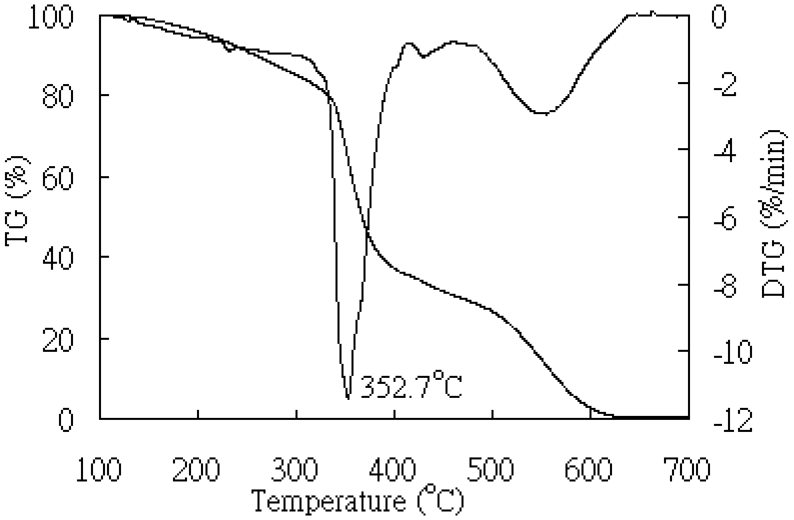

Fig. 34. TG-DTG curves of fSWNT/epoxy

According to the TGA results, the thermal decomposition temperature of the fSWNT/epoxy was 352.7 °C, which was higher than the pure epoxy's thermal decomposition temperature (349.7 °C). On the other hand, the thermal decomposition temperature of the SWNT/epoxy was 348.2 °C, which was lower than the pure epoxy's thermal decomposition temperature. This result was useful to illustrate the chemical bonding formed between SWNTs and polymer chains. In the case of non-functionalized SWNTs, SWNTs could not enhance the thermal stability of the composite, meaning that there was no chemical bonding between SWNTs and epoxy polymer chains. However, for the case of fSWNTs, results showed that the thermal stability of the composite was improved by the addition of 1 wt% fSWNTs. The improved thermal stability implied that chemical bonds were formed between fSWNTs and polymer chains.

4.5 Differential Scanning Calorimetry (DSC)

To further illustrate the thermal properties of the composites, differential scanning calorimetry (DSC) was conducted. DSC curves provide information of the endothermic or exothermic reaction and glass transition temperature (Tg) of the tested sample. Tg depends strongly on the interactions between polymer chains. Through the DSC analysis, the effect of CNTs on the polymer chains could be shown. Fig. 35 depicted the DSC curves of epoxy, SWNT/epoxy and fSWNT/epoxy composite and Table 4 showed comparison of glass transition temperature of the tested samples.

The glass transition is defined as the change in the heat capacity as the polymer matrix changes from the glass state to the rubber state in the DSC test. Glass transition is a second order endothermic transition, which requires the absorption of heat energy through the transition.

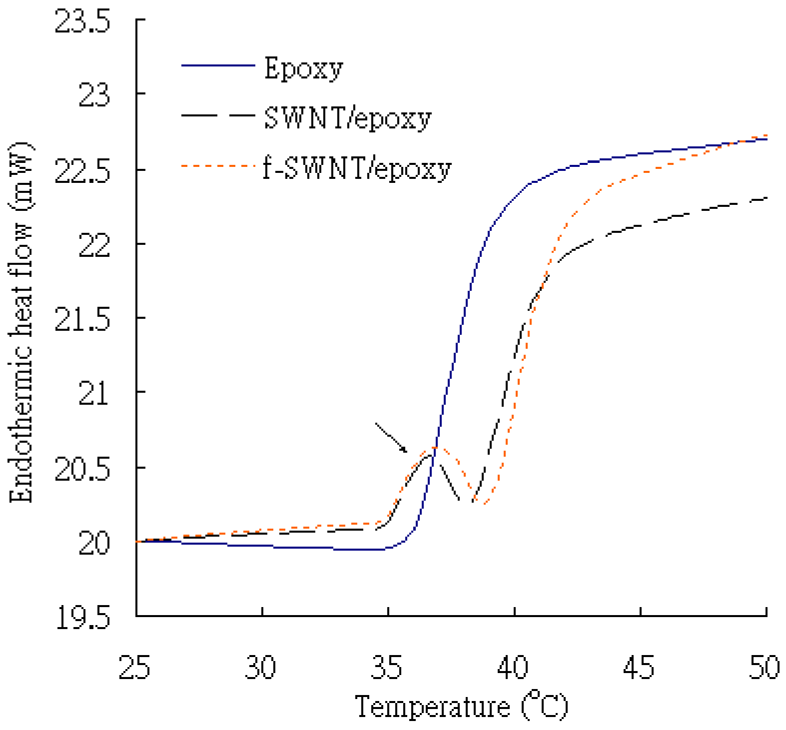

Fig. 35. DSC curves of epoxy, SWNT/epoxy and fSWNT/epoxy

	Epoxy	SWNT/ epoxy	fSWNT/epoxy
Glass transition temperature Tg (^{o}C)	37.89	39.99	40.61
Increment of Tg when comparing with epoxy (%)	-	5.54	7.18

Table 4. Glass transition temperature of tested samples

The results showed that the addition of CNTs increased the Tg of the composites slightly which confirmed the finding from literature [86]. Functionalized SWNTs resulted in 7% increment of Tg. The DSC curves in Fig. 35 provided more information about the Tg. There was a noticeable endothermic peak at around 37^{o}C both for the SWNT/epoxy and fSWNT samples. These peaks indicated that heat energy was absorbed by the SWNTs. It was seen that the peak of the fSWNT/epoxy was wider than SWNT/epoxy, meaning that fSWNTs absorbed more energy than SWNTs. This result matched with the property of the higher thermal conductivity of the fSWNT/epoxy, which distributed energy uniformly inside the composite, and fSWNTs absorbs the energy in an ideal way. Thus, the addition of fSWNTs shifts the T_g of the composite to a higher temperature.

4.6 Scanning Electron Microscope (SEM) observation

The scanning electron microscope (Leica Stereoscan 440) images of the tensile fractured surfaces of the composites were used to study reinforcement behavior of CNTs and failure mechanisms of the composite. Only conductive specimens could be observed by SEM, thus each specimen (Fig. 36) was coated with a thin layer (a few nanometers) of gold in order to become conductive.

Fig. 36. The gold coated specimens for SEM observation

The fractured surfaces of epoxy, SWNT/epoxy and fSWNT/epoxy composites were observed by SEM (Fig. 37 - Fig. 39). It was shown that the matrix (epoxy) of fractured pattern of all specimens were similar. No observable voids were found. The bright regions in the SEM images (Fig. 38 & Fig. 39) were attributed to the high electrical conductivity properties of CNTs.

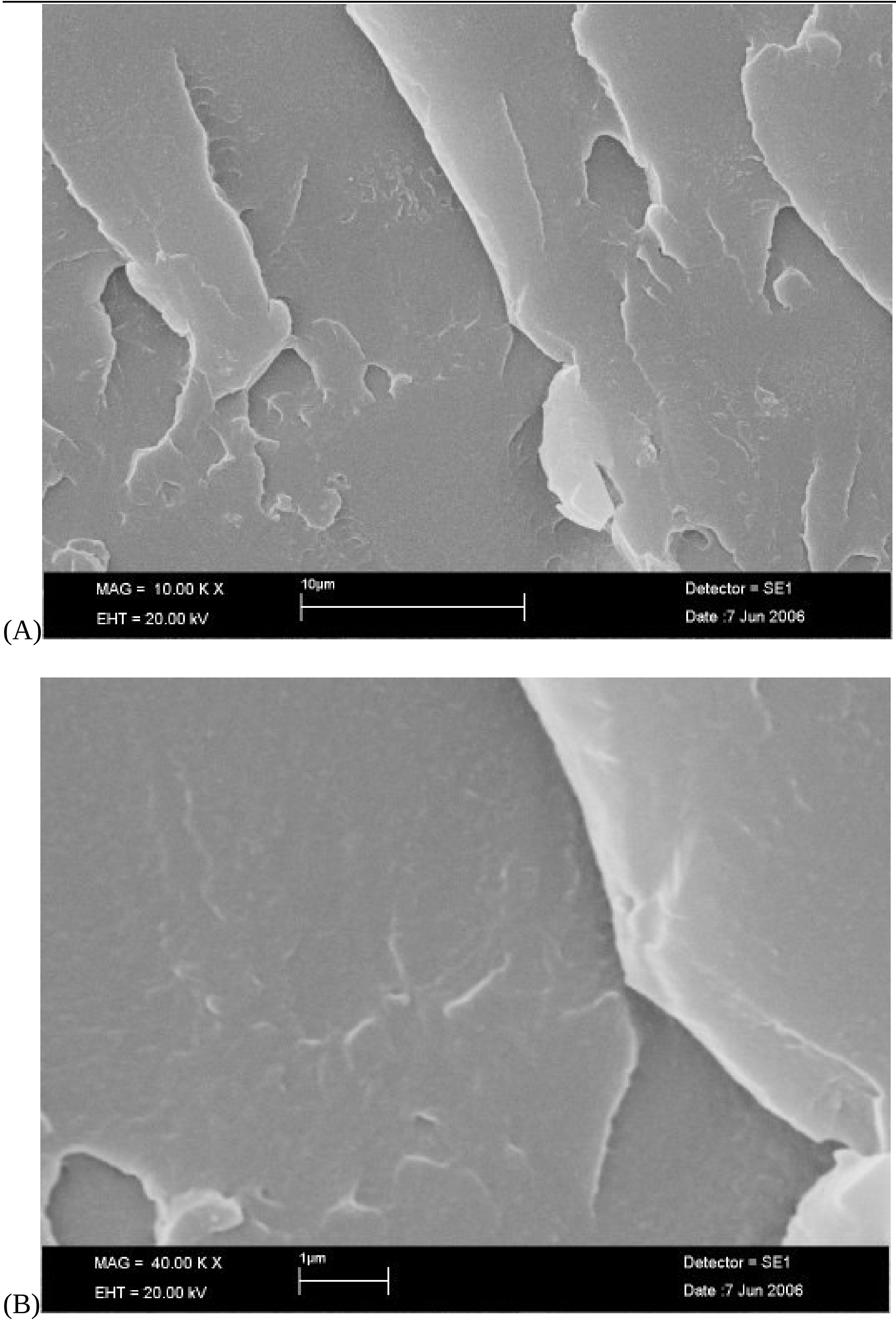

Fig. 37. SEM images of fractured surface of epoxy (A: 10k X; B: 40k X)

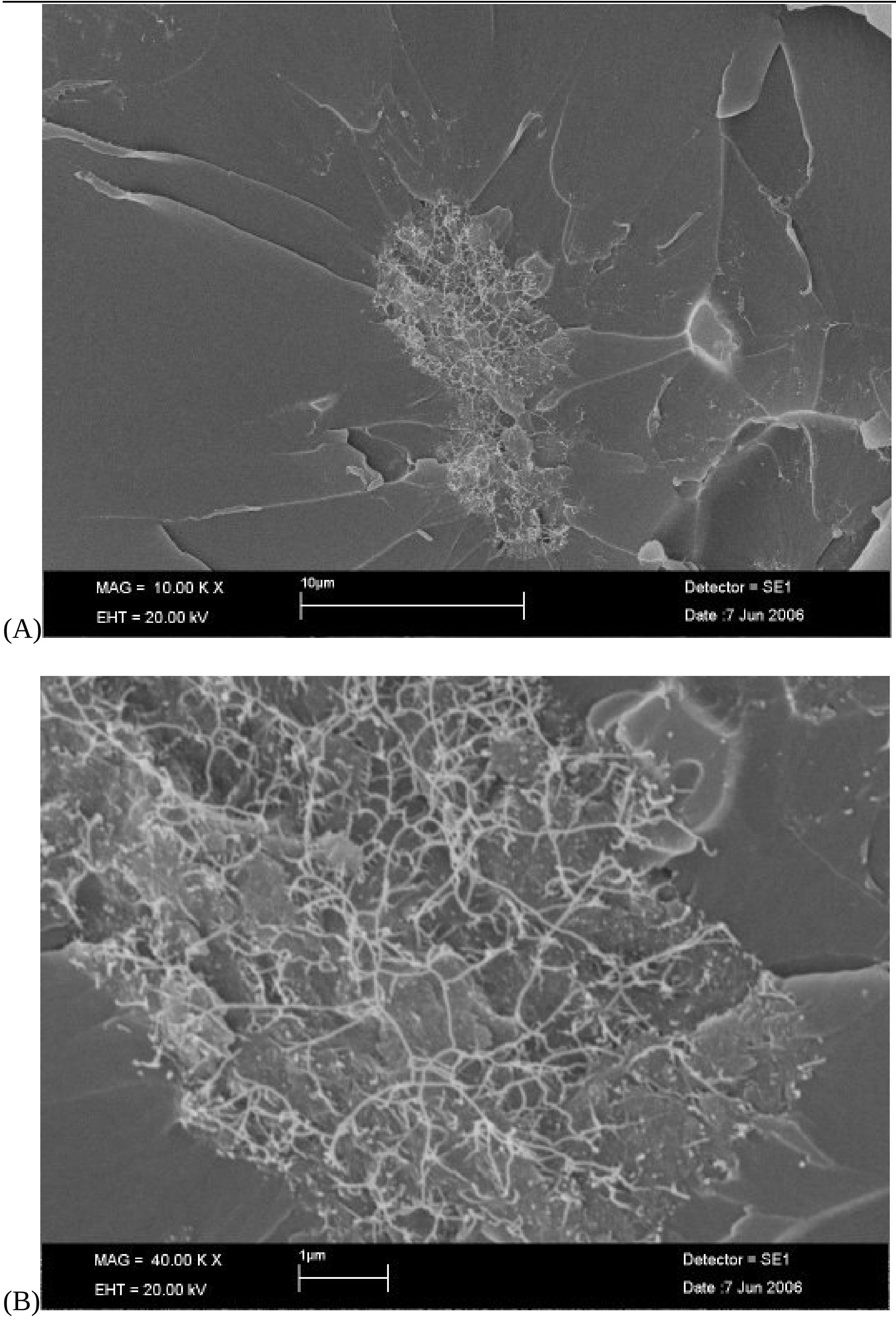

Fig. 38. SEM images of fractured surface of SWNT/epoxy (A: 10k X; B: 40k X)

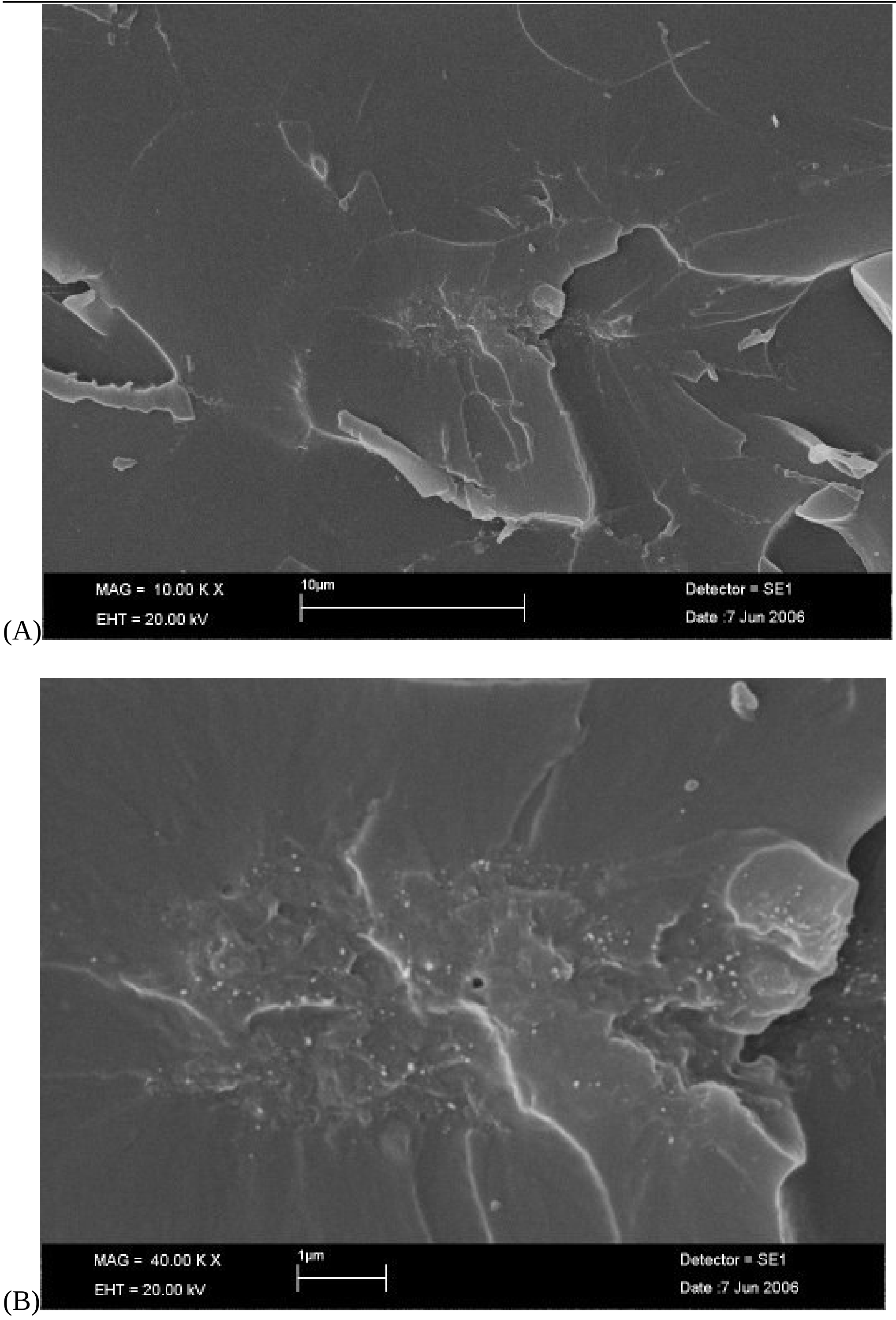

Fig. 39. SEM images of fractured surface of fSWNT/epoxy (A: 10k X; B: 40k X)

As in the Fig. 38, most of the non-functionalized SWNTs tangled together to form bundles cluster and pulled out from epoxy matrix. It meant that the degree of dispersion of non-functionalized SWNTs was poor and the interfacial strength was not high enough to transfer the load from the epoxy matrix to CNTs. As a result, non-functionalized SWNTs were unable to play a significant role in reinforcement, leading to a limited improvement in mechanical strength. By contrast, in Fig. 39, the fSWNTs were dispersed homogenously in epoxy matrix. The Van der Waals force between nanotubes bundles was reduced after functionalization. Fig. 39 also showed that most of the fSWNTs were broken (the white spots), indicating that the strong interfacial bonding between fSWNTs and epoxy matrix were formed and the tensile load was able to transfer from epoxy to CNTs. The functionalized sites of fSWNTs provided opportunity to form chemical bonds with epoxy chains, thereby enhancing the interfacial strength between the fSWNTs and epoxy matrix. In Fig. 39, another noticeable phenomenon showed that the pulled out fSWNTs were obviously shorter than that of the SWNTs in Fig. 38. The possible reasons would be the shortening effect of the CNTs after functionalization. According to Marshall [71], the length of CNTs would be shorter with longer functionalization treatment duration. Although it was known that the CNTs must be longer than a critical length to achieve effective strengthening and stiffening [51], CNTs needed to be functionalized in order to achieve better interfacial strength in polymer matrix. Thus, there exists a trade-off between stress transfer efficiency and the length of CNTs.

4.7 Theoretical study

4.7.1 Modified Halpin-Tsai Equation

Halpin-Tsai Equation (equation (4)) [85] was used for composite with unidirectional reinforcement.

$$E_C = \left[\frac{1+C\eta v_F}{1-\eta v_F}\right]E_M$$
$$\eta = \frac{E_F/E_M - 1}{E_F/E_M + C} \qquad (4)$$
$$C = \frac{2l_F}{D_F}$$

where E_c, E_F, E_M, represents Young's modulus of composite, CNTs and epoxy matrix, $v_{F,}$ l_F and D_F are the volume fraction of CNTs, length of CNTs and diameter of CNTs respectively. Ideally, Halpin-Tsai equation is applied to the composite that has good interfacial bond between fiber and matrix. In addition, it is assumed that the short fibers are laid in the composite in an unidirectional manner.. Thus, original Halpin-Tsai equation is not suitable to be applied to CNTs reinforced composite.

If the reinforcing phase (CNTs) bonds strongly with the matrix (epoxy), the external tensile load will be transmitted from the matrix to the CNTs through the interfacial shear stress. By using modified Halpin-Tsai Equation [8], E_c, can be calculated using the following equations.

$$E_C = \left[\frac{3}{8}\frac{1+C\eta_L v_F}{1-\eta_L v_F} + \frac{5}{8}\frac{1+2\eta_T v_F}{1-\eta_T v_F}\right]E_M$$
$$\eta_L = \frac{E_F/E_M - 1}{E_F/E_M + C}$$
$$\eta_T = \frac{E_F/E_M - 1}{E_F/E_M + 2} \qquad (5)$$
$$C = \frac{2l_F}{D_F}$$

where E_c, E_F, E_M, represents Young's modulus of composite, CNTs and epoxy matrix, v_F, l_F and D_F are the volume fraction of CNTs, length of CNTs and diameter of CNTs, respectively.

However, equation (5) is not strong enough to describe the CNTs reinforced composite. Since the length (μm) of CNTs is much shorter than the thickness (mm) of the composite, the CNTs is unable to exhibit three dimension movement inside the un-cured polymer matrix. Cox [87] suggested adding an orientation factor (α) to Halpin-Tsai Equation. For fiber that can have 2 dimension random orientation, α = 1/3 was used; while α =1/6. was used for the fiber that can have 3 dimension random orientation, After the modification of Halpin-Tsai Equation, equation (5) turned into equation (6) and It was shown as below:

$$E_C = \left[\frac{3}{8}\frac{1+C\eta_L v_F}{1-\eta_L v_F} + \frac{5}{8}\frac{1+2\eta_T v_F}{1-\eta_T v_F}\right]E_M$$
$$\eta_L = \frac{\alpha E_F / E_M - 1}{\alpha E_F / E_M + C} \qquad (6)$$
$$\eta_T = \frac{\alpha E_F / E_M - 1}{\alpha E_F / E_M + 2}$$

To calculate the volume fraction of CNTs, the following equation can be used:

$$v_F = \frac{W_F / \rho_F}{W_F / \rho_F + W_M / \rho_M} \qquad (7)$$

Where, W_F and W_M are the weight fraction CNTs and polymer matrix respectively; ρ_F and ρ_M are the density of CNTs and polymer matrix respectively. And v_F is the volume fraction of CNTs. The physical properties of the CNTs and polymer matrix were shown in Table 5:

SWNT	Value	Ref.
length (μm)	15	[88]
diameter (nm)	1.5	[88]
density (g/cm^3)	1.4	[88]
E (GPa)	1000	[1]
Epoxy	Value	Ref.
E (GPa)	2.33	Exp. Result
density (g/cm^3)	1.12	[90]

Table 5. Physical properties of the CNTs and epoxy

By using equation (7), the volume fraction (v_F) of 1 wt% CNTs was 0.008 and the other parameters for modified Halpin-Tsai Equation (equation (6)) were calculated as in the following table:

C	5000
α	1/6
η_L	0.0139
η_T	0.959

Table 6. Parameter for modified Halpin-Tsai Equation

Since the length (15μm) of CNTs was much shorter than thickness (2mm) of the composite, as mentioned by Cox [87], the orientation factor (α) should be taken as 1/6. The theoretical Young's modulus was then calculated by equation (6).

Theoretical Young's modulus of fSWNT/epoxy composite was 2.85GPa and it was in consensus with the tensile test result. Although the experiment got good agreement with the theoretical calculation, it did not represent the best use of the novel mechanical properties of CNTs. Modified Halpin-Tsai Equation accounted for the randomness and the orientation factors of the CNTs, and got a limited reinforcement by CNTs. For the ideal case, the CNTs should be highly aligned in same orientation and well distributed in the polymer matrix. If the ideal case happened, only the first order approximation of the rule of mixture could represent the tensile strength and Young's modulus of the CNTs reinforced composite.

$$E_C = \eta v_F E_F + v_M E_M$$
$$\sigma_C = \eta v_F \sigma_F + v_M \sigma_M \quad (8)$$

where E_c, E_F, E_M, represents Young's modulus of composite, CNTs and epoxy matrix, σ_c, σ_F, σ_M, represents tensile strength of composite, CNTs and epoxy matrix, v_F, v_M and η are the volume fraction of CNTs, volume fraction of matrix and effectiveness parameter respectively. For two-dimensional random orientations, η =5/8.

4.7.3 Reinforcement mechanism

There are three main mechanisms of load transfer from a matrix to filler. The first one is micromechanical interlocking; but it is not applicable for nanotube composites due to their atomically smooth surface. Fig. 40 schematically showed that, CNTs did not form the cross-link with polymer matrix, thus it could not provide the reinforcement function to the polymer. The second mechanism is the chemical bonding (Fig. 41, Fig. 42) between the nanotubes and the matrix. The third mechanism is a weak Van der Waals bonding between the fiber and the matrix.

An improved matrix/nanotube interaction can be achieved via an equivalent bonding between the functional groups on the nanotube surfaces and the epoxy. Fig. 41 showed the steps of fabricating CNT/polymer composite, (1) the nanotubes are oxidized then (2) functionalized and finally (3) processed to the nanocomposite. In addition, Fig. 42 showed the idea that the functionalized CNTs form cross-link with the polymer matrix to achieve better stress transfer efficiency.

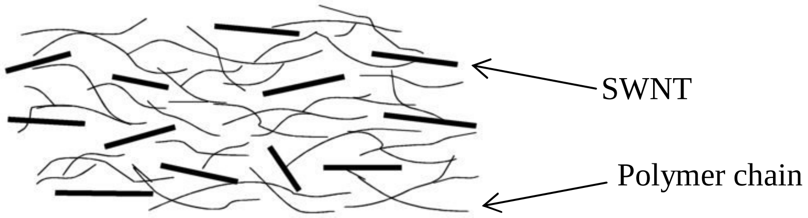

Fig. 40. Schematic diagram for the micro-structure of SWNT/epoxy

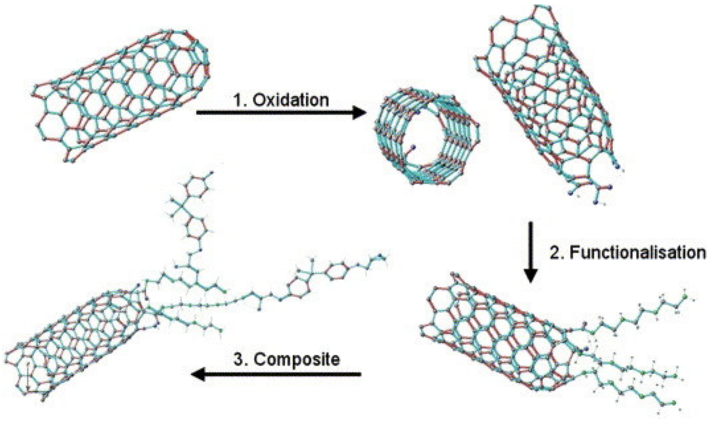

Fig. 41. Schematic diagram for the functionalization process of CNTs

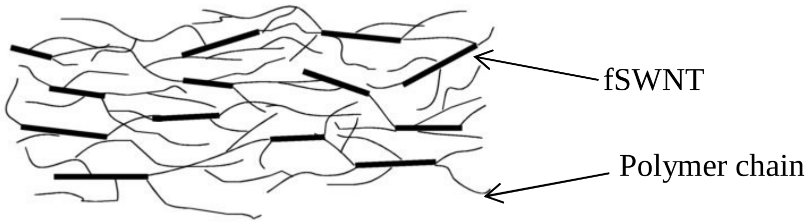

Fig. 42. Schematic diagram for the micro-structure of fSWNT/epoxy

The reaction between fSWNT and epoxy resin could be explained by Fig. 43. The epoxy ring opened and reacted with the COOH of fSWNTs [94]. Actual covalent bonds were formed between fSWNT and polymer chains, thus, the interfacial interaction between them was stronger than that of non-functionalized SWNTs and epoxy polymer chains.

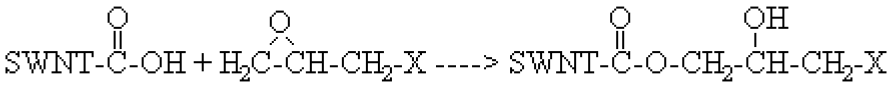

$$\text{SWNT-}\overset{\overset{\text{O}}{\|}}{\text{C}}\text{-OH} + \text{H}_2\overset{\text{O}}{\text{C-CH}}\text{-CH}_2\text{-X} \text{ ----> } \text{SWNT-}\overset{\overset{\text{O}}{\|}}{\text{C}}\text{-O-CH}_2\text{-}\overset{\overset{\text{OH}}{|}}{\text{CH}}\text{-CH}_2\text{-X}$$

Fig. 43. Scheme for fSWNT react with epoxy ring [94]

4.8 Discussion

In fact, many different combinations were conducted during the fabrication process. Different parameters, sonication time, temperature, vacuum time and solvent, were adjusted. It was found that the main factor that affects the quality of the composite is the dispersion issues. As mention before, CNTs agglomerate together easily. The sonication timing would affect the distribution of CNTs inside the polymer matrix. After a series of experiments, it was found that 2-3 hours of sonication time would have the ideal distribution of CNTs. If the sonication time was too short, the CNTs could not have enough time to disperse over. On the other hand, too long of sonication time would not show obvious improvement of dispersion. In addition, it would introduce too much defect to the CNTs and damage the mechanical properties of CNTs finally.

Besides, the use of solvent also affected the mechanical properties of the composite. It was found that, even a small amount of solvent residual would have negative effect to the mechanical properties of the polymer. Although heat was applied to ensure the solvent was evaporated out, there was still a small amount of solvent trapping between the polymer chains. The tensile properties of the epoxy would be reduced with the addition of acetone, because the solvent would have chemical reaction with the polymer matrix. A test was conducted to verify the effect of the solvent on the composite. Two samples of epoxy, one with acetone while another without acetone were tested by tensile test machine. Results showed that the sample with acetone had poor mechanical performance than the one without acetone. Therefore, it was suggested to minimize the use of chemical solvent in processing the composite in future experiments

Chapter 5 CNT/Thermoplastic Composite

Different types of polymer (thermoset and thermoplastic) require different fabricating techniques. So, besides fabricating CNT/thermoset composites, CNT/Thermoplastic composites were also made to investigate the techniques required. It also provided an opportunity to understand the characteristic of different types of CNT/polymer composite. Chapter 4 concluded that the attachment of COOH functional group on the surface of SWNT would enhance the mechanical and thermal properties of the composite. Thus, functionalization of CNTs was also carried out in the experiments. In this chapter, functionalized MWNTs and polypropylene (PP) were used to fabricate CNT/thermoplastic composite by extruder. The reason for selecting MWNTs is that MWNTs has a relatively low price (~HK$10/g) and without much losing of the novel properties when compared with SWNTs [92]. PP is a very common and low-price polymer that is massively used in the industry. Using these two raw materials to fabricate CNT/polymer composite, the price could be reduced and to be used in the industry in the future. Extrusion and injection molding are also common in the processing technique of polymer. In this chapter, melt mixing technique was applied in the fabrication of MWNT/polypropylene composite. This would help to understand the possibility of transferring the techniques to the industry.

After the fabrication of the composite samples, the mechanical properties of the composites were characterized. Tensile test was conducted to obtain the global mechanical properties of the composite. The failure part was used to study further the interfacial bonding between the CNTs and polymer. Tensile property test and micro-hardness test were carried out to examine the mechanical properties of the composites with different MWNT contents. Thermogravimetry Analysis (TGA) and Differential Scanning Calorimetry (DSC) were used to evaluate the thermal properties of the composites. Scanning Electron Microscope (SEM) images were used to investigate the failure mechanism of the composites after tensile test. SEM would also be used to observe the whether pull- out of CNTs happened or not.

5.1 Fabrication of CNTs composite

In order to have a similar fabrication condition as the industry does, a lab scale extruder Hakke MiniLab twin-screw micro extruder was used to disperse the nanotubes into the PP. PP pellets were dried by oven at 80^{o}C for 24 hours to prevent the moisture from affecting the characteristic of the polymer. The functionalization of MWNTs would be same as the functionalization of SWNTs as mentioned in Chapter 3. 0wt%, 0.5wt%, 1wt%, 1.5wt% and 2wt% of purified MWNTs and fMWNTs were mixed with PP pellets before blending in order to have better dispersion of CNTs. The dry mixture of PP and nanotubes were compounded inside the extrusion chamber for 15 minutes in co-rotating mode at 100 rpm and 177^{o}C. The first set of blended mixture would not be used in order to wash out the residues in the machine.

Started from the second set of mixing, the blended mixture was then transferred into the barrel of Thermo Hakke small scale injection molding machine. The temperature of the barrel was kept at 200^{o}C in order to keep the mixture in molten state. The blended materials were injected into a dumbbell shaped mold (mold temperature: 50^{o}C, sample dimension: ~5x1.5x90 mm^3) to form testing composite samples. After cooling down of the mold, the sample was removed (Fig. 44). In order to maintain same testing condition, all samples were stored at an environment with temperature of 25^{o}C and humidity of 40% before performing the tests.

Fig. 44. The CNT/thermoplastic composite samples before test

5.2 Tensile test

One of the important criteria to assess the reinforcement performance of the reinforcement is evaluating the mechanical properties of the composite. Tensile test is a simple and effective method to evaluate the differences between using MWNTs and fMWNTs as reinforcement. It was expected that the reinforcement performance of MWNTs or fMWNTs in PP by using melt mixing would not be as good as in epoxy. The main reason was that, epoxy was a type of thermoset, which contained many branch chains on the polymer chains. As concluded in Chapter 4, the functional groups of CNTs could form bonding with the branch chains of the epoxy’s polymer chains, thus enhancing the mechanical performance of the composite. For the case of PP, PP was a type of thermoplastic, which had long polymer chains without special active functional group. Although the functional groups of fMWNTs were difficult to bond with the polymer chains, it could reduce the surface smoothness of the MWNTs. In addition, functionalization treatments created the charge imbalance around the

MWNTs which resulted in repulsive force between MWNTs. Thus, functionalization improved the dispersion of MWNTs. The nature of more even distribution of fMWNTs further improved the mechanical properties of the composite due to the homogenous interlocking of fMWNTs and polymer chains. Fig. 45 showed the Young's modulus of the CNT-reinforced polymer composites with different CNTs weight percentages.

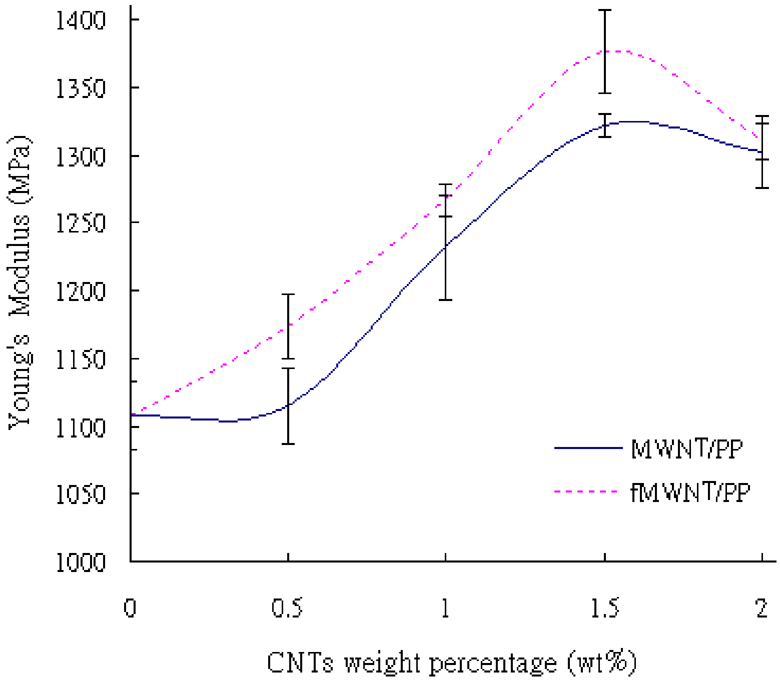

Fig. 45. The Young's modulus of the CNT-reinforced polymer composites with different CNTs weight percentage

There were two areas to be noted in Fig. 45, they were the trend of the curves and the differences between before and after functionalization of MWNTs. As the figure showed that, both MWNTs and fMWNTs had the best reinforcement performance at 1.5 wt%. The increment of the Young's modulus was attributed to the reinforcing effect of MWNTs when MWNTs content between 0.5 wt% to 1.5 wt%, while the drop of the curve after 1.5 wt% was because of the entanglement of MWNTs which mentioned in Chapter 2. It was believed that the entanglement of CNTs was formidable for using melting mixture to fabricate CNT-reinforced polymer composites.

It was because the high viscosity of the melted polymer did not allow distributing CNTs easily. Section 4.1 pointed out that less viscous mixture allowed the CNTs to penetrate into the polymer matrix chain and allowed a better dispersion. It was obvious that the viscosity of melted PP would be higher than the solution of epoxy resin with acetone. Thus the dispersion of MWNTs in PP would not be as good as in epoxy resin with acetone.

Secondly, the differences between before and after functionalization of MWNTs were clearly reflected from the figure. fMWNTs provided a better reinforcing performance against MWNTs. Table 7 showed the numerical result of the tensile test of the composite samples. It could be seen that, the improvement of Young’s modulus of adding fMWNTs was around 4% to 5% higher than adding MWNTs. However, the improvements of Young’s modulus of the two composites were more or less the same when CNTs content went up to 2 wt%. This could also be explained by the agglomeration of CNTs. Although extrusion created a shear mixing to the CNTs and PP polymer chain, the CNTs clusters were still too small (~50μm, detail please refer to the SEM image in Section 5.6) to disperse evenly in such viscous molten PP. The mechanism of dispersion of CNTs in solution and molten status were different. When the COOH groups attached on CNTs, the COOH groups induced charge imbalance on the CNTs molecule and the CNTs was changed from non-polar to polar in nature. Thus, it was easier for functionalized CNTs to disperse in polar solution as acetone. For molten status of PP, it was not easy for CNTs to penetrate into the polymer chain even functionalized CNTs were polar. The only way to disperse CNTs into evenly state was through external force such as high shear force. However, this external force was difficult to disperse the CNTs into nano scale. As a result, the dispersion of CNTs by using extruder would be poorer than using solution mixing.

MWNTs	Young's Modulus (GPa)	Improvement (%)
0 wt%	1.108±0.026	-
0.5 wt%	1.115±0.028	0.648
1 wt%	1.232±0.038	11.221
1.5 wt%	1.322±0.008	19.337
2 wt%	1.302±0.026	17.568
fMWNTs	Young's Modulus (GPa)	Improvement (%)
0 wt%	1.108±0.026	-
0.5 wt%	1.173±0.024	5.916
1 wt%	1.267±0.012	14.354
1.5 wt%	1.376±0.031	24.239
2 wt%	1.310±0.014	18.263

Table 7. Young’s modulus and percentage of improvement of CNT-reinforced polymer composites with different CNTs weight percentage

Fig. 46 showed the failure strain of the composite samples. The most obvious change was the drop of failure strain after adding CNTs. The addition of CNTs led to the reduction of the ductility of the composites. This finding was aligned with other literatures finding which published in the pass [9, 31 & 39]. The main reasons for the reduced ductility were that the CNTs blocked and separated the polymer chains, as a consequence, the polymer chains could not be held together by the Van der Waals force and they intertwined easily. When the composites were under tensile loading, the polymer chains would fall apart easily with little plasticity.

By adding the fMWNTs, there was a little improvement in the failure strain but the result was not very promising. The functionalized site of CNTs reduced the smoothness of the tube surface, so the interlocking/intertwining between fMWNTs and polymer would become more effective when compared with MWNTs. Due to the fact of the relatively smaller functional groups, the improvement of ductility of the composite was not so impressive.

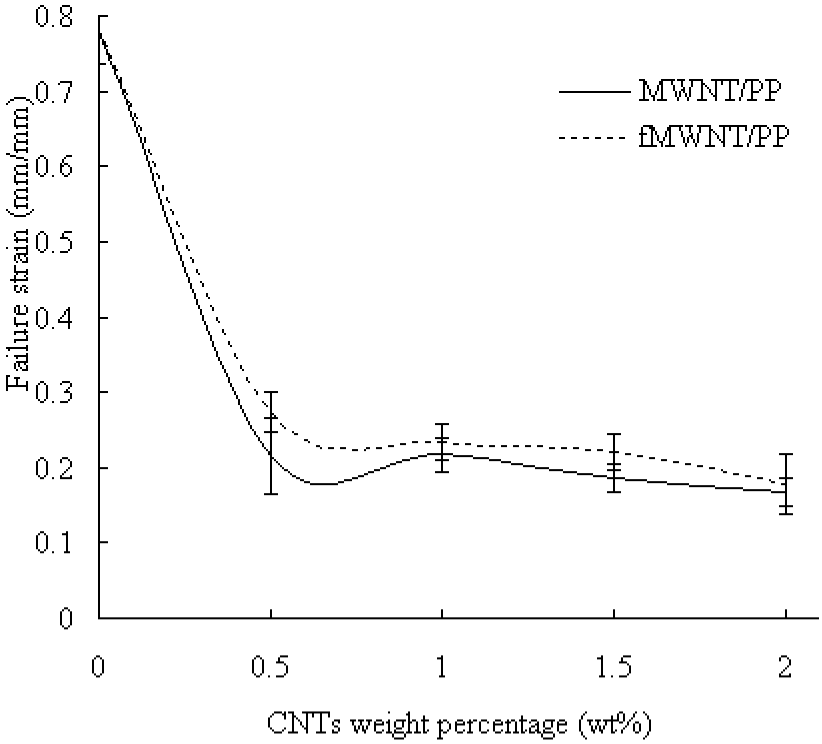

Fig. 46. The failure strain of the CNT-reinforced polymer composites with different CNTs weight percentage

5.3 Microhardness test

The Vickers hardness (Hv) of the composites was measured by Future-tech FM series microhardness testing machine. The Microhardness test method according to ASTM E-384 specifies a range of loads using a diamond indenter to make an indentation that is measured and converted to a hardness value (equation 2 of Section 3.3). The detail testing condition would be same as Section 4.3 so that it would be more convenient to make comparison. Each specimen was measured five times at random locations respectively. The average value of tests was recorded as the hardness value. Fig. 47 showed the hardness values of the different composites. The general trend of the curve was very similar to the tensile test result. MWNTs also provided a reinforce effect to the composite in hardness. Microhardness testing is testing about the property of a relatively large surface of the testing sample, the microhardness value is considered as the macro properties of the CNT/polymer composite.

From the figure, it clearly showed that the optimum CNTs content would be 1 wt% for non-functionalized MWNTs, and 1.5 wt% for fMWNTs. The maximum improvement of hardness value is 21.4% for 1.5 wt% fMWNTs while the improvement of hardness value is 12.1% for 1wt% MWNTs. This phenomenon would also because of the agglomeration of the MWNTs. The agglomeration of MWNTs after 1 wt% reduced the hardness value of the composite. The functionalization of MWNTs, improved the dispersion of MWNTs in the polymer matrix, so the optimum CNTs content raised from 1 wt% to 1.5 wt% for fMWNT/PP. As mentioned at Section 5.2, the reinforcement mechanism of fMWNTs in PP was mainly by interlocking / intertwining between fMWNTs and polymer. The same reason was also applicable for explaining the improved hardness value of fMWNTs. There was only small portion of fMWNTs bonded with the PP polymer chains since the branch chains of PP were relatively stable. Therefore, the percentage of enhanced hardness of fMWNT/PP was not as high as fSWNT/epoxy.

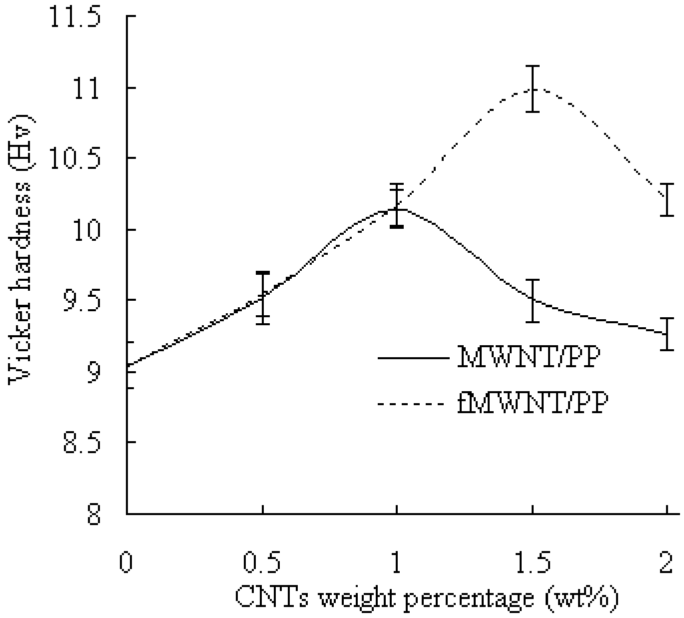

MWNT	Vickers hardness (Hv)
0 wt%	9.05±0.16
0.5 wt%	9.51±0.17
1 wt%	10.14±0.14
1.5 wt%	9.50±0.15
2 wt%	9.27±0.11
fMWNT	Vickers hardness (Hv)
0 wt%	9.05±0.16
0.5 wt%	9.54±0.15
1 wt%	10.17±0.15
1.5 wt%	10.99±0.17
2 wt%	10.20±0.11

Fig. 47. The Vicker hardness of the CNT-reinforced polymer composites with different CNTs weight percentage

5.4 Thermogravimetry Analysis (TGA)

It is a simple and fast way to understand the situation of CNTs in polymer matrix by studying the thermal properties of the composite. There are two reasons for increasing the decomposition temperature of the composite by adding CNTs: (i) CNTs hinder the movement of polymer chains; and (ii) CNTs bond with the polymer chains and reduce the mobility of the polymer chains. The Setaram Labsys TG-DTA/DSC system was used for TGA. The samples were heated from 100 °C to 700 °C at a rate of 10°C/minute with the flow of nitrogen (about 40cc/min). Fig. 48 to Fig. 50 showed the TGA curves of PP, 0.5wt% MWNT/PP and 0.5wt% fMWNT/PP respectively.

From the figures, the decomposition patterns of all the composition samples were very similar and the change of the decomposition temperature was not significant (within 1%).

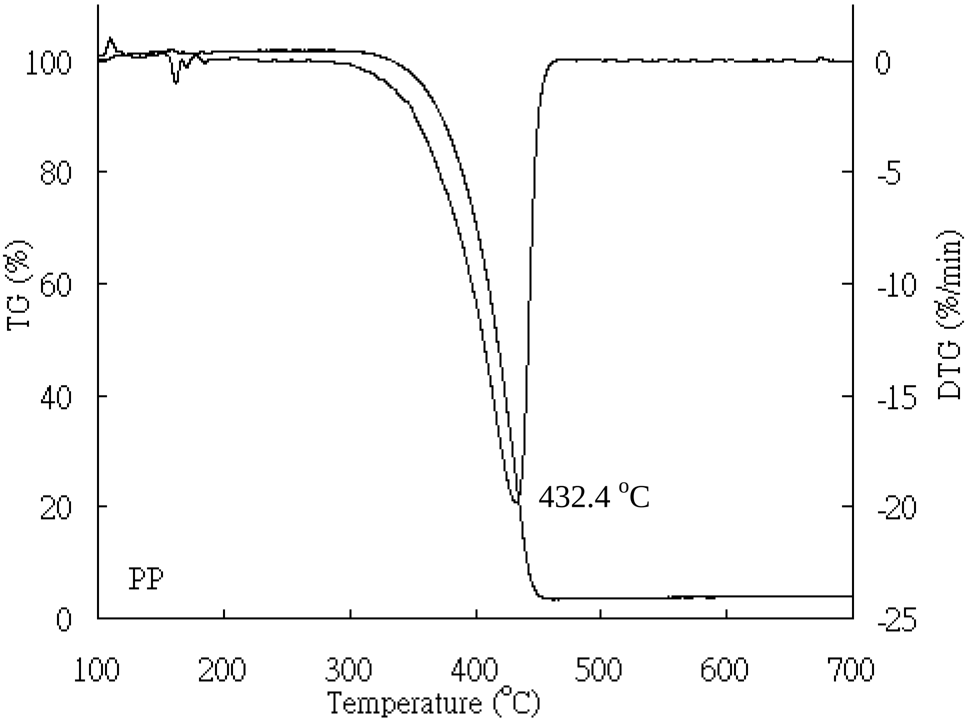

Fig. 48. TG-DTG curves of neat PP

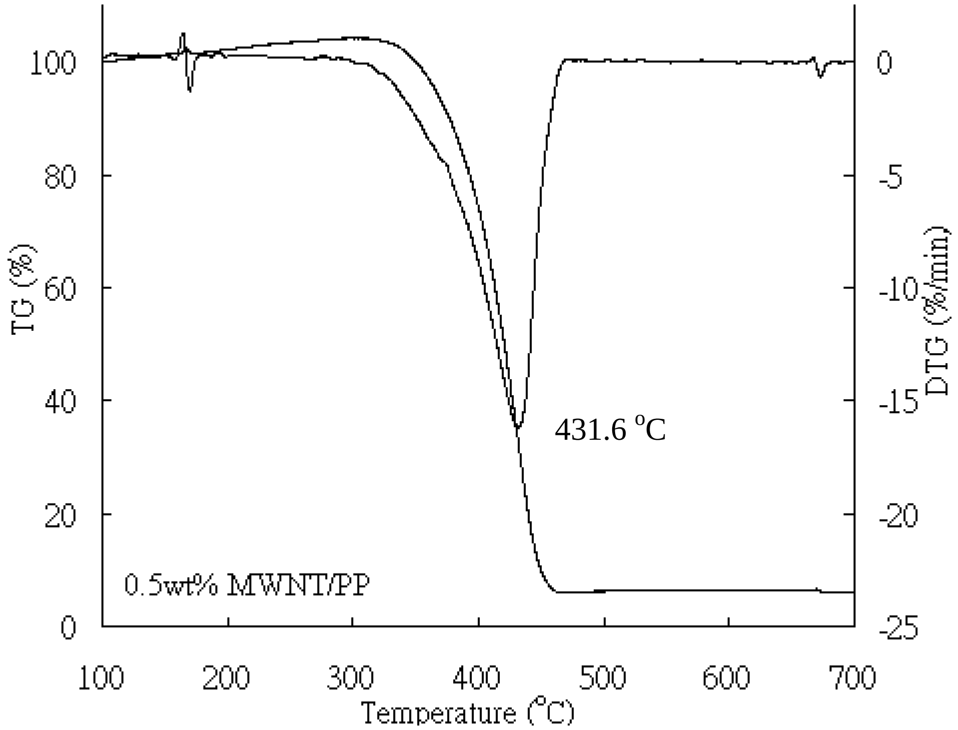

Fig. 49. TG-DTG curves of 0.5wt% MWNT/PP

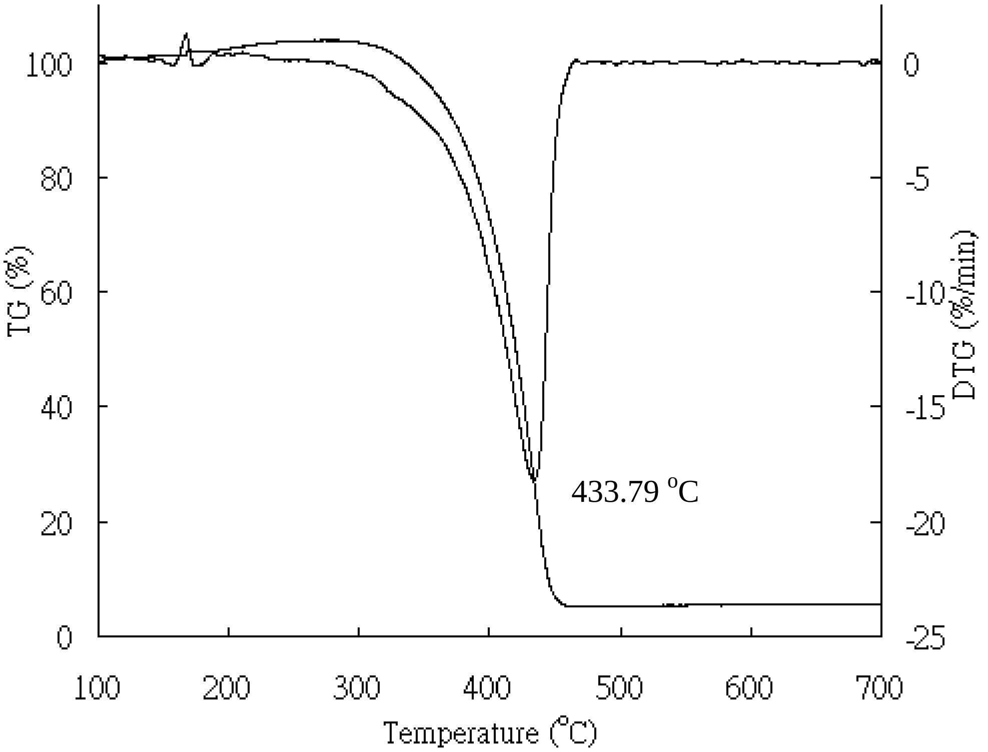

Fig. 50. TG-DTG curves of 0.5wt% fMWNT/PP

Under nitrogen heating environment, the composite was restricted to undergo one-step decomposition process only, in contrary to the different decomposition patterns with SWNT/epoxy at air in Section 4.4. The absence of oxygen avoided the oxidation of polymer. Thus, the TGA curves of three figures were similar. There was only a minor chance (no increment) of decomposition temperature for MWNT/PP, meaning that the MWNTs did not have chemical reaction with the polymer chains. The reinforcement behavior of MWNTs in PP matrix would purely be the mechanical interlocking. For fMWNT/PP, there was only a little increment of decomposition temperature (1.4 ^{o}C), meaning that the chemical bonding between fMWNTs and PP polymer chains was very few and limited. The result of TGA for fMWNT/PP composite also explained why the reinforcement improvement of fMWNT/PP was less than fSWNT/epoxy. The COOH of fSWNT could form bonding with the opened ring of 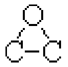 [94] of the epoxy resin. By contrast, the only branch chain of PP is CH_3, which is relatively stable. CH_3 is not easy to form bond with COOH which exists on the tube surface of fMWNT even at high temperature. Thus, few chemical bonding between fMWNT and PP polymer chains led to a limited reinforcement effect. However, UV irradiation on the fMWNT/PP would induce a strengthening effect; UV provides energy for COOH to make bonding with CH_3. The details of the UV effects on the composite will be discussed in the next chapter.

5.5 Differential Scanning Calorimetry (DSC)

Fig. 67 illustrated DSC curves of the different composite samples. The peaks around 161°C were the melting peaks of the samples. The shape of the peaks was consistent, and the widths of melting range were quite similar. There were no significant changes in the melting temperatures for all composite samples, meaning that the addition of CNTs did not affect the melting temperature of the composite samples.

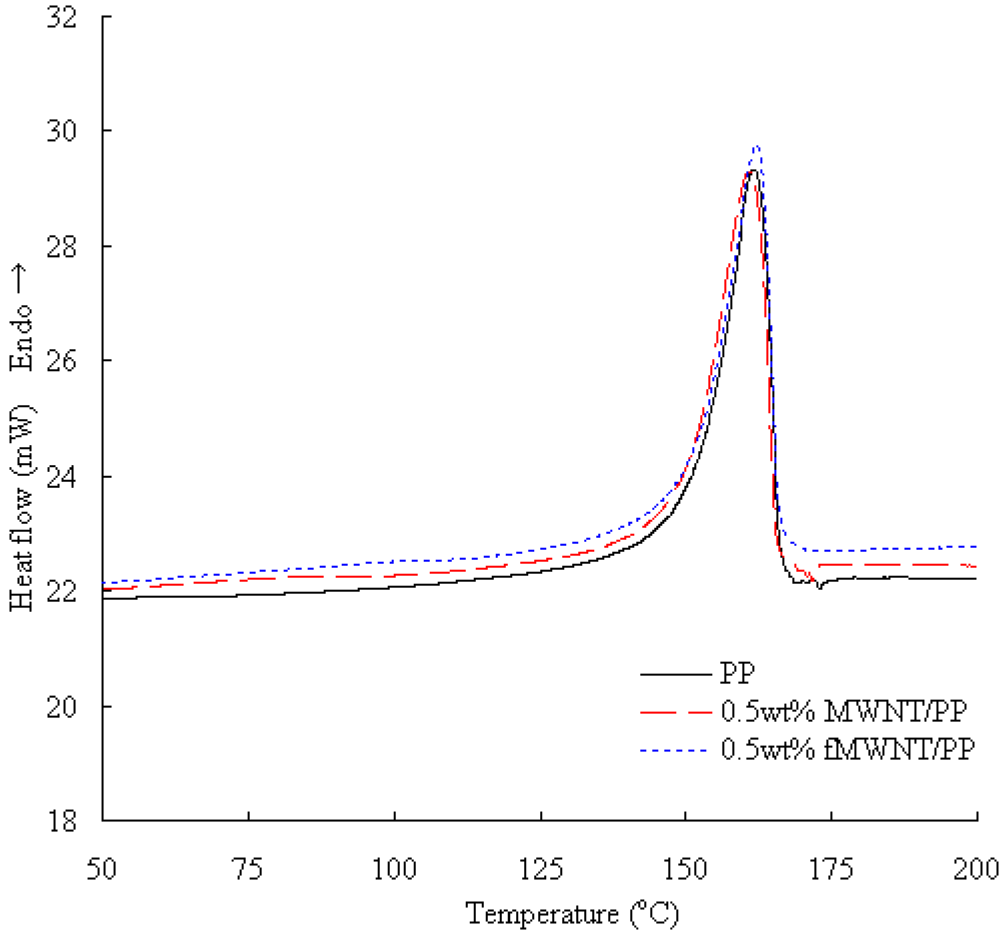

Fig. 51. DSC curves of he CNT-reinforced polymer composites of neat PP, 0.5wt% MWNT/PP and 0.5wt% fMWNT/PP

5.6 Scanning Electron Microscope (SEM) observation

The mechanical tests of the composite samples were used to determine the global properties of the composite. CNTs were in nano-scale, and it was not easy to study the tube performance by the mechanical test on bulky composite samples. Thus, SEM observation was used to help study the CNTs performance in the polymer matrix. SEM (Leica Stereoscan 440) images of the tensile fractured surfaces of the composites were used to study reinforcement behavior of CNTs and failure mechanisms of the composite. All the specimens were coated with a thin layer of gold in order to turn the specimens into observable states for SEM. Fig. 52 to Fig. 56 showed the SEM images of neat PP, 0.5wt% MWNT/PP and 0.5wt% fMWNT/PP specimens. The white lines in the SEM images were the MWNTs/fMWNTs that were mainly due to their high electrical conductivity properties

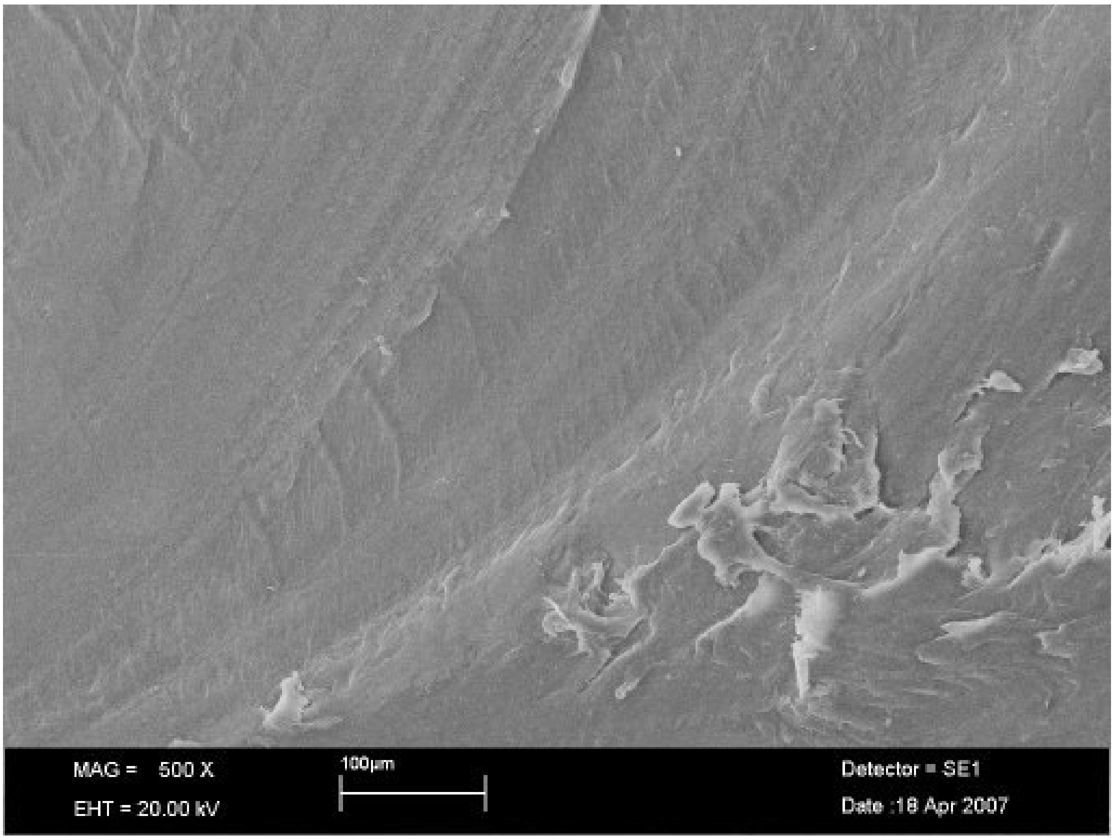

Fig. 52. SEM image of fractured surface of PP (500X)

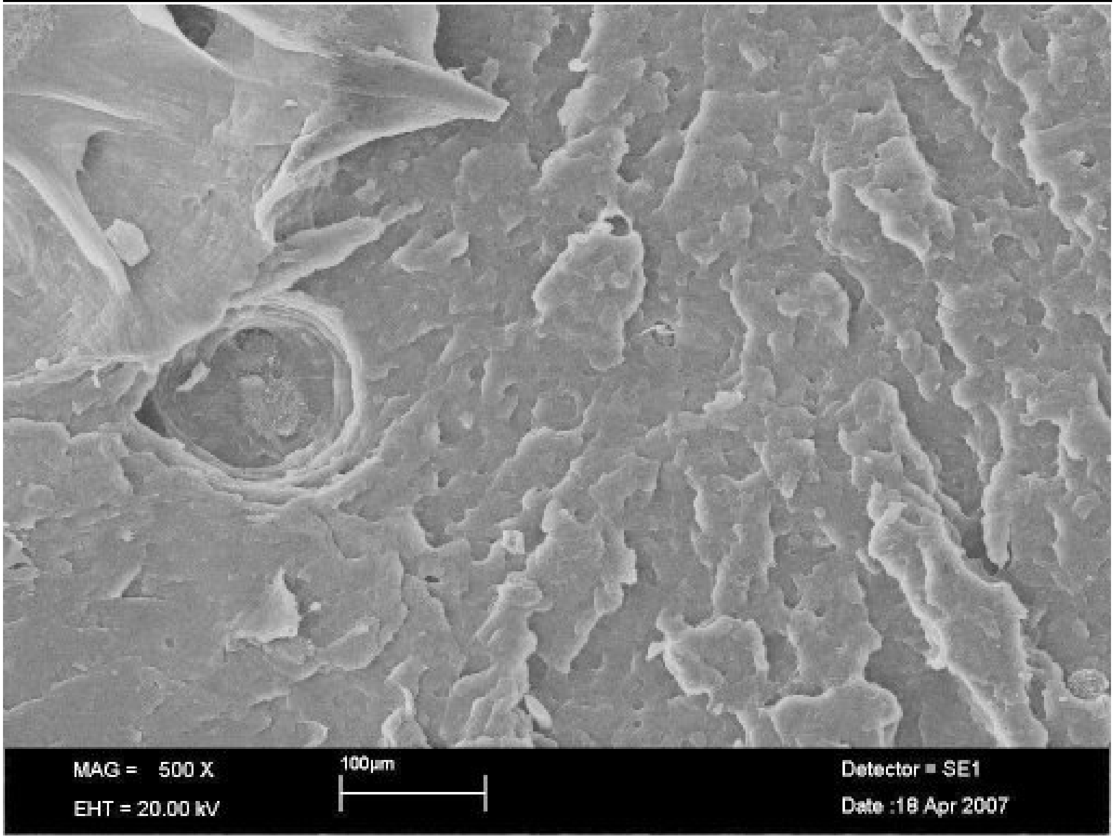

Fig. 53. SEM image of fractured surface of 0.5wt% MWNT/PP (500X)

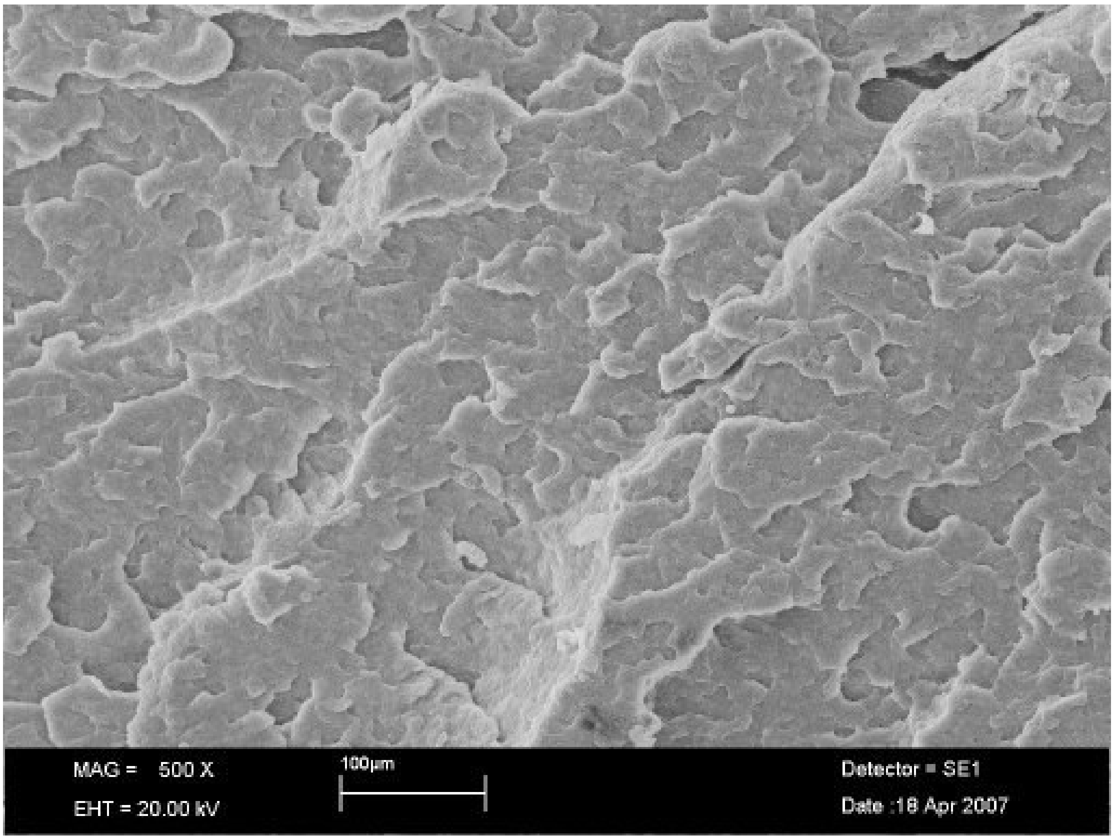

Fig. 54. SEM image of fractured surface of 0.5wt% fMWNT/PP (500X)

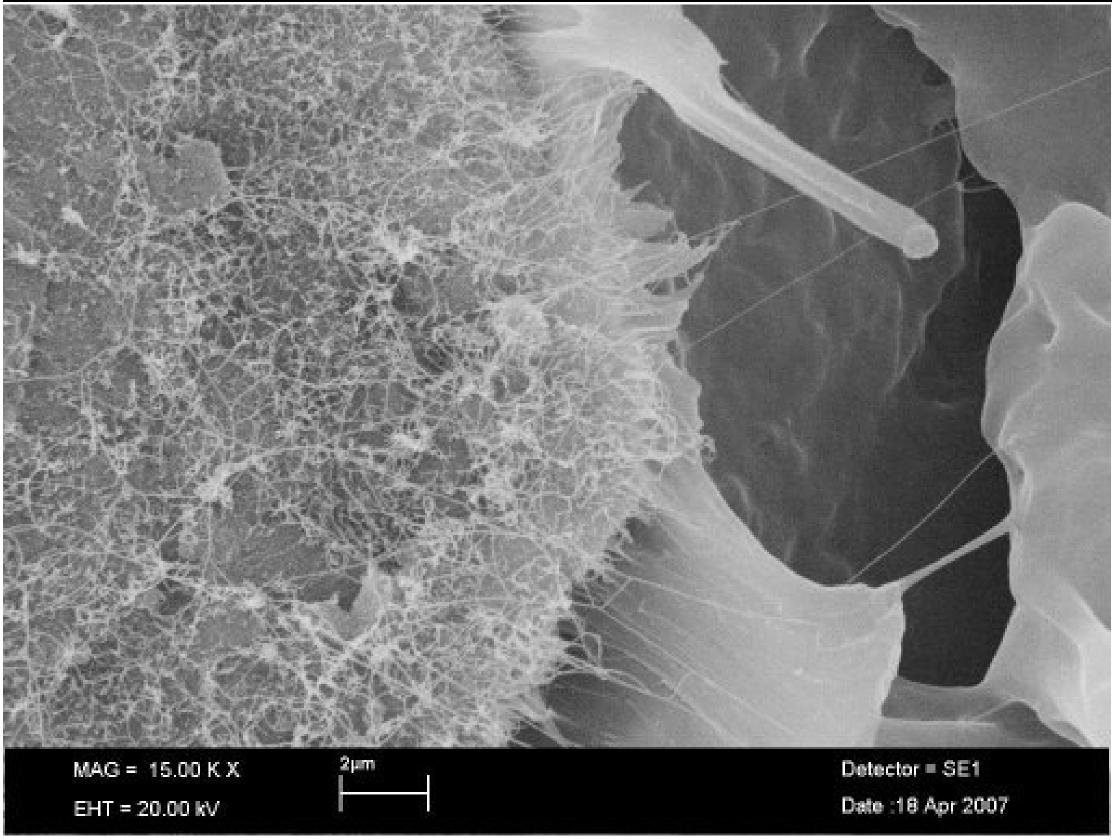

Fig. 55. SEM image of fractured surface of 0.5wt% MWNT/PP (15000X)

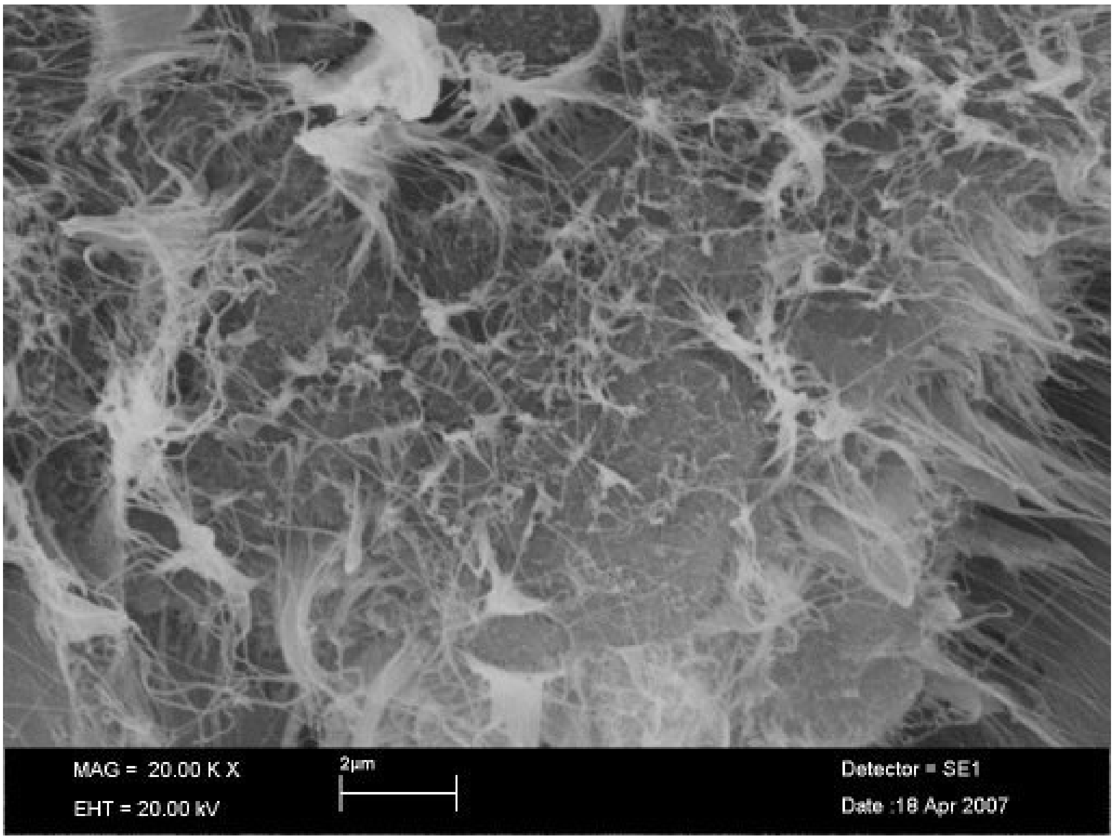

Fig. 56. SEM image of fractured surface of 0.5wt% fMWNT/PP (20000X)

The morphology of the fractured surface of neat PP was very different from the MWNT/PP and fMWNT/PP. From the SEM images, the fractured surface of composites had many lumps after adding MWNTs and fMWNTs, on the other hand, neat PP had a smooth fractured surface. These faceted appearances reflected the brittleness of the composite. More and smaller lumps implied more brittles of the testing sample. By referring to the tensile result (Section 5.2), the failure strain of MWNT/PP and fMWNT/PP were very close. From the SEM images (Fig. 53 & Fig. 54), the size and the number of the lumps of two CNTs composites were also similar. The findings from SEM were consistent with the finding of tensile test.

By using higher magnification of SEM, the interfacial properties between MWNTs and polymer could be easier to study. Fig. 55 and Fig. 56 showed the high magnification SEM images of MWNT/PP and fMWNT/PP respectively. Both MWNTs and fMWNTs agglomerated together. But as Fig. 55 showed, the entanglement of MWNTs were larger and denser than the fMWNTs (Fig. 56). MWNTs were non-polar in nature, while the Van der Waals force between the tube bodies were relative stronger than fMWNTs. Thus, the entanglements of MWNTs were denser than fMWNTs in PP matrix. Another noticeable characteristic was that the interfacial properties of the composite. Some of the fMWNTs in Fig. 56 were wrapped with polymer, because some fMWNTs bonded with PP polymer chains. On the contrary, most of the MWNTs in Fig. 55 fell apart from the polymer. Lack of bonding between MWNTs and polymer chain resulted in poor stress transfer ability, thus the mechanical performance of MWNT/PP was poorer than fMWNT/PP in same CNTs contents. The SEM images confirmed that the stress was transferred from PP to fMWNTs and resulted in the tear-off appearance of fMWNTs from PP matrix.

5.7 Theoretical study

5.7.1 Modified Halpin-Tsai Equation

The tensile experimental results were compared with the numerical calculation by the equation that concluded in Section 4.7. i.e.:

$$
\begin{aligned}
E_C &= \left[\frac{3}{8}\frac{1+C\eta_L v_F}{1-\eta_L v_F}+\frac{5}{8}\frac{1+2\eta_T v_F}{1-\eta_T v_F}\right]E_M \\
\eta_L &= \frac{\alpha E_F / E_M - 1}{\alpha E_F / E_M + C} \\
\eta_T &= \frac{\alpha E_F / E_M - 1}{\alpha E_F / E_M + 2} \\
C &= \frac{2l_F}{D_F}
\end{aligned}
\qquad (9)
$$

where E_c, E_F, E_M, represents Young's modulus of composite, CNTs and epoxy matrix, v_F, l_F and D_F are the volume fraction of CNTs, length of CNTs, and diameter of CNTs respectively.

$$
v_F = \frac{W_F / \rho_F}{W_F / \rho_F + W_M / \rho_M} \qquad (10)
$$

Where, W_F and W_M are the weight fraction CNTs and polymer matrix respectively; ρ_F and ρ_M are the density of CNTs and polymer matrix respectively. And v_F is the volume fraction of CNTs. The physical properties of the CNTs and polymer matrix were shown in Table 8:

MWNT	Value	Ref.
length (μm)	10	[88]
diameter (nm)	20	[88]
density (g/cm^3)	2.6	[88]
E (GPa)	1200	[1]
PP	Value	Ref.
E (GPa)	1.107	Exp. Result
density (g/cm^3)	0.9	[91]

Table 8. Physical properties of the CNTs and epoxy

The parameters for modified Halpin-Tsai Equation (equation (9)) were calculated as following table:

C	1000
α	1/6
η_L	0.152
η_T	0.983

Table 9. Parameters for modified Halpin-Tsai Equation

Since the length (10μm) of MWNTs was much shorter than thickness (1.5mm) of the composite, as mentioned by Cox [87], the orientation factor (α) should be taken as 1/6. The theoretical Young's modulus was then calculated by modified Halpin-Tsai Equation (equation (9)) and showed in Fig. 57.

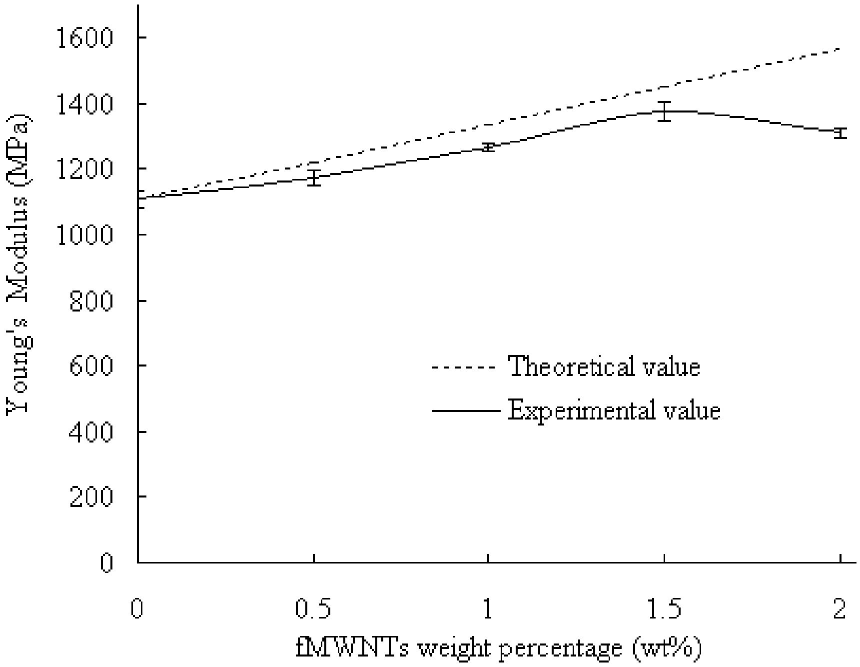

Fig. 57. Comparison of experimental value and theoretical value of Young's modulus of fMWNT/PP composite

As Fig. 57 showed, the theoretical Young's modulus of the composite quite agreed with the experimental results. The theoretical value started to deviate from experimental result after 1.5 wt% of fMWNTs, it is because of the agglomeration of fMWNTs in the composite. Nevertheless, overall speaking, the equation was suitable to predict the Young's modulus of the composite at low CNTs content.

5.7.2 Activation energy for thermal decomposition

According to Horowitz [93], the activation energy for the thermal decomposition, E_t, of the MWNT/PP composites can be estimated from the corresponding TGA curves by using a integral method. The equation for the activation energy for thermal decomposition was expressed as follows:

$$\ln[\ln(1-\alpha)^{-1}] = \frac{E_t\theta}{RT_{\max}^2} \qquad (11)$$

where, α is the decomposed fraction, E_t is the activation energy of decomposition, T_{max} is the temperature at maximum rate of weight loss, R is the universal gas constant (8.314 $mol^{-1}K^{-1}$) and θ is ($T-T_{max}$).

By plotting the $\ln[\ln(1-\alpha)^{-1}]$ vs θ, the activation energy of decomposition (E_t) can be determined. Fig. 58 to Fig. 60 showed the graphs of $\ln[\ln(1-\alpha)^{-1}]$ vs θ and a straight line is fitted into the graph. The slope of the straight line equal E_t/RT_{max}^2 and thus activation energy can be calculated.

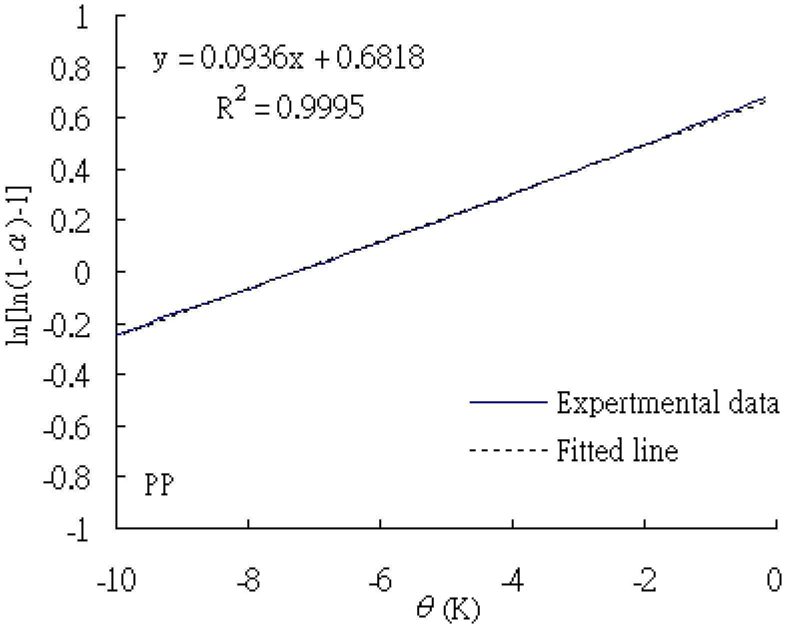

Fig. 58. Plot of $\ln[\ln(1-\alpha)^{-1}]$ vs θ for determination of the activation energy of decomposition of PP

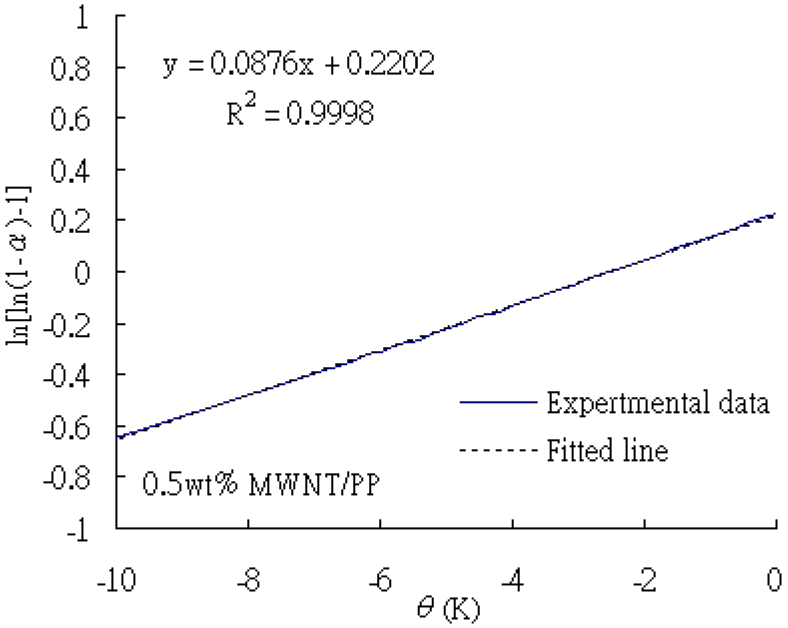

Fig. 59. Plot of $\ln[\ln(1-\alpha)^{-1}]$ vs θ for determination of the activation energy of decomposition of 0.5wt% MWNT/PP

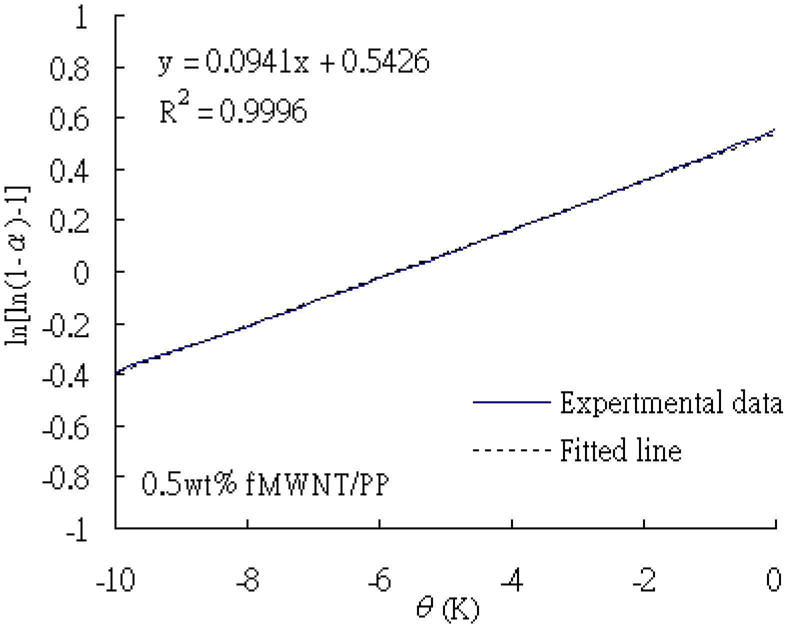

Fig. 60. Plot of $\ln[\ln(1-\alpha)^{-1}]$ vs θ for determination of the activation energy of decomposition of 0.5wt% fMWNT/PP

	E_t/RT_{max}^2	T_{max}	Activation energy of decomposition
PP	0.0936	432.40	145.50 kJ/mol
0.5wt% MWNT/PP	0.0897	431.54	138.88 kJ/mol
0.5wt% fMWNT/PP	0.0941	433.79	147.22 kJ/mol

Table 10. Activation energy of decomposition of the composites

Energy is the most fundamental parameter to assess the stability of a system. Thus, the activation energy of decomposition would be easier to directly compare the stability of the composites. The experimental data was successfully fitted with the theoretic calculation. Fig. 58 to Fig. 60 showed that there was very good fitting, the lowest R-square value was 0.9995 meaning the estimated value was reasonably close to theoretical value. Table 10 showed the numerical value of the activation energy of decomposition. It showed that the decomposition temperature of the composite was not directly proportional to the activation energy of decomposition of the composite. The thermal stability of composite was enhanced by adding of fMWNTs. On the other hand, the thermal stability of the composite reduced after adding MWNTs. It may due to the poor dispersion of MWNT in PP matrix. According to Chen [83] in literature, the dispersion of the CNTs inside the polymer would affect the thermal stability of the composite. Thus, the poor dispersion of MWNTs in PP matrix resulted in low activation energy of decomposition.

5.8 Discussion

The serials of experiments of fMWNT/PP proved the possibility and performance of using industrial process to fabricate CNT/thermoplastic composite. There were some problems using extruder to disperse the MWNTs inside PP matrix, since the gap between the extruding screws is too big for dispersing nano-scale material. One solution is to blend the MWNTs with PP pellets prior to entering the extrusion chamber. The hand stirring of MWNTs and PP would help reduce the size of MWNTs agglomeration. It is observable that the dispersion of MWNTs would be better inside the composite after stirring. During the hand stirring, the PP pellets may act as the balls for ball milling.

Another upcoming issue from this serial of experiments was the mechanical reinforcement performance of the MWNTs and fMWNTs. As it can be seen from the experiment result, the MWNTs cannot provide a significant reinforcement to the composite. However, the main reason would be the inert properties of the CNTs. The surfaces of MWNTs are too smooth to interlock with the PP polymer chains. Agglomeration of MWNTs also is a reason to restrict the best use of CNTs novel properties as explained in Section 5.2. The improvement after functionalization of CNTs would greatly improve the reinforcement performance for fSWNT/epoxy in Chapter 4. The main reason would be the functionalized site could bond with the epoxy polymer chains. However, the situation for fMWNTs and PP would be different. Although the improvement of the mechanical properties by using functionalized MWNTs was better than non-functionalized MWNTs, its improvement would not be as significant as fSWNT/epoxy. fMWNTs could not bond with the stable branch chain of PP polymer chains easily. The interfacial bonding between fMWNTs and PP was weaker than fSWNT and epoxy. Thus, the stress could not be transferred from PP to fMWNTs effectively. In order to improve the bonding between CNTs and polymer, specific function group could be functionalized on the CNTs, but it requires additional chemical process, which is time consuming. Another method to improve the interfacial bonding would be high-energy irradiation, such as, X-ray and UV light. The high-energy irradiation would excite the molecules of CNTs and polymer chains; which in turn stimulate forming bonds between them. Lastly, this chapter also verified that the modified Halpin-Tsai equation could predict the Young’s modulus for low CNTs content’s composite (for both thermoset and thermoplastic).

Chapter 6 Effects of UV Exposure

UV degradation has been a critical problem for polymers. Most of the polymer would be aging under sunlight [95-96]. CNTs reinforced polymer composites also expose to the same problem when they are used in outdoor applications. However, there are only a very limited number of scientific studies focusing on this issue for CNT/polymer composites. Najafi et al. [17] reported that the radiation of UV-ozone (UV wavelength: 254 nm) on MWNTs under an ambient condition would oxidize the surface of the nanotubes, producing quinines, esters, and hydroxyl functional groups. They also reported that the addition of CNTs fillers had a reinforcement effect against the degradation by UV irradiations for a thin film nanocomposite [19]. This chapter intended to investigate the effects of UV irradiation on the MWNT reinforced polymer composite in order to understand the UV effect on MWNT/polymer composites.

Polypropylene (PP) was used as a matrix. MWNTs functionalized with carboxylic acid groups at their tubes' ends and defect site by acid treatment were used as nano-fillers. The fMWNTs (0 – 2 wt%) were blended with PP by a co-rotating twin-screw extruder (same as the fabrication process which mentioned at Section 5.1), in order to enhance the dispersion of the fMWNTs. The mechanical and thermal properties of pre UV irradiation fMWNT/PP and post UV irradiation fMWNT/PP composite at different weight percentages were compared. SEM examination was conducted to investigate the dispersion quality of the fMWNTs and the failure patterns of the composites.

6.1 Experimental condition

In order to study the effect of UV exposure on the composite sample , UV irradiation was conducted under ambient condition in a UV lamp chamber (40 cm × 40 cm × 13.5 cm) which had a layer of reflective aluminum foil inside to ensure all the sample would have an even exposure to UV. The temperature during UV irradiation was maintained at around 25 °C. The PP and fMWNT/PP composite samples were irradiated under a 25 W ultraviolet lamp (Sylvania, Japan) for 72 hours. The specimens were exposed to UV for 36 hours on each side. The distance between the UV lamp and specimens was about 100 cm. The primary wavelength of the lamp was 254 nm. Fig. 61 showed the spectral energy distribution of the lamp:

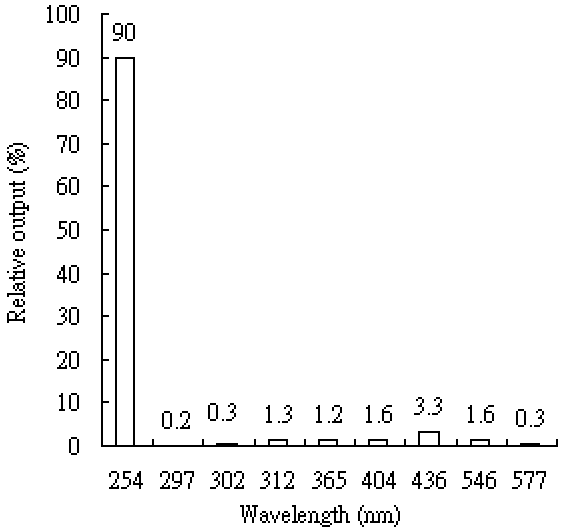

Fig. 61. The spectral energy distribution of the UV lamp

6.2 Tensile test

Tensile test was used to determine the mechanical properties of the composite sample. Fig. 62 showed the change of Young’s modulus at various fMWNTs content before and after the UV irradiation. It showed that the Young’s modulus gradually increased from around 1110 MPa to 1380 MPa for 0 to 1.5 wt% of both pre and post UV irradiation composite samples. In the case of pre UV irradiation, the maximum improvement of Young’s modulus for the composite samples was around 24%. On the contrary, in the case of post UV irradiation, the maximum improvement was around 11%. It was expected that the mechanical properties of the composites would increase due to the interlocking between the fMWNTs and polymer chains. Thus, fMWNTs were able to play the role of reinforcement. The reduction of stiffness after 1.5wt% of fMWNTs was due to the agglomeration of fMWNTs. The agglomeration of CNTs would cause slippage inside the clusters which in turn reduced stress transfer efficiency and the reinforcement performance [10]. It was obvious that the effect of UV exposure on the Young’s modulus of the composite sample was narrow down and reached similar values at 1.5wt% of fMWNTs.

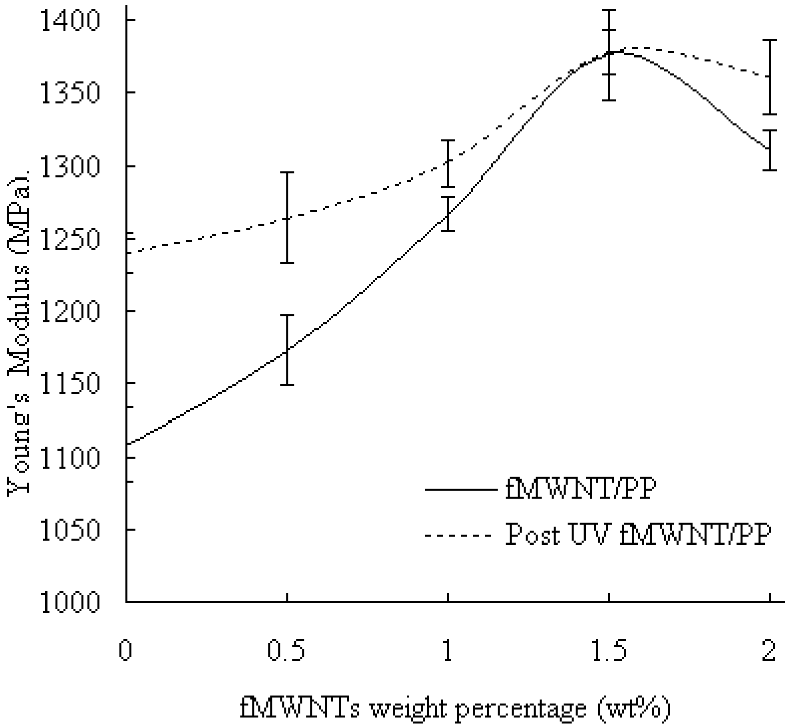

Fig. 62. The Young’s Modulus of the composite samples before and after UV irradiation.

In cooperate with Fig. 63, UV irradiation strengthened the Young’s modulus of PP composite but weakened the failure strain of the composite. From Fig. 63, it was found that the Young’s modulus increased by adding fMWNTs, but the failure strain reduced. It was a trade off between utilizing the Young's modulus and the failure strain of the material. But after UV irradiation, the situation could be different. The UV irradiation resulted in nearly a half of reduction of the failure strain value of neat PP. This reduced value was approximate to the value of fMWNTs containing composite. For the fMWNT/PP, UV irradiation imposed only a limited effect to its tensile property. Both the pre and post UV irradiation composite samples got very similar failure strain value. According to the literature [19], fMWNTs were able to provide an irradiation protection to the composite material. The further explanation on the UV irradiation protection of fMWNTs could be seen in Section 6.4. Microhardness test also provided some useful information to understand the structural change of the composite after exposing the UV irradiation.

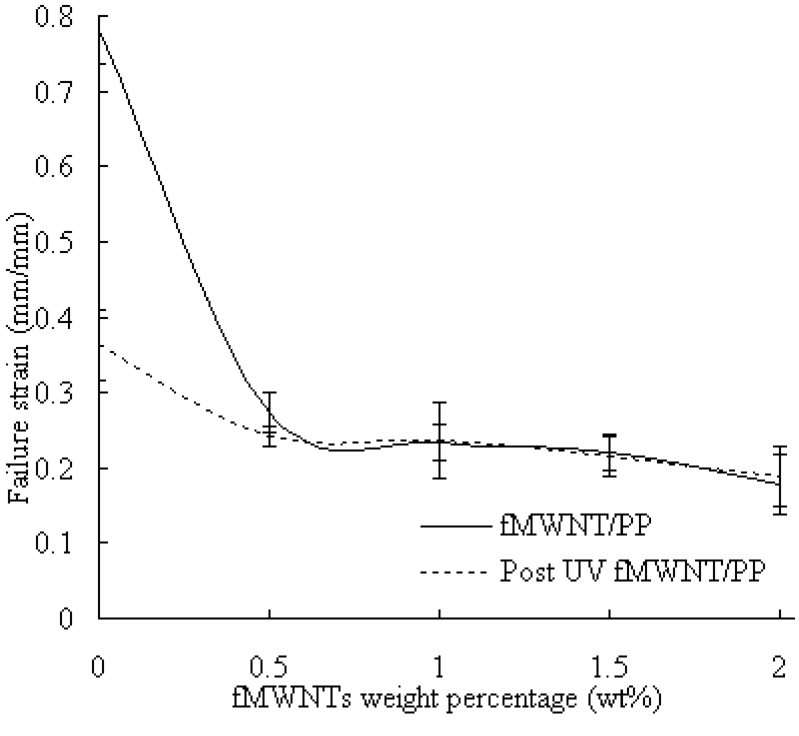

Fig. 63. Failure strain of the composite samples before and after UV irradiation.

6.3 Microhardness test

The values of Vicker's hardness of the samples were listed in Table 11. The result showed that, the behavior of the hardness test result was consistent with the tensile test result. The hardness value generally increased with the increase of the fMWNTs content and 1.5 wt% of fMWNTs achieved the best reinforcement result among others. Fig. 64 showed the improvement of hardness value when compared with neat PP before and after UV irradiation. It was obvious that, fMWNT/PP resulted in a uniform positive improvement in hardness value after UV irradiation. The drop of hardness value after 1.5 wt% of MWNTs was explained by the phenomenon of agglomeration of MWNTs. It was noted that the improvement of hardness value of composite with 0.5 wt% fMWNTs after UV irradiation was specially high. It was different from other weight percentage's composite. In order to get more information about this phenomenon, the cross-section of 0.5 wt% fMWNT/PP was examined in a more detailed manner. The Vicker's hardness value of 0.5 wt% fMWNT/PP cross-section was shown in Fig. 65. This would help explain the effect of UV irradiation.

	fMWNT (wt%)	**Vickers hardness (Hv)**	**Improvement (%)**
Pre UV irradiation	0	9.05±0.16	0
	0.5	9.54±0.15	5.45
	1	10.17±0.15	12.42
	1.5	10.99±0.17	21.44
	2	10.20±0.11	12.75
Post UV irradiation	0	8.89±0.10	0
	0.5	9.95±0.23	11.93
	1	10.35±0.12	16.43
	1.5	11.00±0.17	23.78
	2	10.33±0.16	16.28

Table 11. The value of Vickers hardness of the composite samples

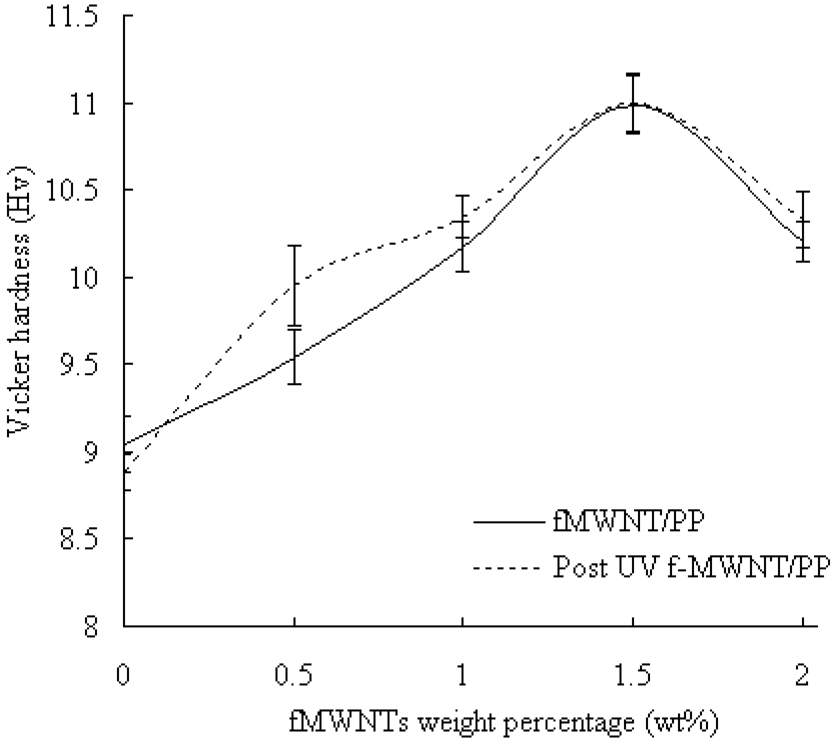

Fig. 64. The Vickers hardness of the composite samples

Fig. 65 showed that the Vicker's hardness value of 0.5 wt% fMWNT/PP cross-section was a "U" shape against the distance from sample surface. It implied that UV irradiation only changed the microstructure of the composite surface, and hardened the outermost surface of the sample. This hardened layer resembled a layer of protection to the composites. At low fMWNTs concentration (e.g. 0.5 wt%), UV was able to penetrate into the inner part of the composite. Thus, the hardness between the inner and outer part was not the same. The hardened layer was the dominating part to strengthen the composite across the cross-section. For the higher fMWNTs concentration, it was not easy for UV to penetrate into the inner part of the composite. The hardened layer reached the threshold with very thin region and resulted in a very limited reinforcement effect after UV irradiation. The result of the Vicker's hardness value of fMWNT/PP cross-section also provided a possible reason to explain why the difference between Young's modulus of the composite samples narrowed down and reached a similar value 1.5wt% of fMWNTs before and after UV irradiation.

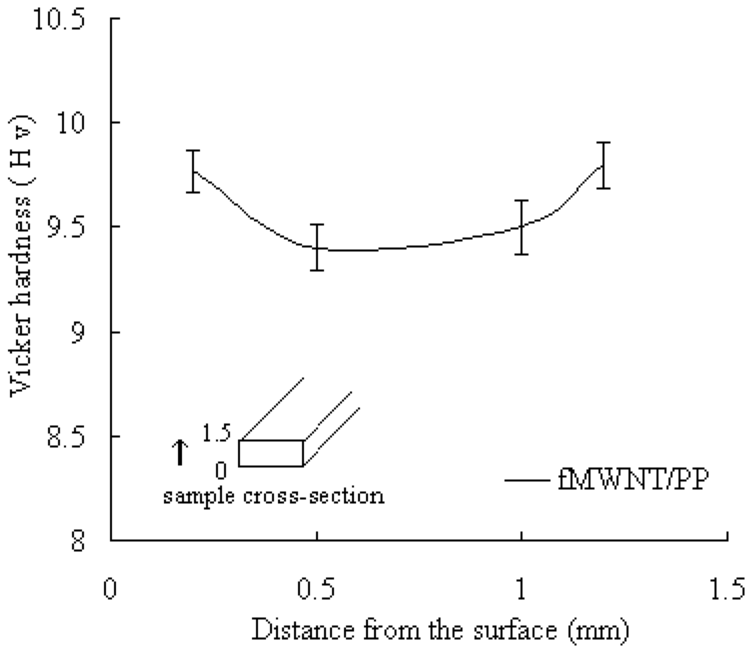

Fig. 65. The Vickers hardness value against the cross section distance of 0.5wt% fMWNT/PP.

6.4 Thermogravimetry Analysis (TGA)

The thermal stability of the composites can be illustrated by thermogravimetric analysis (TGA). The temperature at the maximum weight loss in differential thermogravimetric (DTG) curve indicates the thermal stability. Setaram Labsys TG-DTA/DSC (the accuracy was ±1 μg) system was used for TGA. The samples (about 5mg) were heated from 25 ^{o}C to 600 ^{o}C at a rate of 10^{o}C/minute with the flow of nitrogen. Fig. 66 illustrated the DTG curves of the composite samples. CNTs had extremely high thermal conductivity [81-82]. The uniformity of the dispersion of fMWNTs resulted in higher thermal conductivity of the composite, therefore higher thermal stability [83]. The general patterns of the curves were similar meaning that all the composite have gone through a similar decomposition process.

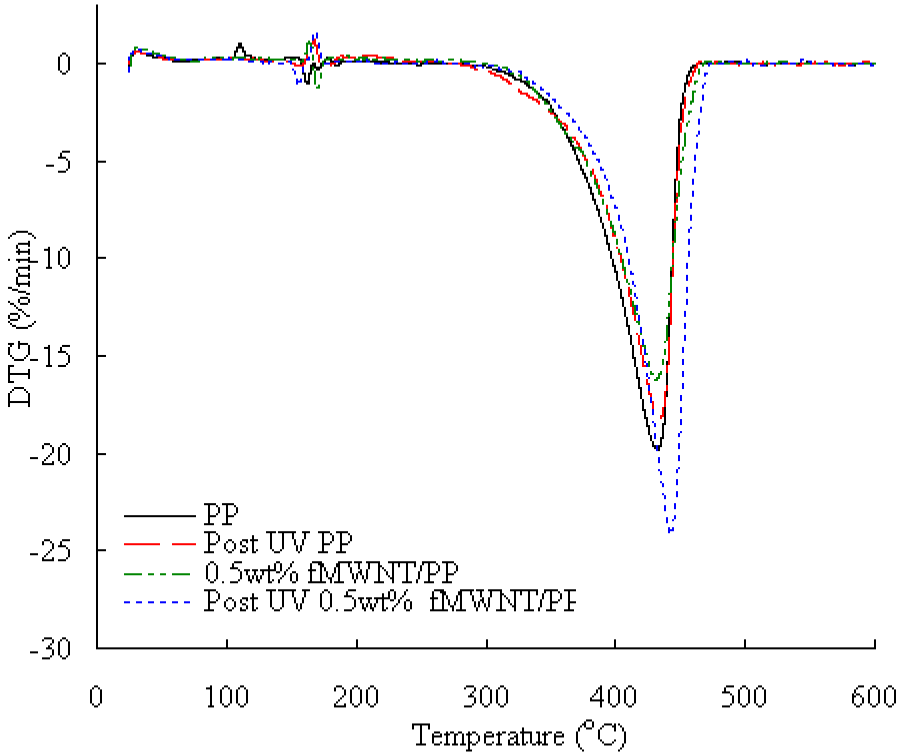

Fig. 66. The differential thermogravimetric (DTG) curves of the composite samples.

The thermal decomposition temperature of neat PP, post UV irradiation PP, 0.5wt% fMWNT/PP and post UV irradiation 0.5wt% fMWNT/PP were 432.4^{o}C, 433.79^{o}C 431.54^{o}C and 442.22 ^{o}C respectively. Results showed that the thermal stability values of the samples only showed a small change in post UV irradiation PP and pre UV irradiation fMWNT/PP. After UV irradiation, the thermal stability of 0.5 wt% fMWNT/PP increased by around 10^{o}C. The change of this thermal stability led to an indication that the microstructure fMWNT/PP had changed after UV irradiation. As Najafi et al. [17] reported that the radiation of UV-ozone on MWNTs under an ambient condition oxidized the surfaces of the nanotubes, it was believed that the UV irradiation induced the formation of chemical bonding between fMWNTs and PP polymer chains. The hardening effect of the outermost layer of the fMWNT/PP could also be explained by the UV oxidization of fMWNTs.

6.5 Differential Scanning Calorimetry (DSC)

Fig. 67 showed DSC curves of the composite samples with different conditions. The peaks around 160^{o}C were the melting peaks of the samples. The shapes of the peaks were consistent, and the widths of melting range were similar. There were no significant changes in the melting temperatures (T_m) (Table 12) for all composite samples. This result agreed with Valentini and Seo’s [95-96] findings. UV irradiation did not affect the melting temperature of the composite samples.

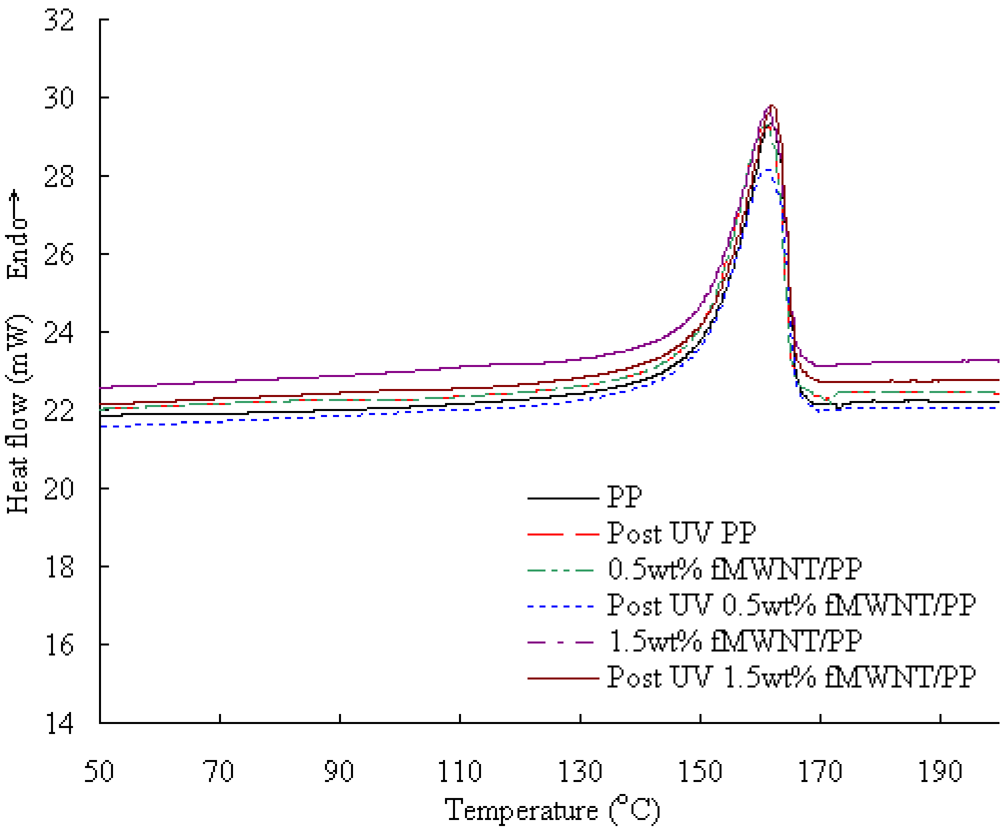

Fig. 67. The DSC curves of the composite samples

	fMWNTs (wt%)	**T_m (^{o}C)**
Pre UV irradiation	0	161.83
	0.5	161.00
	1.5	161.50
Post UV irradiation	0	161.67
	0.5	161.33
	1.5	162.17

Table 12. Melting temperature (T_m) of the composite samples by DSC tests

6.6 Scanning Electron Microscope (SEM) observation

Fig. 68 to Fig. 73 showed the SEM images of the fracture surfaces of the composite samples after tensile tests. The white lines in the SEM images Fig. 69 to Fig. 73 were the fMWNTs which reflected their high electrical conductivity properties. It was obvious that the failure pattern of pre UV irradiation PP was very different from the others. The fracture surface of pre UV irradiation PP was relatively smooth, but the fracture surfaces of fMWNT/PP and post UV irradiation fMWNT/PP were very rough. The roughness of the fracture surface was related to the ductility of composite. More brittle sample would have rougher fracture surface. The similar failure patterns of Fig. 69, Fig. 70 and Fig. 72 implied they should have similar failure mechanism and strength. In fact, the results of tensile test and hardness test of fMWNT/PP and MWNT/PP were different. This was explained by higher magnification (15000X) of SEM images (Fig. 71 and Fig. 73). Although the failure patterns of the pre and the post UV irradiation fMWNT/PP was similar in a macroscopic view, they were different under microscope.

Fig. 73 showed that more fMWNTs were torn off than in Fig. 71. This could be illustrated by the bonding formed between the fMWNTs and PP polymer chains. After UV irradiation, the oxidized defect site and function groups on fMWNTs were able to form bonding with the polymer chains. When the tensile force was applied to the test sample, the tensile stress was transferred from the polymer chains to the fMWNTs. As a result, the fMWNTs were torn from the polymer matrix. fMWNTs were able to play the role of reinforcement. For the case of pre UV irradiation fMWNT/PP, it was observed that some fMWNTs were torn off, but the quantity was much smaller than the post UV irradiation sample. Thus, the reinforcing effect was smaller than the post UV irradiation's samples.

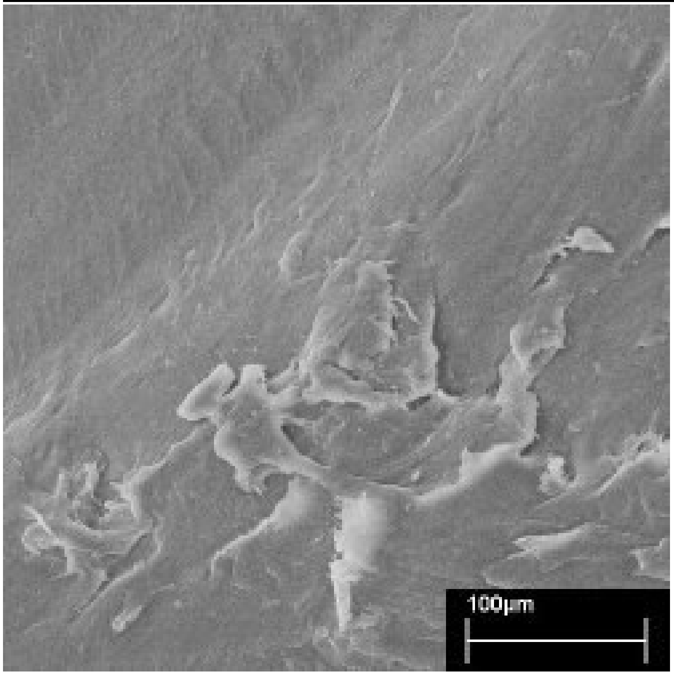

Fig. 68. SEM image of fractured surface of PP (500X)

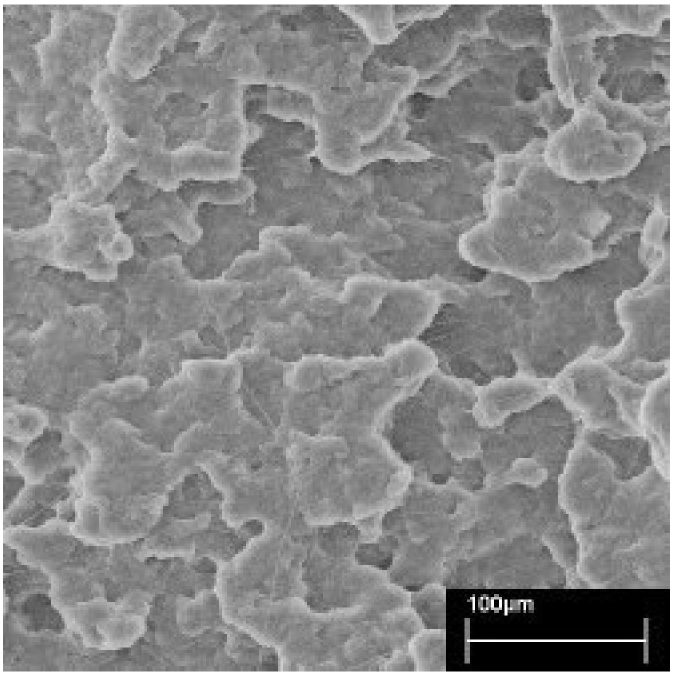

Fig. 69. SEM image of fractured surface of post UV PP (500X)

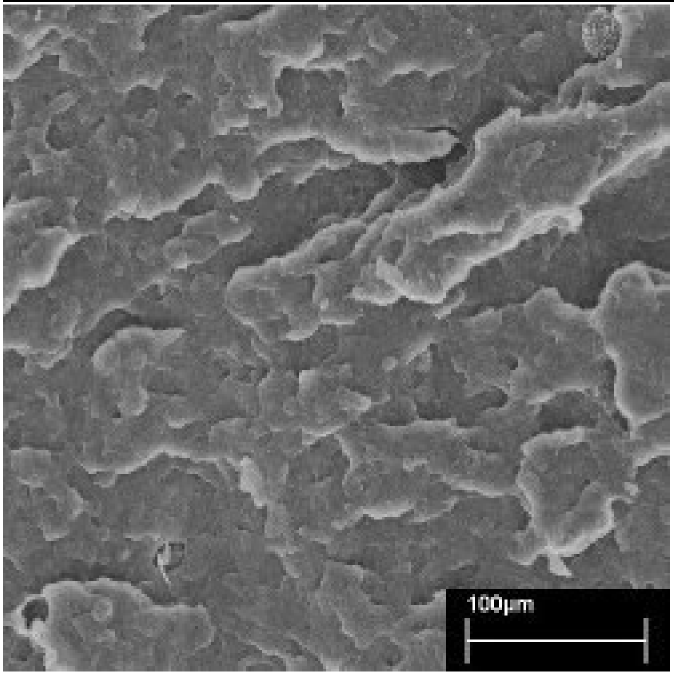

Fig. 70. SEM image of fractured surface of 0.5wt% fMWNT/PP (500X)

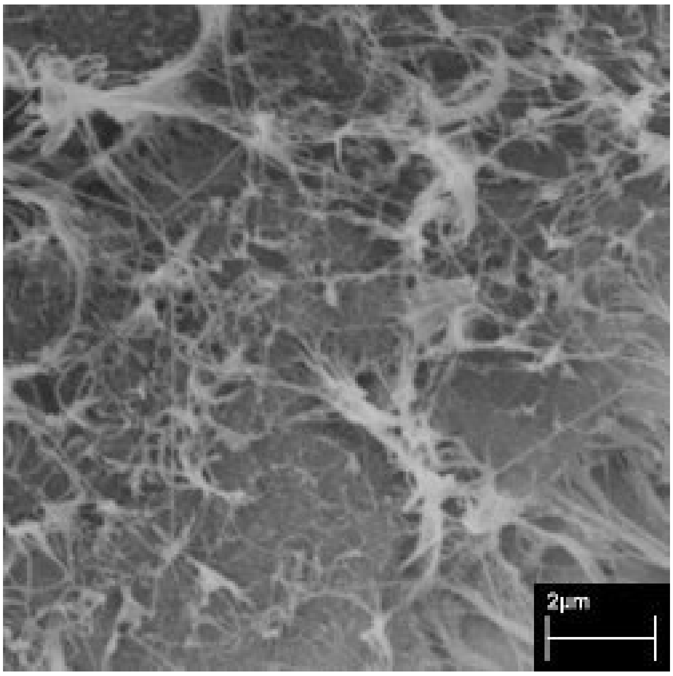

Fig. 71. SEM image of fractured surface of 0.5wt% fMWNT/PP (15000X)

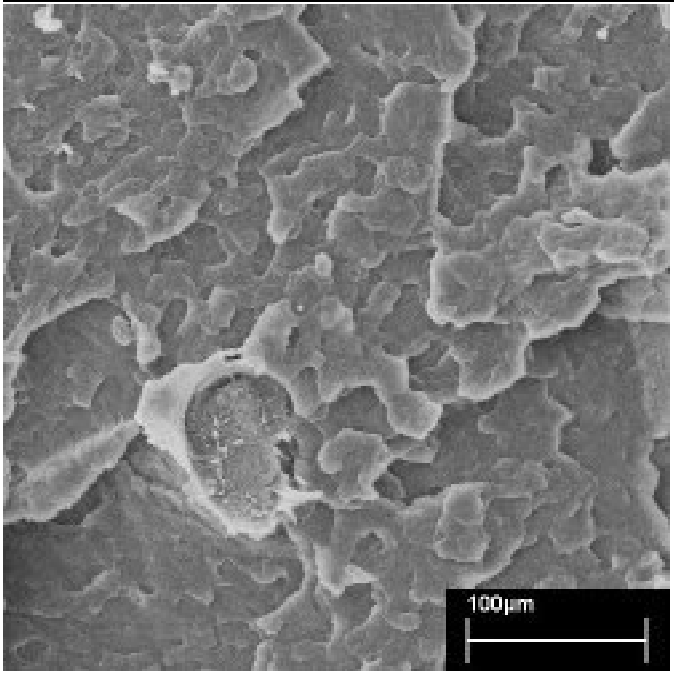

Fig. 72. SEM image of fractured surface of post UV 0.5wt% fMWNT/PP (500X)

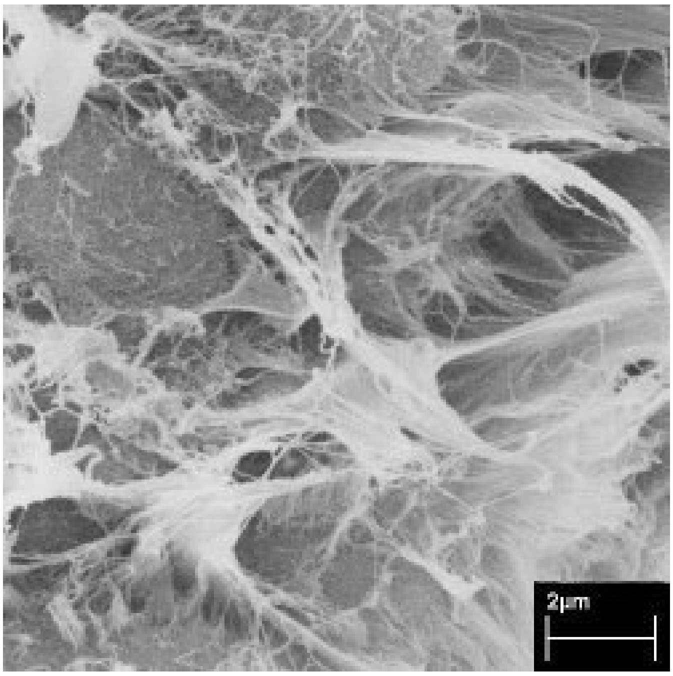

Fig. 73. SEM image of fractured surface of post UV 0.5wt% fMWNT/PP (15000X)

6.7 Theoretical study

This chapter would like to investigate the effects of UV exposure on fMWNT/PP composite. The theoretical calculation of mechanical properties of CNT/polymer composite had been developed in Section 4.7. Thus, it will not repeat the theoretical calculation in this section. This section would like to discuss about the mechanism of the UV effect on the composite. Fig. 74 showed the schematic diagram to illustrate the UV effect on fMWNT/PP composites.

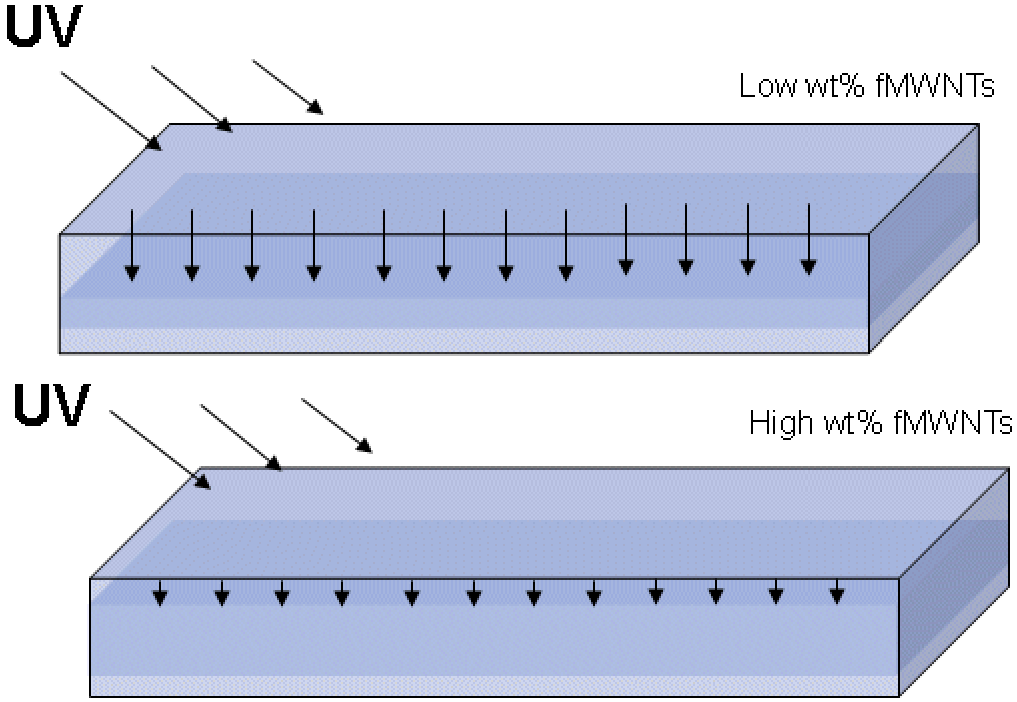

Fig. 74. Schematic diagram for the UV effect on fMWNT/PP composites

UV light would activate the COOH groups on the MWNTs surface [19, 96]. The COOH is thus energized to bond with the branch of PP polymer easily. For MWNTs, the carbon-carbon bond is very stable. Even after UV irradiation, MWNTs still cannot have enough energy to form bonding with other polymer molecules. Thus, it is easier for fMWNTs to have chemical reaction with polymer. Due to this reason, fMWNTs was selected to fabricate the composite samples in this chapter.

At low concentration of fMWNTs, UV can penetrate into the core of the composite. The region of the composite that contact with UV will have formed more cross-linkage and the hardened layer will be thicker. On the other hand, the UV cannot penetrate into the deep core of the composite for high concentration of fMWNTs. Thus, the effect of UV will be higher for low concentration of fMWNTs but not for high concentration of fMWNTs.

6.8 Discussion

In this study, the effects of UV irradiation on fMWNTs reinforced polymer composites were investigated. Through the mechanical and thermal property analysis, it was found that a low concentration of fMWNTs has better reinforcement performance to PP after UV irradiation. In addition, UV irradiation could form a protective layer on the composites. SEM images also illustrated the reinforcement mechanism of pre and post UV irradiation composites. The result of hardness value across the cross section of the samples in the form of a “U” shape provided evidence that UV could not penetrate into the core of the samples. It also found that, the concentration of fMWNTs could affect the penetration of UV in the composites. In application, CNTs could be used as an agent to protect against UV irradiation as mentioned by literature [17].

The result of this chapter could contribute to the idea of UV protection coating. At the beginning of this chapter, it was mentioned that UV degradation had been a critical problem for polymers. If the CNT/polymer coating on the outdoor application can be put to effective, it possesses three features: (i) UV shield and (ii) Mechanical strengthening and (iii) Light in weight. The CNT/polymer composite would be certainly suitable for applying in sport’s brackets, motorcar’s shell body and etc.

Chapter 7 Conclusions and Suggestions for Future Work

This study has focused on the development of CNT-reinforced polymer composites. The fabrication skills of the composite were successfully developed. CNTs can improve the mechanical performance of a polymer composite. Functionalization of CNTs can further improve the dispersion and interfacial bonding with a polymer matrix. It was also found that the concentration of the CNTs will affect the absorption of UV light by the composite. Moreover, CNTs can act as absorbers of UV irradiation and protect the inner parts of the composite. CNT-reinforced polymer composites would be applicable in outdoor activities, such as sport equipment.

7.1 Conclusions

Throughout a series of experiments and tests, the fabrication skills for CNT-reinforced polymer composites were developed. Although the fabrication procedures of CNT/thermoset and CNT/thermoplastic are completely different, the main factor that affects the quality of the composite remains the dispersion quality of CNTs. For the solvent-solution mixing composite fabrication process, CNTs were dispersed inside the solvent by an ultra-sonicator. The sonication time was directly related to the dispersion of CNTs inside the polymer matrix in a liquid state. However, sonication for too long or with excess power will damage the CNTs tube body. The best duration of sonication was between 2-3 hours. In addition, Chapter 4 mentioned that the reduction of viscosity of the polymer matrix would also improve the dispersion of CNTs. It was found that the heating of CNT/resin mixture reduced the viscosity of the mixture so that the CNTs can disperse more homogenously into the resin. The heating also helped to evaporate the residues solvent which can weaken the mechanical properties of the composite.

In the melt mixing composite fabrication process, the per-mixing of CNTs and polymer pellets helped to improve the dispersion quality of the CNTs. The gap between the extrusion screws is in millimeter scale, it is relatively large for dispersing the nano-scale CNTs agglomerates. The polymer pellets acted as balls in ball milling during per-mixing. Polymer pellets can break down the CNTs agglomerates into a smaller scale and enhance the dispersion quality of CNTs. After per-mixing, the quality of the composite was obviously better than the one that without per-mixing. Thus, per-mixing is a very important treatment for CNT/thermoset composites.

Beside the sonication, heating and per-mixing of CNTs polymer mixtures, functionalization of CNTs is a critical treatment for CNTs to improve both the dispersion of CNTs and the interfacial bonding between CNTs and polymers. As Section 3.2.4 mentioned, sonication functionalization is a suitable method to functionalize the CNTs since it is relatively milder than reflux functionalization. Reflux functionalization involves using heat energy to break the carbon-carbon bond of the CNTs tube’s body. If the energy is high, many carbon-carbon bonds will be broken at the same moment. However, sonication functionalization just uses mechanical force to make the defect site on the CNTs tube’s body easier for the acid to open and oxidize. Functionalized CNTs are much easier to disperse in the resin solution. The dispersed functionalized CNTs are suspended in the mixture for a longer time. The dispersion of functionalized CNTs is also more homogeneous when compared with the non-functionalized CNTs. As Chapter 4 mentioned, dispersion of the CNTs is very important for reinforcing the composite. The agglomeration of CNTs will affect the mechanical properties of the composite as the agglomeration will slip inside the composite and finally the CNTs will not be able to bear the load transferred from the polymer. By functionalization, the size and number of CNTs agglomerations is reduced. This is an important first step in the fabrication of a high performance CNTs composite.

The experiments in Chapter 4 and Chapter 5 showed that CNT-reinforced polymer composites have at least 20% Young’s modulus and hardness improvement. Both SWNTs and MWNTs provide similar reinforcement improvements. This agrees with the literature which suggests [92] that there is no distinct difference between using SWNTs and MWNTs as reinforcements. It is very clear that using CNTs can improve the mechanical properties of the composite, but it is not good enough to indicate the best use of the novel properties of CNTs. The agglomeration of CNTs is still happened inside the composite and the interfacial bonding between CNTs and polymer is not good enough. Through thermal analysis, the glass transition temperature and decomposition temperature were not changed very much which implies the chemical bonding in the composite system was not changed very significantly. The inert characteristics of CNTs make it difficult to bond them with polymer chains. SEM images also showed that many CNTs formed clusters and they were pulled out from the polymer matrix. Therefore, the non-functionalized CNTs are not good enough for fabricating high performance CNT-reinforced polymer composites.

For the reasons above, functionalization of CNTs was introduced into this study. By functionalizing CNTs, a very promising improvement of mechanical properties was achieved. There is about a 40% improvement of Young’s modulus by only using 1 wt% of fSWNT in epoxy. There was also about a 25% improvement of Young’s modulus by using 1.5 wt% of fMWNT in PP. By the SEM observation, functionalizing the CNTs caused a great improvement of dispersion of CNTs. In addition, functionalized CNTs were able to form cross-links with a polymer matrix, thus, enhancing the stress transfer efficiency between CNTs and the polymer matrix. The SEM observations showed a good agreement with the mechanical test results. The mechanical properties of the composite were greatly improved by adding functionalized CNTs when compared with the addition of non-functionalized CNTs. Functionalization of CNTs enhanced the dispersion and interfacial bonding between CNTs and polymer chains. Functionalization of the CNTs provided a prospective method for reinforcing the polymer. Functionalization of CNTs may play an important role in the further development of CNTs reinforced composites.

The effect of UV on functionalized and non-functionalized MWNT/PP was also studied by a series of experiments. UV light can energize the function group of CNTs and bond with the polymer chains. The concentration of the CNTs will affect the penetration of UV irradiation, and a lower concentration of the CNTs would produce a thicker layer of bonded fMWNT – PP; and the other way round. This layer of bonding is stronger than the inter part of the composite and it could act as protection layer. In addition, CNTs are also good UV absorbers. The CNT-reinforced polymer composites can also used as a UV protection coating for outdoor applications.

In conclusion, CNTs would be a potential candidate for reinforcing polymers. The unique properties of CNTs make them a multi-functional filler for fabricating composites. At this moment, the novel properties of CNTs are not fully unitized yet. More studies are needed to make CNTs dispersion easier and to improve bonding with polymer chains. If CNTs can perfectly bond with the polymer chains, the reinforcement performance would as good as describe from rules of mixture.

7.2 Suggestions for future work

With the previous experience of fabricating CNT/thermoset and CNT/thermoplastic composites, the direction for further fabrication of other CNTs composite should be clearer. The dispersion and interfacial bonding issues of CNTs need to be totally solved in order to best use the novel properties of CNTs. These issues are mainly caused by chemical factors, such as the electrostatic balance of CNTs tube bodies and the compatibility of the functional groups with the polymer chains. The most promising method to solve these problems may be functionalization of CNTs. One potential area worth further study would be a simplified functionalization process and shortened duration of functionalization. Besides studying the chemical techniques for CNTs, the process of fabrication of CNT-reinforced polymer composites is also worth further study. A method for mass production of CNT-reinforced polymer composites is needed so as to broaden the use of CNTs.

Thermoplastics would be more suitable to be the matrix of CNTs reinforced composites on an industrial scale, as most factories would probably prefer to use melting-mixing to fabricate their products. Melting-mixing is flexible, allowing processing by extrusion, injection molding, blow molding etc. Different shapes of CNTs composites could be formed such as thin films, block shapes and fibers. Among of these forms, CNT-reinforced thermoplastic fibers would be preferred for the following reasons:

1. Thermoplastic is easy to recycle;
2. Fiber would be more flexible for further applications (Fig. 75);
3. Fiber can be used to form laminate structures; and
4. More constraints to control the orientation of the CNTs while fabricating fiber.

In fact, some companies [99-100] would recycle PET bottles and fabricate them into fabrics for other uses, for example, carpets.

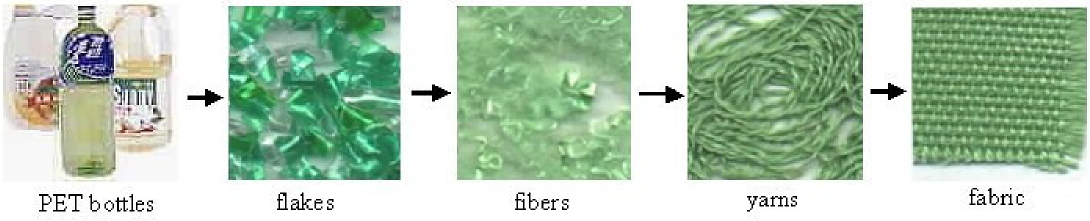

Fig. 75. Recycling of PET bottles [100]

Melt-mixing would avoid the use of solvents and eliminate the contamination problem that solution-mixing involves. The dispersion of CNTs would be enhanced by the use of high-shear mixing and longer processing times. According to the literature [101], the CNTs can be aligned by the elongational flow. By adding a long orifice to increase the flow traveling distance, it is possible to enhance the alignment of the CNTs. The viscosity of the CNTs polymer liquid should be reduced to make aligning the CNTs easier. The degree of alignment for CNTs is related to the stiffness of the CNT/PET composite. Thus, a factor of degree of alignment of CNTs may be incorporated in the Halpin-Tsai equation. Ideally, it will become possible to apply a simple rule of mixture (equation 8) in the well-aligned CNT-reinforced polymer composites [102]. Single-screw extruders and double-screw extruders could be used. By using this method, it may become possible to transfer this technique into the plastic industries. In addition, this method creates the prospect of recycling thermoplastic composites and creating an environmental friendly use of plastic.

7.3 Industrial applications

Large amount of studies [7-10, 22-24, and 64-70] of CNT-reinforce polymer composite were carried out in the past decade, and it is believed that more research on CNTs will keep on doing in the future Through the extensive investigation of CNTs in the future, the dispersion and interfacial bonding problems of CNTs can be solved eventually. Sport rackets, protective equipments and surface coating are the potential applications of CNT-reinforce polymer composites in the manufacturing industry. Possessing its novel mechanical properties, CNTs could replace the traditional reinforcing materials such as glass fiber, carbon fiber and Kevlar in producing sport rackets and protective equipments to achieve light in weight but strong in strength properties.

The sport racket and hamlet can be manufactured by injection molding as mentioned in section 7.2, while the armor can be made by the CNTs composite fiber. Although the manufacturing cost of these equipments is higher than the one that uses traditional reinforcing materials, market for the high cost equipment still exists because the users of sport racket and armor are most probably professionals who are willing to pay higher price to get lighter and stronger equipments. In addition, the results in chapter 7 and other literatures [17, 19] showed that CNTs could resist UV irradiation. Thus, CNT-reinforced polymer composite can be used as protective coating against UV degradation in outdoor application, for example, the coating of pipeline and vehicle’s body. In addition, this layer of coating also provides mechanical protection to the subject. The results from section 4.3 and 5.3 illustrated that the adding of CNTs showed an improvement in hardness value. The increased hardness helps avoid the subject being scratched. In short, CNTs could replace the role of traditional reinforcing materials in sport and protection equipments areas.

References

[1] Fiedler B., Gojny F.H., Wichmann M.H.G., Nolte M. C.M. and Schulte K. , Fundamental aspects of nano-reinforced composites, Comp Sci & Tech, 66 (2006) , pp.3115-3125

[2] S. Iijima, Helical microtubules of graphitic carbon, Nature, 354 (1991), p. 56-59

[3] M. M. J. Treacy, T. W. Ebbesen, and J. M. Gibson, Exceptionally high Young's modulus observed for individual carbon nanotubes, Nature (London), 381 (1996), pp.678 – 680

[4] P. Poncharal, Z. L. Wang, D. Ugarte, and W. A. de Heer, Nanobeam Mechanics: Elasticity, Strength, and Toughness of Nanorods and Nanotubes, Science, 283 (1999), pp.1513-1517

[5] R. Haggenmueller, H.H. Gommans, A.G. Rinzler, J.E. Fischer and K.I. Winey, Aligned single-wall carbon nanotubes in composites by melt processing methods, Chem Phys Lett, 330 (2000), pp. 219–225

[6] B. Fiedler, H. Gojny, M.H.G. Wichmann, M.C.M. Nolte and K. Schulte, Fundamental aspects of nano-reinforced composites , Comp. Sci & Tech., 66 (2006), pp.3115-3125

[7] P.J.F. Harris, Carbon nanotube composites, Int Mat Reveiws, 49(2004), pp.31-43

[8] K.T. Lau, S.Q. Shi and H.M. Cheng, Micro-mechanical properties and morphological observation on fracture surfaces of carbon nanotube composites pre-treated at different temperatures, Comp Sci & Tech, 63 (2003), pp.1161-1164

[9] E. T. Thostenson, Advances in the science and technology of carbon nanotubes and their composites: a review, Comp Sci & Tech, 61 (2001), pp.1899-1912

[10] D. Qian, E. C. Dickey, R. Andrews and T. Rantell, Load transfer and deformation

mechanisms in carbon nanotube-polystyrene composites, Appl Phys Lett, 76 (2000), pp. 2868–2870

[11] X.L. Xie, Y.W. Mai and X.P. Zhou, Dispersion and alignment of carbon nanotubes in polymer matrix: A review, Mat Sci & Engg, R49 (2005) pp. 89-112

[12] P. M. Ajayan, L. S. Schadler, C. Giannaris and A. Rubio, Single-walled carbon nanotube-polymer composites: Strength and weakness, Adv Mat, 12(2000), pp. 750 – 753

[13] B. W. Smith, Z. Benes, D. E. Luzzi, and J. E. Fischer, Structural anisotropy of magnetically aligned single wall carbon nanotube films, Appl Phys Lett, 77 (2000), pp. 663-667

[14] Y. Chen, D.T. Shaw and L. Guo, Field emission of different oriented carbon nanotubes, Appl Phys Lett, 76 (2000), pp. 2469-2472

[15] H.H. Gommans, J.W. Alldredge, H. Tashiro, J. Park, J. Magnuson and A.G. Rinzler, Fibers of aligned single-walled carbon nanotubes: Polarized Raman spectroscopy, J Appl Phys, 88 (2000), pp. 2509-2513

[16] R. Sen, B. Zhao, D. Perea, M.E. Itkis, H. Hu, J. love, E. Bekyarova and R.C. Haddon, Preparation of Single-Walled Carbon Nanotube Reinforced Polystyrene and Polyurethane Nanofibers and Membranes by Electrospinning, NanoLetters, 4 (2004), pp. 459-465

[17] E. Najafi, J.Y. Kim, S.H. Han and K. Shin, UV-ozone treatment of multi-walled carbon nanotubes for enhanced organic solvent dispersion, Coll. and Surf. A: Physicochemical and Engineering Aspects, 284-285(2006), pp. 373-378

[18] M.L. Sham and J.K. Kim, Surface functionalities of multi-wall carbon nanotubes after UV/Ozone and TETA treatments, Carbon, 44(2006), pp.768-777

[19] E. Najafi and K. Shin, Radiation resistant polymer–carbon nanotube

nanocomposite thin films, Colloids and Surfaces A: Physicochemical and Engineering Aspects, 257-258 (2005), pp. 333-337

[20] J. Li, M.L. Sham, J.K. Kim, and G. MaromMorphology and properties of UV/ozone treated GNP/epoxy nanocomposite, Comp Sci & Tech, 67 (2007), pp. 296-305

[21] T. Kimura, H. Ago and M. Tobita, Polymer Composites of Carbon Nanotubes Aligned by a Magnetic Field, Adv Mat, 14 (2002), p. 1380

[22] P. M. Ajayan, O. Stephan, C. Colliex, and D. Trauth, Aligned Carbon Nanotube Arrays Formed by Cutting a Polymer Resin-Nanotube Composite, Science, 265 (1994), p. 1212

[23] F. H. Gojny, M. H. G. Wichmann, U. Köpke, B. Fiedler and K. Schulte, Carbon nanotube-reinforced epoxy-composites: enhanced stiffness and fracture toughness at low nanotube content,Comp Sci & Tech, 64 (2004), pp.2363-2371

[24] B. Vigolo, A. Pénicaud, C. Coulon, C. Sauder, R. Pailler, C. Journet, P. Bernier and P. Poulin, Macroscopic Fibers and Ribbons of Oriented Carbon Nanotubes, Science, 290 (2000), p. 1331.

[25] C.A. Cooper, D. Ravich, D. Lips, J. Mayer and H.D. Wagner, Distribution and alignment of carbon nanotubes and nanofibrils in a polymer matrix, Comp Sci & Tech, 62 (2002), p. 1105

[26] M. Zhang, S. Fang, A.A. Zakhidov, S.B. Lee, A.E. Aliev, C.D. Williams, K.R. Atkinson, and R.H. Baughman, Strong, Transparent, Multifunctional, Carbon Nanotube Sheets, Science, 307 (2005), pp. 1215-1219

[27] C. Park, Z. Ounaies, K. A. Watson, R. E. Crooks, J. Smith, S. E. Lowther, J. W. Connell, E. J. Siochi, J. S. Harrison and T. L. St Clair, Dispersion of single wall carbon nanotubes by in situ polymerization under sonication,Chem Phys Lett,

364(2002), pp.303-308

[28] D.S. Bethune, C.H. Kiang, M.S. Devries, G. Gorman, R. Savoy and J. Vazquez et al., Cobalt-catalyzed growth of carbon nanotubes with single-atomic-layerwalls, Nature, 363 (1993), pp. 605–607

[29] S. Iijima and T. Ichihashi, Single-shell carbon nanotubes of 1-nm diameter, Nature, 363 (1993), pp. 603–605

[30] K. Balasubramanian and M. Burghard, Chemically Functionalized Carbon Nanotubes, Small, 1 (2005) , pp.180 – 192

[31] M. Yu, O. Lourie, M.J. Dyer, T.F. Kelly and R.S. Ruoff, Strength and breaking mechanism of multiwalled carbon nanotubes under tensile load, Science, 287 (2000), pp. 637–640

[32] J.W. Che, T. Cagin and W.A. Goddard, Thermal conductivity of carbon nanotubes, Nanotechnology 11 (2000), pp. 65–69

[33] M.A. Osman and D. Srivastava, Temperature dependence of the thermal conductivity of single-wall carbon nanotubes, Nanotechnology, 12 (2001), pp. 21–24

[34] S. Berber, Y. Kwon and D. Tománek, Unusually high thermal conductivity of carbon nanotubes, Phys Rev Lett, 84 (2000), pp. 4613–4616

[35] B.T. Kelly, Physics of graphite, Applied Science, London (1981)

[36] G. Overney, W. Zhong and D. Tomanek, Structural rigidity and low-frequency vibrational-modes of long carbon tubules, Z Phys D—At Mol Clusters, 27 (1993), pp. 93–96

[37] J.P. Lu, Elastic properties of single and multilayered nanotubes, J Phys Chem Solids, 58 (1997), pp. 1649–1652

[38] J.P. Salvetat, G.A.D. Briggs, J.M. Bonard, R.R. Bacsa, A.J. Kulik and T. Stockli

et al., Elastic and shear moduli of single-walled carbon nanotube ropes, Phys Rev Lett 82 (1999), pp. 944–947

[39] L. Jin, C. Bower and O. Zhou, Alignment of carbon nanotubes in a polymer matrix by mechanical stretching, Appl Phys Lett, 73 (1998), pp. 1197

[40] A. Haque and A. Ramasetty, Theoretical study of stress transfer in carbon nanotube reinforced polymer matrix composites, Comp Struct, 71(2005), pp.68-77

[41] R. Andrews, D. Jacques, A.M. Rao, T. Rantell, F. Derbyshire, Y. Chen, J. Chen and R.C. Haddon, Nanotube composite carbon fibers,Appl Phys Lett, 75 (1999), pp. 1329-1333

[42] J. Foster, S. Singamaneni, R. Kattumenu and V. Bliznyuk, Dispersion and phase separation of carbon nanotubes in ultrathin polymer films, J Colloid and Interface Sci, 287(2005), pp.167-172

[43] K.T. Lau, M. Lua, C.K. Lam, H.Y. Cheung, F.L. Sheng and H.L. Li, Thermal and mechanical properties of single-walled carbon nanotube bundle-reinforced epoxy nanocomposites: the role of solvent for nanotube dispersion, Comp Sci & Tech, 65 (2005), pp. 719-725

[44] J. Chen, M.A. Hamon, H. Hu, Y. Chen, A.M. Rao, P.C. Eklund and R.C. Haddon, Solution Properties of Single-Walled Carbon Nanotubes, Science, 282 (1998), pp. 95-99

[45] A. Eitan, K.Y. Jiang, D. Dukes, R. Andrews, and L.S. Schadler, Surface Modification of Multiwalled Carbon Nanotubes: Toward the Tailoring of the Interface in Polymer Composites, Chem Mater,15 (2003), pp. 3198-3201

[46] J. Zhu, J.D. Kim, H. Peng, J.L. Margrave, V.N. Khabashesku and E.V. Barrera, Improving the Dispersion and Integration of Single-Walled Carbon Nanotubes in

Epoxy Composites through Functionalization, Nanoletters, 3 (2003), pp. 1107–1113

[47] M. Holzinger, J. Abraha, P. Whelan, R. Graupner, L. Ley, F. Hennrich, M. Kappes and A. Hirsch, Functionalization of Single-Walled Carbon Nanotubes with (R-)Oxycarbonyl Nitrenes, J Am Chem Soc, 125 (2003), pp. 8566-8569

[48] T. Tiano, M. Roylance and J. Gassner, Functionalization of single-wall nanotubes for improved structural composites, 32nd SAMPE Conf, 2000, pp.192-199

[49] C. Velasco Santos, A.L. Martinez Hernandez, M. Lozada Cassou, A. Alvarez Castillo and V.M. Castano, Chemical functionalization of carbon nanotubes through an organosilane, Nanotechnology, 13 (2002), pp. 495-499

[50] A. Dufresne, M. Paillet, J.L. Putaux, R. Canet, F. Carmona, P. Delhaes and S. Cui, Processing and characterization of carbon nanotube/poly(styrene-co-butyl acrylate) nanocomposites, J Mater Sci, 37 (2002), pp. 3915-3719

[51] K.T. Lau, Interfacial bonding characteristics of nanotube/polymer composites, Chem Phys Lett, 370(2003), pp.399-405

[52] L. Jin, C. Bower and O. Zhou, Alignment of carbon nanotubes in a polymer matrix by mechanical stretching, Appl Phys Lett, 73 (1998), pp. 1197–1199

[53] M.S.P. Shaffer and A.H. Windle, Fabrication and characterization of carbon nanotube/poly(vinyl alcohol) composites, Adv Mater, 11 (1999), pp. 937–941

[54] A. Dufresne, M. Paillet, J.L. Putaux, R. Canet, F. Carmona and P. Delhaes et al., Processing and characterization of carbon nanotube/poly(styrene-co-butyl acrylate) nanocomposites, J Mater Sci, 37 (2002), pp. 3915–3923

[55] F. Dalmas, L. Chazeau, C. Gauthier, K. Masenelli-Varlot, R. Dendievel and J.Y. Cavaillé et al., Multiwalled carbon nanotube/polymer nanocomposites: processing and properties, J Polym Sci Part B: Polym Phys, 43 (2005), pp.

1186–1197

[56] Q.Q. Li, M. Zaiser and V. Koutsos, Carbon nanotube/epoxy resin composites using a block copolymer as a dispersing agent, Phys Status Solidi a—Appl Res, 201 (2004), pp. R89–R91

[57] T. Ogasawara, Y. Ishida, T. Ishikawa and R. Yokota, Characterization of multi-walled carbon nanotube/phenylethynyl terminated polyimide composites, Compos Part A: Appl Sci Manuf, 35 (2004), pp. 67–74

[58] O. Breuer and U. Sundararaj, Big returns from small fibers: a review of polymer/carbon nanotube composites, Polym Compos, 25 (2004), pp. 630–645

[59] R.E. Gorga and R.E. Cohen, Toughness enhancements in poly(methyl methacrylate) by addition of oriented multiwall carbon nanotubes, J Polym Sci Part B: Polym Phys, 42 (2004), pp. 2690–2702

[60] E.T. Thostenson and T.-W. Chou, Aligned multi-walled carbon nanotube-reinforced composites: processing and mechanical characterization, J Phys D: Appl Phys, (2002), pp. L77–L80

[61] Z. Jin, K. Pramoda, G. Xu and S.H. Goh, Dynamic mechanical behavior of melt-processed multi-walled carbon nanotube/poly(methyl methacrylate) composites, Chem Phys Lett, 337 (2001), pp. 43–47

[62] P. Potschke, A.R. Bhattacharyya, A. Janke and H. Goering, Melt mixing of polycarbonate/multi-wall carbon nanotube composites, Compos Interf, 10 (2003, pp. 389–404

[63] J.C. Kearns and R.L. Shambaugh, Polypropylene fibers reinforced with carbon nanotubes, J Appl Polym Sci, 86 (2002), pp. 2079–2084

[64] C. Velasco-Santos, A.L. Martinez-Hernandez, F.T. Fisher, R. Ruoff and V.M. Castano, Improvement of thermal and mechanical properties of carbon nanotube

composites through chemical functionalization, Chem Mater, 15 (2003), pp. 4470–4475

[65] K.W. Putz, C.A. Mitchell, R. Krishnamoorti and P.F. Green, Elastic modulus of single-walled carbon nanotube/poly(methyl methacrylate) nanocomposites, J Polym Sci Part B: Polym Phys, 42 (2004), pp. 2286–2293

[66] F.H. Gojny, J. Nastalczyk, Z. Roslaniec and K. Schulte, Surface modified multi-walled carbon nanotubes in CNT/epoxy-composites, Chem Phys Lett, 370 (2003), pp. 820-824

[67] A. Allaoui, S. Bai, H. M. Cheng and J. B. Bai, Mechanical and electrical properties of a MWNT/epoxy composite, Comp Sci & Tech, 62 (2002), pp. 1993–1998

[68] J.W. Xiong, Z. Zheng, X.M. Qin, M. Li, H.Q. Li and X.L. Wang, The thermal and mechanical properties of a polyurethane/multi-walled carbon nanotube composite, Carbon, 44 (2006), pp. 2701-2707

[69] J. Li, L.F. Tong, Z.P. Fang, A.J. Gu and Z.B. Xu, Thermal degradation behavior of multi-walled carbon nanotubes/polyamide 6 composites, Polym Degrad Stab, 91(2006), pp. 2046-2052

[70] K.A. Ananda, U.S. Agarwalb and R. Joseph, Carbon nanotubes induced crystallization of poly(ethylene terephthalate),Polymer, 47 (2006), pp.3976-3980

[71] M.W. Marshall, S. Popa-Nita and Joseph G. Shapter, Measurement of functionalised carbon nanotube carboxylic acid groups using a simple chemical process, Carbon, 44 (2006), pp.1137-1141

[72] I.M. Ward and J. Sweeney, The mechanical properties of solid polymers, Wiley (2004)

[73] W. Chen and X.M. Tao, Production and characterization of polymer

nanocomposite with aligned single wall carbon nanotubes, Appl Surf Sci, 252 (2005), pp.3547-3552

[74] C. Park, Z. Ounaies, K. A. Watson, R. E. Crooks, J. Smith, S. E. Lowther, J. W. Connell, E. J. Siochi, J. S. Harrison and T. L. St Clair, Dispersion of single wall carbon nanotubes by in situ polymerization under sonication, Chem Phys Lett, 364(2002), pp.303-308

[75] C. Liu ,H.T. Cong ,F. Li,P.H. Tan, H.M. Cheng, K. Lu, B.L. Zhou, Semi-continuous synthesis of single-walled carbon nanotubes by a hydrogen arc discharge method, Carbon, 37 (1999), pp.1865-1868

[76] F. Li, H.M. Cheng,, Y.T. Xing, P.H. Tan and G. Su, Purification of single-walled carbon nanotubes synthesized by the catalytic decomposition of hydrocarbons, Carbon, 38 (2000), pp. 2041-2045

[77] P.X. Hou, C. Liu, Y. Tong, S.T. Xu, M. Liu and H.M. Cheng, Purification of single-walled carbon nanotubes synthesized by the hydrogen arc-discharge method, J Mater Res, 16(2001), pp.2526-2529

[78] J. Liu, A.G. Rinzler, H. Dai, J.H. Hafner, R. K. Bradley, P.J. Boul, A. Lu, T. Iverson, K. Shelimov, C.B. Huffman, F. Rodriguez-Macias, Y.S. Shon, T. R. Lee, D.T. Colbert, R.E. Smalley, Fullerene Pipes, Science, 280 (1998), pp. 1253 – 1256

[79] L. S. Schadler, S. C. Giannaris, and P. M. Ajayan, Load transfer in carbon nanotube epoxy composites, Appl Phys Lett, 73 (1998), pp.3842-3844

[80] C.A. Mitchell, J.L. Bahr, S. Arepalli, J.M. Tour and R. Krishnamoorti, Dispersion of Functionalized Carbon Nanotubes in Polystyrene, Macromolecules, 35 (2002), pp. 8825 -8830

[81] L.X. Benedict, S.G. Louie and M.L. Cohen, Heat capacity of carbon nanotubes,

Solid State Commun 100 (1996), pp. 177.

[82] S. Berber, Y.K. Kwon and D. Tomanek, Unusually High Thermal Conductivity of Carbon Nanotubes, Phys Rev Lett, 84 (2000), pp. 4613-4616

[83] G.X. Chen, H.S. Kim, B.H. Park and J.S. Yoon, Multi-walled carbon nanotubes reinforced nylon 6 composites, Polymer, 47 (2006), pp. 4760-4767

[84] A. Omrani, A. A. Rostami and M. Ghaemy, Kinetics and thermal properties of epoxy resin cured with Ni(II)-tris-(O-pheneylendiamine) bromide, J Appl Poly Sci, 101 (2006), pp.1257 – 1265

[85] J.C. Halpin, S..W Tsai, Effects of environmental factors on composite materials. AFML-TR-67-423, June 1969

[86] M. Lu, K.T. Lau, J.C. Xu and H.L. Li, Coiled carbon nanotubes growth and DSC study in epoxy-based composites, Colloids and Surfaces A, 257-258 (2005), pp. 339-343

[87] H.L. Cox, The elasticity and strength of paper and other fibrous materials, Brit J Appl Phys ,3(1952), pp. 72–79

[88] Shenzhen Nanotech Port Co. Ltd, http://www.nanotubes.com.cn

[89] C. Park, Z. Ounaies, K. A. Watson, R. E. Crooks, J. Smith & S. E. Lowther et al, Dispersion of single wall carbon nanotubes by in situ polymerization under sonication, C Phys Lett, 364 (2002), pp.303-308

[90] Huntsman Advanced Materials, http://www.huntsman.com/

[91] Polymers: A Property Database, http://www.polymersdatabase.com/

[92] J.N. Coleman, U. Khan, W.J. Blau and Y.K.G. Ko, Small but strong: A review of the mechanical properties of carbon nanotube–polymer composites, Carbon, 44(2006), pp.1624-1652

[93] H.H. Horowitz and G. Metzger, A New Analysis of Thermogravimetric Traces,

Anal Chem 35 (1963), pp. 1464-1468

[94] M. Moniruzzaman, F.M. Du, N. Romero and K.I. Winey,Increased flexural modulus and strength in SWNT/epoxy composites by a new fabrication method, Polymer, 47(2006), pp. 293-298

[95] H. Kaczmarek, D. Odak, P. Malanowski and H. Chaberska, Effect of short wavelength UV-irradiation on ageing of polypropylene/cellulose compositions, Polym Degrad Stab, 88 (2005), pp.189-198

[96] K.C.C. Tse, F.M.F. Ng and K.N. Yu, Photo-degradation of PADC by UV radiation at various wavelengths, Polymer Degradation and Stability, 91 (2006), pp. 2380-2388

[97] L. Valentini, J. Biagiotti, J. M. Kenny and S. Santucci, Morphological characterization of single-walled carbon nanotubes-PP composites, Comp. Sci. & Tech. 63 (2003), pp.1149-1153

[98] M.K. Seo, J.R. Lee and S.J. Park, Crystallization kinetics and interfacial behaviors of polypropylene composites reinforced with multi-walled carbon nanotubes, Mat Sci & Engg, 404 (2005), pp.79-84

[99] Recycle of polymer, http://www.lotfi.net/recycle/plastic.html

[100] Recycle PET Fiber, http://www.hojo.com.tw/pet_fiber.htm

[101] M. Sennett, E. Welsh, J. B. Wright, W. Z. Li, J. G. Wen, Dispersion and alignment of carbon nanotubes in polycarbonate, 76 (2003), pp. 111-113

[102] S.L. Ruan, P. Gao and T.X. Yu, Ultra-strong gel-spun UHMWPE fibers reinforced using multiwalled carbon nanotubes, Polymer, 47 (2006), pp.1604-1611

Appendix

Experimental procedures of tensile test

1. The main power was turned on.
2. The testing machine was turned on.
   (both the power of back of machine, portable control)
3. The computer was turned on
4. The software “Testwork 4” was launched.
5. Tensile test method as used: Open method > tensile > simplified tensile
6. Data aqr: 10Hz, speed: fast for metal (3mm/min); slow for plastic
   i. The unit can be changed as follow: Method > edit method > global unit
   ii. The test method can be changed as follow: Method > open methods
7. Disable “return to zero” by Method > test flow
8. Sample attached to the machine by follow:
   i. The upper part was clamped first
   ii. “Down” button of the portal control was pressed, and the fine tune can be used.

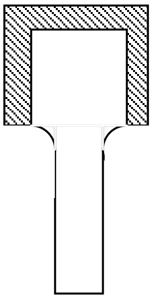

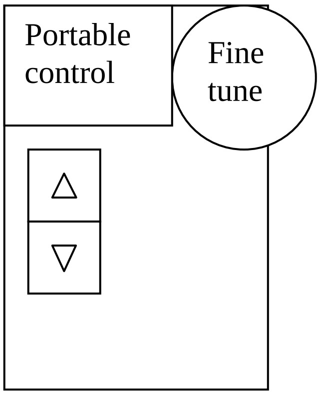

   iii.
9. Zero of the channel was set. (right click in the channel)
10. Pre-load was set (~80N for metal)
11. Start button was pressed.
12. The data was saved:
   i. print preview > save
   ii. export > specimen
   iii. export > sample
   iv. right click in the graph > save picture

Experimental procedures of thermogravimetric analysis

1. The cooling water was turned on to allow the water flow into the machine. (half open, ~45°, near the window)
2. The power of the machine was turned on. (back of the machine)
3. The pipe of air/ oxygen/ Ar was connected to the machine.
4. The valve of bottle of the supply gas was turned to ~2.
5. The tap of the gas supply was turn on such that the liquid indication is in around 30-40 at indication pipe.
6. The sample was weighed and place into a crucible.
7. The furnace was opened by operating the switch in front of the machine.
8. The crucible was placed on the top of the rod by a tweezer.
9. The rod was stabilized before the furnace was closed.
10. Computer was turned on.
11. 3 programmes can be used in the folder Setsoft.
12. Collection > control the experimental set up
    Database > file management
    Processing > Data output
13. The machine was cool down before turning off (<25°C)

Collection

1. Experiment > Data collection > OK
2. “Catalog” was pressed to choose the pre-saved experiment procedures. Otherwise go to step 3.
3. The sequence of the experiment can be modify to suit for different needs.
   Ramp: heating…
   Isotherm: ….
   Valve should be open: oooo oooo
   Data was saved (ticked), tare was ticked
4. “save as” was press to save the experiment sequence if needed. (Type the required information when new window was pop up.
5. “to experiment” was pressed to start the experiment and filled in the required data.
6. Displace > Real time drawing > LABSYS TG-TG

Processing

1. Experiment > open an experiment> search the files > OK
2. Palette icon was clicked.
3. The interested signal was double clicked. (e.g. time, TG)
4. “Extract data point” was 50
5. Data were exported to a text file

Experimental procedures of differential scanning calorimetry

1. Machine was turn on the
2. Pyris Manager > start pyres > data analysis > click “offline” to make DSC online
3. Two similar weight empty pans were found (Baseline testing was done first.). The pans were put into the DSC machine station as follow:

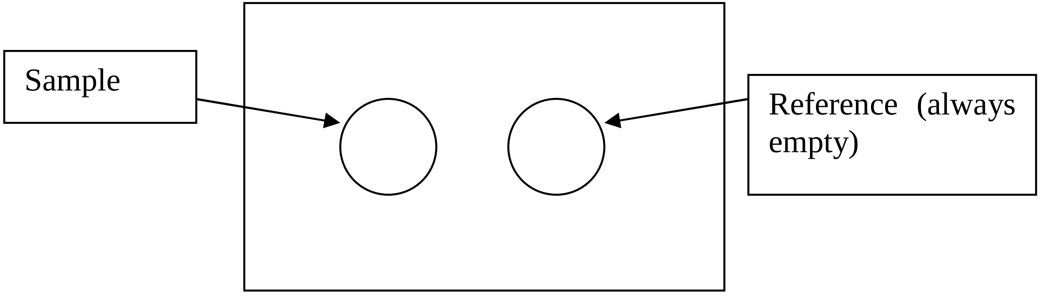

4. Data input (sample ID, save route), key in sample weight (0 for baseline)
5. Initial state > input initial temp: 25°C > y-initial: 20mW
   (1st time no baseline file, 2nd time use the baseline file)
6. Program: add step (temp scan), temperature from x to y, rate: 10°C/min
   View program (for confirming setting purpose)
7. View > calibrate (see whether the heat rate is 10°C/min setting)
8. Button was clicked “Go to temp” to cool down the temperature.
9. Button T↔t was clicked to see the “heat flow again time” curve, after a steady heat flow, button “start/stop” was clicked to start the experiment.
10. After finished the experiment, the data were export as a text file.
11. Step 3 to 10 was repeated for real testing. The sample was placed (sample weight: ~5mg) in one and the other was left as reference.

Experimental procedures of extrusion

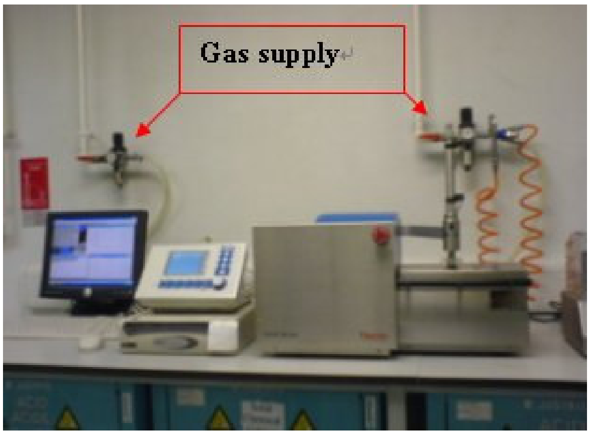

1. The gas supply was turned on (both feeder and driver)
2. The computer and main power was turned on. (back of the machine)
   (The gas sound will be hear)
3. The fastening screw were opened as followed order
   5 2 6
   3 1 4
4. The extruder screws and chamber were cleaned.
5. Anti-heat oil was put onto the fastening screws.
6. The fastening screws and feeder were then locked.
7. The software (Minilab) was then opened.
8. Maximum pressure: 200, 100
   Screw: co-rotating
9. Click ✎ for setting parameters:
   Mixing time, mixing speed
   Operation temperature (TS-E1) : x; Alarm: x+20,
   TM-D2: x+20; P-D1:180; P-D3:90
   cooling

TS-E1 x☐ ☐ ☐ ←x+20

TM-D2 ☐ ←x+20

P-D1 ☐ ←180

P-D3 ☐ ←90

10. ☺(load configuration to the machine)→ T (pre-heat)→ ▦ Calibrate the sensors
11. After pre-heat, the fastening screws were tightened again.
12. The material (4-5g) was filled by using the funnel.
13. Button ⚡ was clicked to start the machine

14. The feeder piston will be moved down to feed the material into the extruder screws.
15. Wait for material mixing
16. The control manual of the extruder:

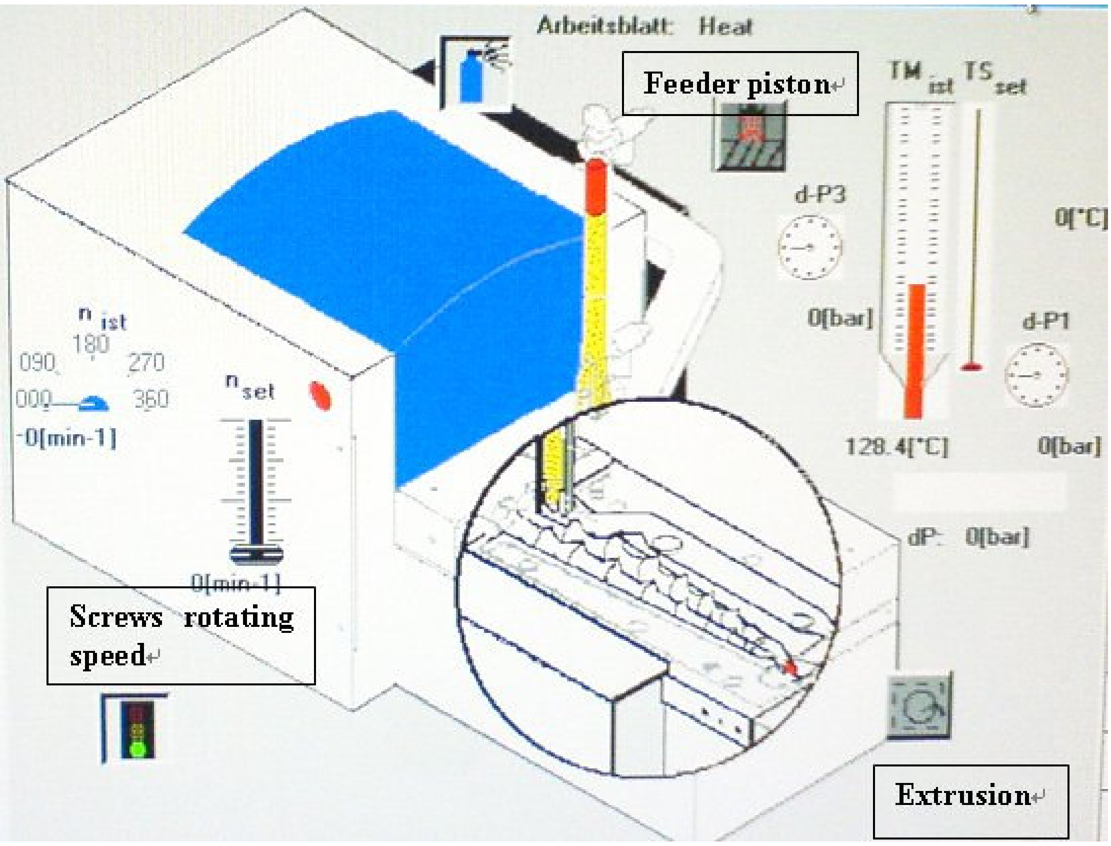

Feeder piston

Screws rotating speed

Extrusion

17. After mixing, the “Extrusion” button can be press and extrude the material out.
18. The fastening screws and housing were released for cleaning. (>1hr)
19. The machine was cooled down before shut down.